PREPARATION AND ANALYSIS OF BIODEGRADABLE DENDRITIC MACROMOLECULES FOR ENHANCED TUMOR ACCUMULATION

by

Janset Yener

B.S., Chemistry, Boğaziçi University, 2013

Submitted to the Institute for Graduate Studies in Science and Engineering in partial fulfillment of the requirements for the degree of

Master of Science

Graduate Program in Chemistry

Boğaziçi University

2015

PREPARATION AND ANALYSIS OF BIODEGRADABLE DENDRITIC MACROMOLECULES FOR ENHANCED TUMOR ACCUMULATION

APPROVED BY:

Assoc. Prof. Amitav Sanyal .....
(Thesis Supervisor)

Assoc. Prof. Rana Sanyal .....

Assist. Prof. Hüseyin Esen .....

DATE OF APPROVAL: 18.06.2015

To My Family and Beloved Harun

ACKNOWLEDGEMENTS

I would like to express my most sincere gratitude to my thesis supervisor Assoc. Prof. Amitav Sanyal for his endless patience, attention and scientific guidance throughout this study. I appreciate her support and useful comments throughout my laboratory work.

I wish to express my deepest thanks to Assoc. Prof. Rana Sanyal for her valuable scientific advices and helpful discussions regarding all my research in this laboratory.

I wish to express my thanks to Assist. Prof. Hüseyin Esen for his careful and constructive review of the final manuscript.

I wish to express my great thanks to Harun Utku Aksoy for both his endless help, patience and eternal love.

I also wish my endless thanks to Özgül Gök for her endless patience, attention, support and scientific guidance during my whole research and laboratory work.

I would like to extend my deepest thanks and respects to my masters Filiz Emlik Çalık, Burcu Sümer, Sadık Kağa, Mehmet Arslan and Nergiz Cengiz for their care, endless patience and support during my whole research and laboratory work.

I would like to thank my labmates Sesil Genç, Hazal İpek, Yasemin Nursel Üzüm, Merve Karaçivi, Laura Chambre, Yavuz Öz, Hasan Can Helvacı, Ahmet Genç, Buğra Aktan, Duygu Aydın, Özlem Kalaoğlu Altan, Tuğçe Nihal Gevrek, Gizem Yeter Baş, Evrim Aslan, İsmail Altınbaşak, Azize Kıraç, Büşra Karagöz, Bianca Golba, and Elif Erdinç for their friendship and endless support. I would also thank all my friends and the members of the faculty in Chemistry Department.

I want to thank TUBITAK 2210-D for funding my project.

ABSTRACT

PREPARATION AND ANALYSIS OF BIODEGRADABLE DENDRITIC MACROMOLECULES FOR ENHANCED TUMOR ACCUMULATION

The most important problem in cancer treatment is that many of the side effects of drugs used. While these drugs kill cancer cells, they also damage healthy cells. To reduce the side effects of these drugs, to extend the time the drug molecules stay in the body and to increase the water solubility of drugs which are hydrophobic in their nature, they can be loaded into polymeric structures. Drug delivery using micelles which are composed of dendrimers is an effective way of delivering drugs to their targets. Due to the hydrophobic environment of the core of micelles, water insoluble drugs can easily be solubilized and thus loaded for delivery at the required targets. In this thesis, several micellar structures were obtained using novel polymer-dendron conjugates synthesized via Diels-Alder "Click" reaction by utilizing furan-protected maleimide functionalized p(DEGMEMA) polymers with different generations synthesized via atom transfer radical polymerization (ATRP) and acetal dendrons of first and second generations containing anthracene unit at their focal point. Also, micellar stabilities were measured via fluorescence spectroscopy and dynamic light scattering (DLS). Sizes of these micelles were found to be less than 200 nm, a size suitable for drug delivery uses. In swelling studies, observed that dendron-polymer conjugate based micelles were highly stable rather than micelles formed from polymer itself under the addition an organic solvent, such as THF.

ÖZET

GELİŞTİRİLMİŞ TÜMÖR BİRİKİMİNE SAHİP BİYOBOZUNUR DENDRİTİK MAKROMOLEKÜLLERİN HAZIRLANMASI VE ANALİZİ

Kanser tedavisinde en önemli sorun, kullanılan ilaçların yan etkilerinin çok olmasıdır. Bu ilaçlar kanser hücrelerini öldürmekle beraber, sağlıklı hücrelere de zarar vermektedirler. Bu ilaçların yan etkilerini azaltmak, vücutta kalma sürelerini uzatmak ve hidrofobik yapılarının suda çözünürlüklerini arttırmak için ilaç molekülleri polimerik yapılara yüklenebilmektedir. Dendrimerlerden oluşan miseller kullanılarak hedeflenen bölgeye yapılan ilaç teslimi etkili bir yoldur. Misel çekirdeklerinin hidrofobik ortam olmaları nedeniyle, suda çözünmeyen ilaçlar kolay çözünür hale getirilebilir ve istenilen hedeflere teslimat için yüklenebilirler. Bu tezde, atom transfer radikal polimerizasyonu (ATRP) üzerinden sentezlenen, furan korumalı maleimit ile fonksiyonlandırılmış farklı jenerasyonlu p(DEGMEMA) polimeri ile odak noktasında antrasen içeren, birinci ve ikinci jenerasyona sahip asetal dendronların Diels - Alder reaksiyonu ile oluşturdukları yeni polimer dendron konjugatları kullanılarak çeşitli misel yapıları elde edilmiştir. Ayrıca, misel stabiliteleri floresan spektroskopisi ve dinamik ışık saçılımı (DLS) aracılığı ile ölçülmüştür. Bu misellerin, tıbbi kullanım için uygun olan en az 200 nm boyutunda oldukları bulunmuştur. Şişirme çalışmalarında, dendron-polimer konjuge misellerin THF gibi bir organik çözücü ilavesi altında, polimerin kendisi ile oluşan misellerden daha dayanıklı oldukları gözlenmiştir.

TABLE OF CONTENTS

LIST OF FIGURES.....x

LIST OF TABLE xiv

LIST OF SYMBOLS.....xv

LIST OF ACRONYMS/ABBREVIATIONS.....xvi

1. INTRODUCTION.....1

1.1. Cancer and Chemotherapy.....1

1.2. Polymer Therapeutics.....2

1.2.1. Enhanced Permeability and Retention Effect (EPR Effect).....4

1.2.2. Polymeric Architectures For Drug Delivery and Its Effect on Pharmacokinetics.....6

1.3. Dendrimers.....9

1.4. Structure of Polymeric Micelles.....12

1.5. Dendron - Polymer Conjugates.....13

1.6. Dendron – Polymer Conjugates Based Micellar Structures.....15

1.7. Critical Micelle Concentration (CMC).....16

1.8. Atom Transfer Radical Polymerization.....18

1.9. Click Chemistry.....19

1.9.1. Diels-Alder Reaction.....19

1.9.2. Diels-Alder Reaction in Polymer and Macromolecular Chemistry.....20

2. AIM OF THE STUDY.....24

3. RESULTS AND DISCUSSION.....25

3.1. Synthesis of the Building Blocks.....25

3.1.1. Synthesis of Dendrons.....26

3.1.2. Synthesis of Multiarm Star Polymers.....28

3.2. Synthesis of Dendron-Polymer Conjugates 36
3.3. Micelle Formation from Polymer-Dendron Conjugate 43
3.3.1. Critical Micelle Concentration (CMC) 43
3.3.1.1. Critical Micelle Concentration (CMC) Measurements 45
3.3.1.2. Swelling and Ultra-Dilution Studies of Micelles 55
4. EXPERIMENTAL 58
4.1. Materials and General Methods 58
4.2. Synthesis 58
4.2.1. Synthesis of Anthracene Functionalized Poly(ester) Acetal Dendrons 58
4.2.1.1. Synthesis of 1st Generation Anthracene Functionalized Acetal Dendron 58
4.2.1.2. Synthesis of 2nd Generation Anthracene Functionalized Acetal Dendron 60
4.2.2. Synthesis of Furan-Protected Maleimide-Containing Polymers 60
4.2.2.1. Synthesis of Furan-Protected Maleimide-Containing Linear Initiator 60
4.2.2.2. Synthesis of G1-Maleimide Initiator 61
4.2.2.3. Synthesis of G2-Maleimide Initiator 62
4.2.2.4. Synthesis of furan protected maleimide end-functionalized Linear-p(DEGMEMA) (12) 63
4.2.2.5. Synthesis of furan protected maleimide end-functionalized G1-p(DEGMEMA) (14) 64
4.2.2.6. Synthesis of furan protected maleimide end-functionalized G2-p(DEGMEMA) (16) 65
4.2.3. Synthesis of Dendron-Polymer Conjugates 66
4.2.3.1. Synthesis of Dendron-Polymer Conjugate (C1) 66
4.2.3.2. Synthesis of Dendron-Polymer Conjugate (C2) 67
4.2.3.3. Synthesis of Dendron-Polymer Conjugate (C3) 68

4.2.3.4. Synthesis of Dendron-Polymer Conjugate (C4).....69
4.2.3.5. Synthesis of Dendron-Polymer Conjugate (C5).....70
4.2.3.6. Synthesis of Dendron-Polymer Conjugate (C6).....71
4.3. Micelle Formation from Dendron-polymer Conjugates and Measurements 72
4.3.1. Micelle Preparation Method 73
5. CONCLUSION.....74
REFERENCES 75

LIST OF FIGURES

Figure 1.1. Schematic illustration of normal cell division vs. cancer cell division [2]. ... 1
Figure 1.2. Various drug delivery systems employed in polymer therapeutics [4]. 3
Figure 1.3. Schematic illustration of EPR effect with released drug. 5
Figure 1.4. Pharmaceutical carriers [7]. 5
Figure 1.5. Schematic illustration of EPR effect with drug carrier system. 6
Figure 1.6. Polymeric architectures which can be used for drug delivery [8]. 7
Figure 1.7. Passage of a polymer through linear and branched polymers from a pore during renal filtration [19] 8
Figure 1.8. Poly(ethylene oxide) Bow-tie hybrids. 8
Figure 1.9. Schematic representation of general structure of dendrimer [12]. 9
Figure 1.10. General structure of a dendron a part of the dendrimer [13]. 10
Figure 1.11. Synthesis of dendrimers via divergent and convergent method [1]. 11
Figure 1.12. Dendrimer as platform for multiple ligands as a tool for various applications [12]. 12
Figure 1.13. Schematic illustration of polymer micelle formation. Amphiphilic copolymers self-assemble to have a hydrophobic core and a hydrophilic corona structure in aqueous environments [21]. 13
Figure 1.14. Schematic representation of a linear–dendrimer diblock copolymer (left) and a linear–hyperbranched diblock copolymer (right) [23]. 14
Figure 1.15. General Scheme for the Synthesis of Functionalized Hydrogels [24]. 14
Figure 1.16. Schematic for drug release from a pH-sensitive micelle [25]. 15
Figure 1.17. General scheme of micelle [27]. 16
Figure 1.18. Schematic representation of linear and branched AMs [28]. 17
Figure 1.19. Mechanism of ATRP [33]. 18
Figure 1.20. Representation of the DA and retro-DA reactions [41]. 19
Figure 1.21. Segment block dendrimers consisting of polyester and polyaryl ether dendrons [43]. 21
Figure 1.22. A furan AB2 monomer with aromatic ether moieties at C3 and C4 in conjunction with a maleimide bearing a reactive phenolic moiety [41]. 21

Figure 1.23. Dendronization of polymer via Diels–Alder reaction [46]. 22
Figure 1.24. Synthesis of dendron–polymer block copolymers via the Diels–Alder "click" reaction [47]. 23
Figure 2.1. General scheme of micelle. 24
Figure 3.1. General scheme of dendron-polymer synthesis via Diels-Alder "Click" cycloaddition reaction. 25
Figure 3.2. General scheme of anthracene functionalized G1-acetal dendron 3 and G2 acetal dendron 4 synthesis. 26
Figure 3.3. ^{1}H NMR of dendron 3 and dendron 4. 27
Figure 3.4. General scheme for the synthesis of multiarm star polymers. 28
Figure 3.5. General scheme for the synthesis of furan-protected maleimide containing initiators. 29
Figure 3.6. ^{1}H NMR spectra of Linear Maleimide Based Initiator (6). 30
Figure 3.7. ^{1}H NMR spectra of G1-Maleimide Based Initiator (8). 30
Figure 3.8. ^{1}H NMR spectra of G2-Maleimide Based Initiator (10). 31
Figure 3.9. Synthesis of furan-protected maleimide-containing linear and multiarm star polymers. 32
Figure 3.10. ^{1}H NMR spectra of Linear Maleimide Based Polymer (12). 34
Figure 3.11. ^{1}H NMR spectra of G1-Maleimide Based Polymer (14). 34
Figure 3.12. ^{1}H NMR spectra of G3-Maleimide Based Polymer (16). 35
Figure 3.13. Dendron-polymer conjugate via Diels-Alder cycloaddition reaction. 36
Figure 3.14. ^{1}H NMR spectrum of polymer-dendron conjugate (C1). 37
Figure 3.15. ^{1}H NMR spectrum of polymer-dendron conjugate (C2). 38
Figure 3.16. ^{1}H NMR spectrum of polymer-dendron conjugate (C3). 38
Figure 3.17. ^{1}H NMR spectrum of polymer-dendron conjugate (C4). 39
Figure 3.18. ^{1}H NMR spectrum of polymer-dendron conjugate (C5). 39
Figure 3.19. ^{1}H NMR spectrum of polymer-dendron conjugate (C6). 40
Figure 3.20. GPC traces of polymer 12, dendron 3 and dendron-polymer conjugate C1. 40
Figure 3.21. GPC traces of polymer 12, dendron 4 and dendron-polymer conjugate C2. 41
Figure 3.22. GPC traces of polymer 14, dendron 3 and dendron-polymer conjugate C3. 41

Figure 3.23. GPC traces of polymer 14, dendron 4 and dendron-polymer conjugate C4. 42
Figure 3.24. GPC traces of polymer 16, dendron 3 and dendron-polymer conjugate C5. 42
Figure 3.25. GPC traces of polymer 16, dendron 4 and dendron-polymer conjugate C6. 43
Figure 3.26 Formation of micelles at critical micelle concentration [32]. 44
Figure 3.27. Excitation graph of pyrene loaded micelles formed from conjugate C1. 45
Figure 3.28. CMC graph of micelles formed from conjugate C1. 46
Figure 3.29. CMC graph of micelles formed from conjugate C2. 47
Figure 3.30. CMC graph of micelles formed from conjugate C3. 47
Figure 3.31. CMC graph of micelles formed from conjugate C4. 48
Figure 3.32. CMC graph of micelles formed from conjugate C5. 48
Figure 3.33. CMC graph of micelles formed from conjugate C6. 49
Figure 3.34. CMC graph of micelles formed from polymer 12. 49
Figure 3.35. CMC graph of micelles formed from polymer 14. 50
Figure 3.36. CMC graph of micelles formed from polymer 16. 50
Figure 3.37. Sizes of Conjugates with Changing Polymer Segment. 51
Figure 3.38. Sizes of Conjugates with Changing Dendron Segments. 52
Figure 3.39. Size of Polymers at 250 ^{o}C. 53
Figure 3.40. Size of Linear Polymer and Its Conjugates. 54
Figure 3.41. Size of G1-Polymer and Its Conjugates. 54
Figure 3.42. Size of G2-Polymer and Its Conjugates. 55
Figure 3.43. Change in the size of micelles of G1-Dendron & Linear Polymer (C1) upon addition of THF. 56
Figure 3.44. Change in the size of micelles G2-Dendron & Linear Polymer (C2) upon addition of THF. 56
Figure 3.45. Change in the size of micelles of linear polymer upon addition of THF. ... 57
Figure 4.1. Divergent synthesis of anthracene functionalized poly (ester) acetal dendron. 59
Figure 4.2. Furan-Protected Maleimide-Containing Linear Initiator Synthesis. 61
Figure 4.3. G1-Maleimide Initiator Synthesis. 62

Figure 4.4. G2-Maleimide Initiator Synthesis. 63
Figure 4.5. Linear Maleimide Based Polymer Synthesis. 64
Figure 4.6. G1-Maleimide Based Polymer Synthesis. 65
Figure 4.7. G2-Maleimide Based Polymer Synthesis. 66
Figure 4.8. Synthesis of dendron-polymer conjugate (C1). 67
Figure 4.9. Synthesis of dendron-polymer conjugate (C2). 68
Figure 4.10. Synthesis of dendron-polymer conjugate (C3). 69
Figure 4.11. Synthesis of dendron-polymer conjugate (C4). 70
Figure 4.12. Synthesis of dendron-polymer conjugate (C5). 71
Figure 4.13. Synthesis of dendron-polymer conjugate (C6). 72

LIST OF TABLES

Table 3.1. Synthesis and Characterization of Linear and Multiarm Star Polymers. …. 35

Table 3.2. CMC values of conjugates and polymers at 25°C. ……..…… 48

LIST OF SYMBOLS

G_1	Generation 1 dendron
G_2	Generation 2 dendron
G_3	Generation 3 dendron
λ	Wavelength

LIST OF ACRONYMS/ABBREVIATIONS

EPR	Enhanced Permeability and Retention
ATRP	Atom Transfer Radical Polymerization
Bis-MPA	2,2-bis(hydroxymethyl)propionic acid
CCA	1,2 cyclohexanedicarboxylic acid
$CDCl_3$	Deuterated Chloroform
CH_2Cl_2	Dichloromethane
CMC	Critical Micelle Concentration
DCC	Dicyclohexylcarbodiimide
DDS	Drug Delivery System
DEGMEMA	Di(ethylene glycol) methyl ether methacrylate
DLS	Dynamic Light Scattering
DMAP	N,N Dimethylaminopyridine
DOX	Docetaxel
EPR	Enhanced Permeability and Retention
Et_2O	Diethyl ether
FT-IR	Fourier Transform Infrared
G_1	Generation 1 dendron
G_2	Generation 2 dendron
G_3	Generation 3 dendron
GPC	Gel Permeation Chromatography
NMR	Nuclear Magnetic Resonance
PEG	Poly(ethylene glycol)
PEGMA	Poly(ethylene glycol) methyl ether methacrylate
PMDETA	N,N,N',N',N''-Pentamethyldiethylenetriamine
ROP	Ring Opening Polymerization
STEM	Scanning Transmission Electron Microscope
TEA	Triethylamine
THF	Tetrahydrofuran

1. INTRODUCTION

1.1. Cancer and Chemotherapy

Cancer is a leading cause of death that accounted for 8.2 million deaths which corresponds to around 15% of all deaths worldwide in 2012 [1]. It is a general term used for a group of diseases which involve unregulated cell growth. Normal cells grow and divide in a controlled way and when they become damaged by mutations they kill themselves by apoptosis. But in the case of cancerous cells, when mutations which affect the normal cell division process occur, the cell starts to proliferate in an uncontrollable manner (Figure 1.1). Cancerous tumors are malignant, which means they can spread into, or invade, nearby tissues. In addition, as these tumors grow, some cancer cells can break off and travel to distant places in the body through the blood or the lymph system and form new tumors far from the original tumor. This process is called as metastasis and it is responsible for spread of disease to other organs.

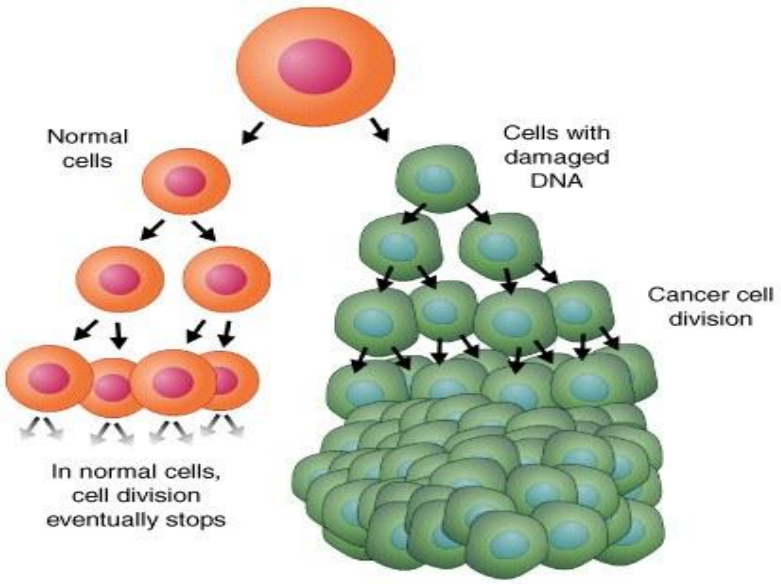

Figure 1.1. Schematic illustration of normal cell division vs. cancer cell division [2].

Chemotherapy is a drug treatment that uses powerful chemicals to kill fast-growing cells in the body. Chemotherapy is most often used to treat cancer, since cancer cells grow and multiply much more quickly than most cells in the body. Unfortunately, chemotherapy not only kills fast-growing cancer cells, but also kills or slows the growth of healthy cells that grow and divide quickly. Examples are cells found in your mouth, intestines and hair. Damage to healthy cells may cause side effects, such as mouth sores, nausea, and hair loss. Challenges in the area of chemotherapy are selective targeting at drugs to diseased organs. Advancements in this area will lead to less side effects and improved efficacy of treatment.

1.2. Polymer Therapeutics

Side effects and limitations of chemotherapy drugs have been addressed by scientists using drug delivery. Researchers improve efficacy and reduce toxicity of cancer therapy together with the advances in polymer based drug carriers. These innovative and associated nanomedicine technologies are named as “Polymer Therapeutics”.

The advantages of utilizing a polymer based therapeutic system are primarily to improve the potential of the respective drug by enhancing water solubility, particularly relevant for some drugs with low aqueous solubility, stability against degrading enzymes or reduced uptake by reticulo-endothelial system (RES), and targeted delivery of drugs to specific sites of action in the body (1), (6). The idea of conjugating drugs to polymers as drug delivery systems was introduced by Ringsdorf in 1975. According to Ringsdorf’s model the polymer should be biocompatible and biodegradable and the drugs should be attached to the backbone via a cleavable linker. Additionally the polymer should have solubilizing groups and targeting moieties [3].

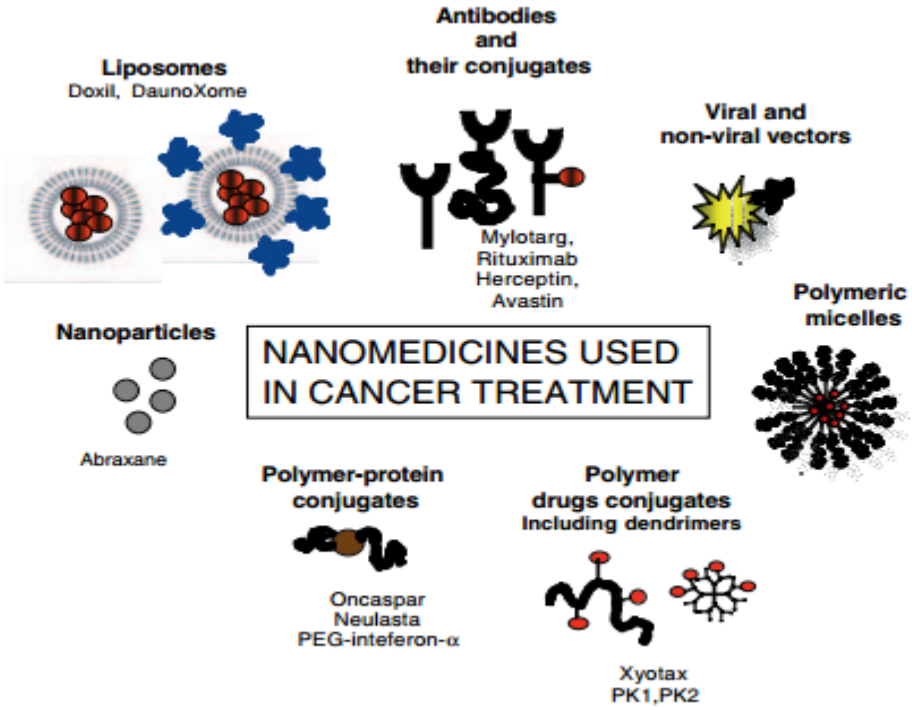

Figure 1.2. Various drug delivery systems employed in polymer therapeutics [4].

The current interest in polymer-drug conjugates arises due to their solution to several problems related to conventional chemotherapy. These problems include short half-life due to renal clearance, low solubility and toxicity to healthy cells [5]. Firstly, chemotherapy drugs have a low molecular weight, so they have a short half-life in the blood stream and they are eliminated rapidly. Conjugating drugs to large molecular weight polymers reduces their elimination from the body and prolongs their half-life, resulting in a better pharmacokinetic profile. This situation increases the efficacy of chemotherapy. Chemotherapeutic drugs generally have a hydrophobic nature and require toxic solubilizers in drug formulation. To solubilize chemotherapeutic drugs, conjugating them to a water soluble polymer is a common approach. So, polymers which are chosen for the preparation of drug–polymer conjugates should ideally be water-soluble, nontoxic and non-immunogenic.

Water soluble polymers such as poly(ethylene glycol) (PEG), poly(vinyl alcohol) (PVA), poly(hydroxypropyl methacrylate) (HPMA) and poly(glycolic acid) (PGA) are

widely used polymers for drug conjugation. Their hydrophilic character increases the solubility of drug in aqueous media.

Another major problem related to chemotherapy is toxicity. Chemotherapy drugs cannot differentiate normal cells and cancerous cells, so all rapid dividing cells get affected and this situation causes serious side effects to the patient receiving chemotherapy. Additionally, the toxicity of the drug for healthy tissue limits the dose which can be administered to the patient. In that case, the use of polymer-drug conjugates helps to reduce the toxicity. Polymer-drug conjugates can localize the drug concentration at one place and decrease the distribution of the drug to healthy tissues. Namely, the polymer-drug conjugate accumulates in the tumor tissue due to a phenomenon called "enhanced permeability and retention effect" (EPR effect) which will be discussed in the following section. Finally, after accumulation in tumor tissue, the drug is released from the polymer just at the right place for maximum effectiveness and minimum toxicity for healthy tissue.

Another important point of using polymer-drug conjugates is attachment of a targeting group, such as an antibody which is specific for the receptors which are overexpressed on the cancer cells. In that case, the accumulation of polymer-drug conjugates in cancer tissue is increased with the help of targeting groups.

1.2.1. Enhanced Permeability and Retention Effect (EPR Effect)

Tumors and many inflamed areas of body have hyper-permeable vasculature and poor lymphatic drainage which passively provides increased retention of macromolecules into tumor and inflamed area of body [6,7]. This phenomenon is called enhanced permeability and retention (EPR) effect. EPR effect is primarily utilized for passive targeting due to accumulation of pro-drug into tumor or inflamed area. Small molecules are able to diffuse through the endothelium cells on the walls of the blood vessels and enter both the healthy and tumor tissue (Figure 1.3). On the other hand, low molecular drugs covalently coupled with high-molecular-weight carriers are not eliminated efficiently due to hampered lymphatic drainage and therefore accumulate only in tumors (Figure 1.5).

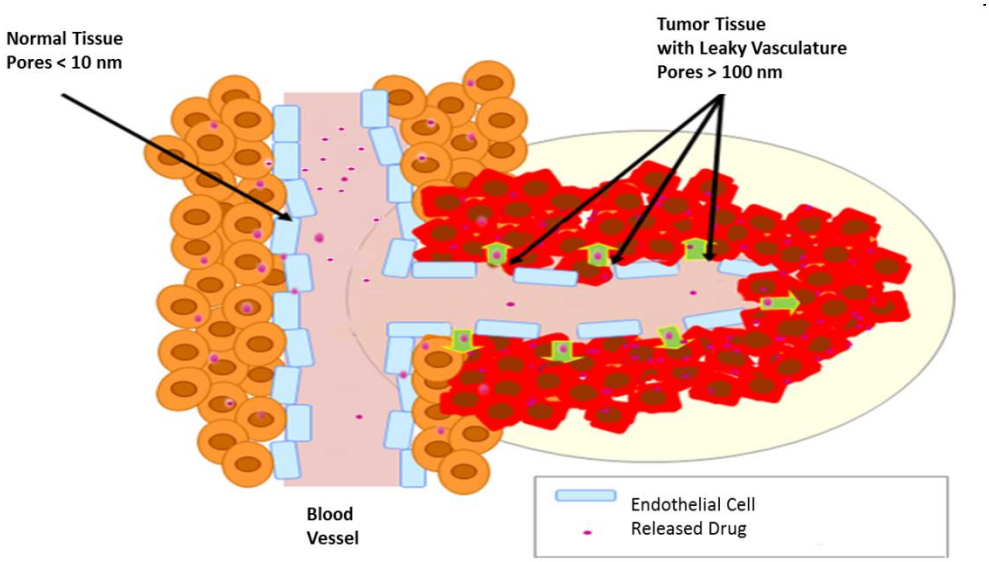

Figure 1.3. Schematic illustration of EPR effect with released drug.

While EPR effect enhances the passive targeting ability due to higher accumulation rate of drug in tumor and subsequently due to accumulation, pro-drug slowly releases drug molecules which provide high bioavailability and low systemic toxicity [7]. To minimize drug degradation and loss to prevent harmful side-effects of chemotherapy drugs and to increase drug bioavailability and the amount of the drug accumulated in the required region via EPR effect, various drug delivery and drug targeting systems are currently under development (Figure 1.4).



Figure. 1.4. Pharmaceutical carriers [7].

Colloidal drug carrier systems such as micellar solutions, vesicle and liquid crystal dispersions, as well as nanoparticle dispersions consisting of small particles of 10–400 nm diameter show great promise as drug delivery systems. When developing these formulations, the aim is to obtain systems with optimized drug loading and release properties, long shelf-life and low toxicity [8].

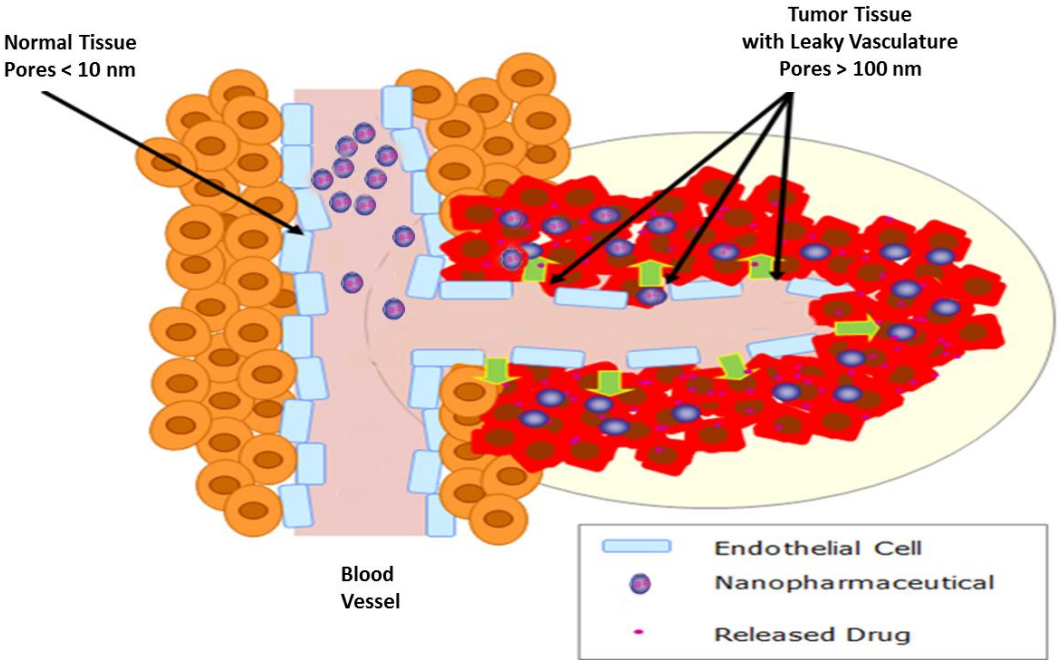

Figure 1.5. Schematic illustration of EPR effect with drug carrier system.

1.2.2. Polymeric Architectures For Drug Delivery and Its Effect on Pharmacokinetics

Design of polymer architectures in drug delivery systems has an important effect on the accumulation of polymer-drug conjugates in the tumor tissue. Branching degree, flexibility and molecular conformation of these conjugates have a great and direct impact on the rate of renal clearance. Commonly used polymeric architectures include graft polymers, star polymers, multivalent polymers, dendrimers and dendronized polymers (Figure 1.6.).

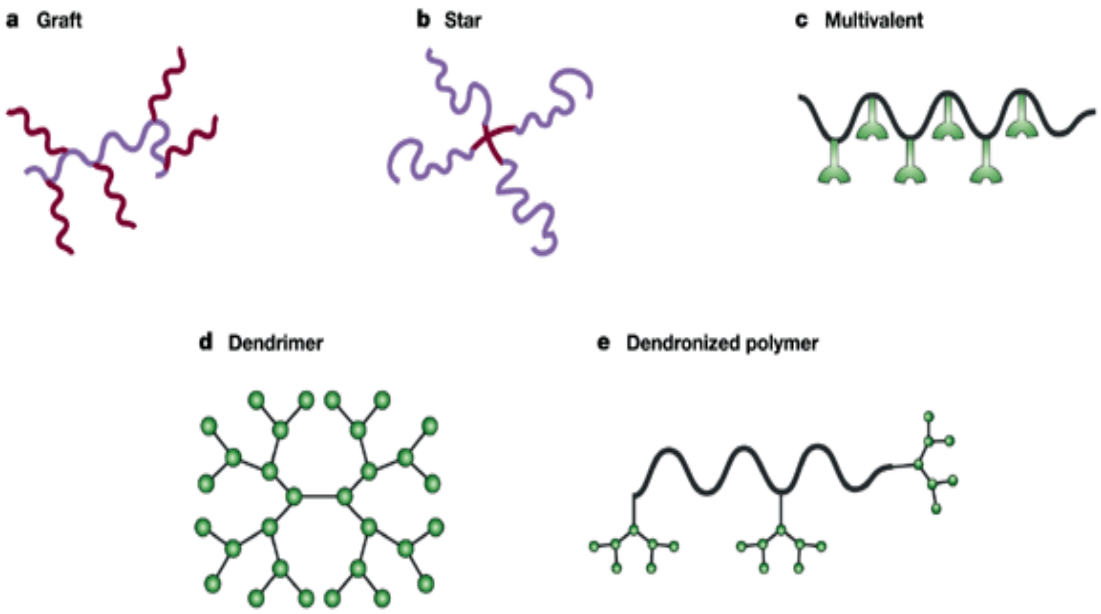

Figure.1.6. Polymeric architectures which can be used for drug delivery [4].

Compared to linear elongated polymers, more branched and compact ones, especially star polymers and dendrimers, have increased residence time in the bloodstream because of its less flexibility during the elimination from kidneys. So, in this prolonged life time, polymer-drug conjugates with branched structure have more chance to reach and accumulate in the tumor tissue [9].

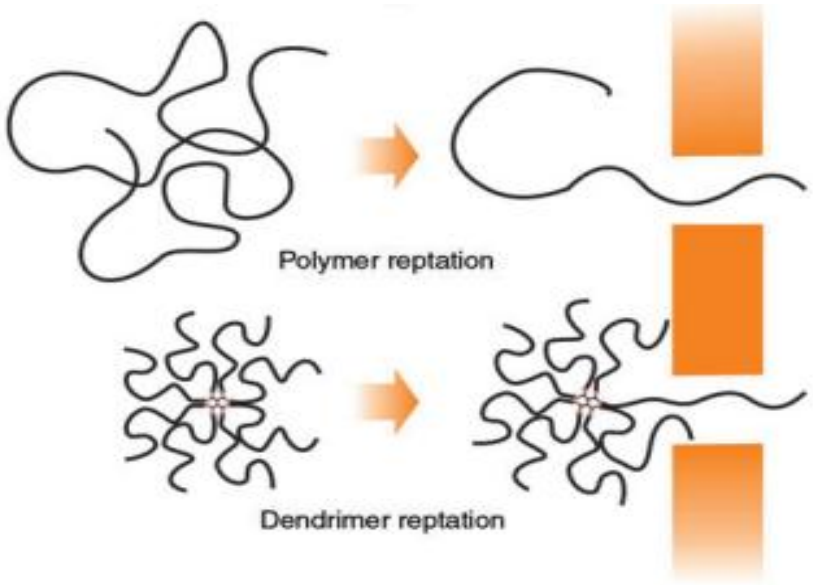

Figure 1.7. Passage of a polymer through linear and branched polymers from a pore during renal filtration [9].

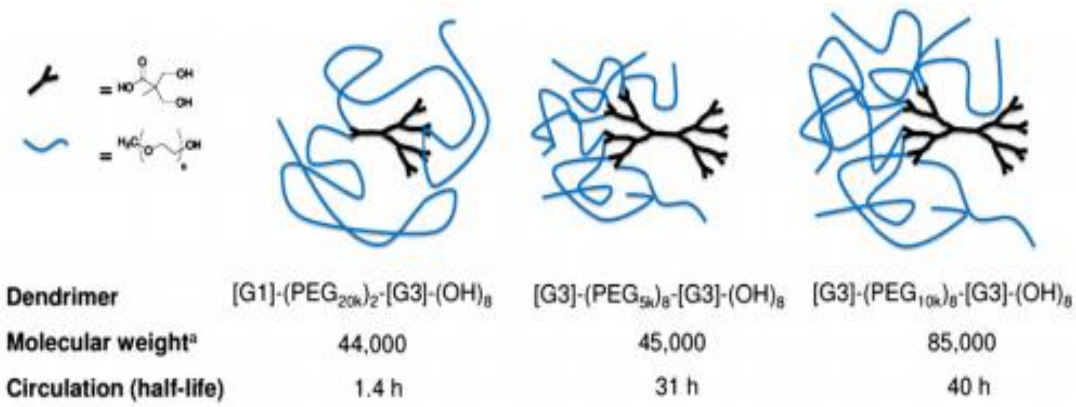

Figure 1.8. Poly(ethylene oxide) Bow-tie hybrids [10].

Pharmacokinetics of dendrons based on 2,2-bis(hydroxymethyl)propionic acid can be tuned by varying generation size (G1, G2, and G3) and PEG chain molecular weight (5000, 10,000, and 20,000) [10].

In a recent study, the groups of Fréchet and Szoka reported the pharmacokinetics of bow-tie dendrimer based on poly(ethylene glycol) (PEG) and 2,2-bis(hydroxymethyl)propionic acid with varying molecular weights and chain numbers to determine the effect of molecular weight and architecture [10]. The polymers were comprised of G3 hydroxyl-terminated branching on one side, and G1, G2, or G3 branching on the opposite side featuring PEG chains of 5000, 10,000, and 20,000 molecular weights. Examples of a [G1]- (PEG20k)2-[G3]-(OH)8, [G3]-(PEG5k)8-[G3]-(OH)8, and a [G3]-(PEG10k)8-[G3]-(OH)8 are shown in Figure 1.8.

Importantly, an architecturally dependent response was observed, where the number of PEG macromolecules attached to the bow tie dramatically affected circulation time. A [G1]-(PEG20k)2-[G3]-(OH)8 polymer of 44,000 Da has a half life of 1.5 h whereas a [G3]-(PEG5k)8- [G3]-(OH)8 of similar molecular weight has a half life of 31 h. Next, the two largest [G3]-(PEG10k)8-[G3]-(OH)8 and [G3]- (PEG20k)8-[G3]-(OH)8 macromolecules were injected intravenously into tumor bearing C57BL6 mice previously injected subcutaneously with B16F10 melanoma cells. Both polymers showed similar biodistribution characteristics, with high levels of material found in the tumors (10% to 15%) and blood (18% to 20%) at 48 h [10].

1.3. Dendrimers

Dendrimers are novel three dimensional, hyperbranched globular nanopolymeric archi-tectures. The expression dendrimer is derived from a Greek termdendron that means “tree”, which is logical in view oftheir typical structure with a number of branching units. These hyperbranched molecules were first discovered by Fritz Vogtle in 1978, by Donald Tomalia and co-workers in the early 1980s, and at the same time, but independently by George R. Newkome [11]. It is synthesized with stepwise organic reactions resulting the structure mainly copmposed of three different units: a core, repeating units and surface groups (Figure 1.9) [12]. Branching units are symmetrically placed around the core contribute to its uniform structure. The number of branching units from the core to the periphery refers to the generation of the dendrimer.

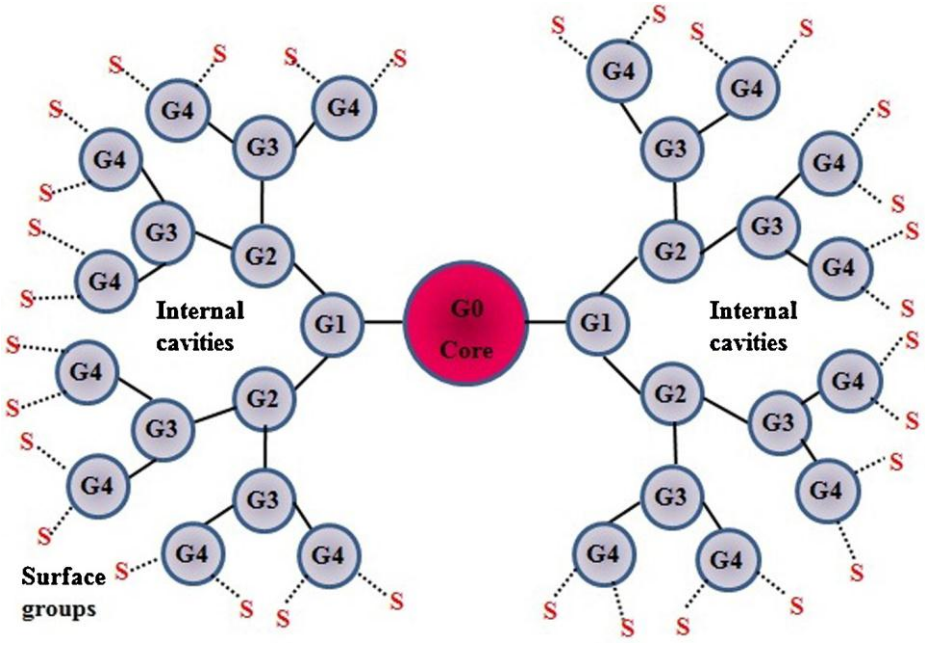

Figure 1.9. Schematic representation of general structure of dendrimer [12].

Each part of a dendrimer can be used for different purposes. Internal cavities play crucial role in the encapsulation of agents in delivery for specific purposes. The functional groups which are located at the surface usually interact with surroundings and define the physical and chemical properties of the dendrimers. The core of a dendrimer can be

perceived as a protected part, so can be used to attach a catalytically or optically isolated site.

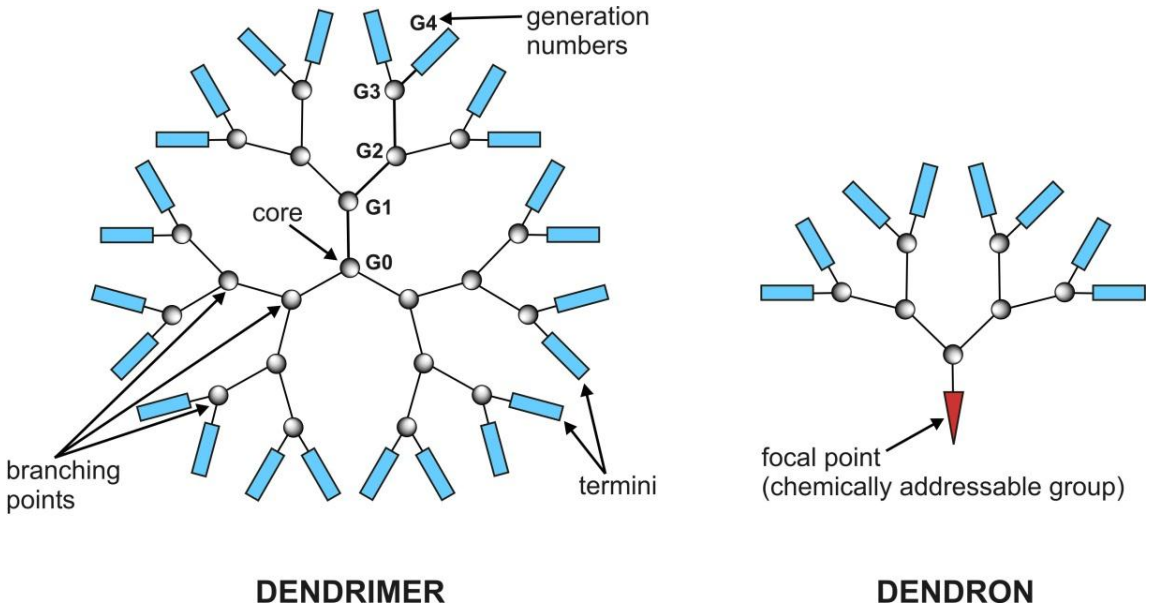

Figure 1.10. General structure of a dendron a part of the dendrimer [13].

A part of the dendrimer starting from the core and ending at the periphery is called dendron. It does not contain the ‘core’ part. The starting point from which repeating units built the dendron is called as the focal point, which may also contain chemically reactive groups on it (Figure 1.10). Several dendrons can be combined together to obtain a dendrimer.

Dendrimers can be synthesized with two different approaches, namely, “divergent” and “convergent” approaches. In divergent method, we start from a reactive core to grow different generation and then periphery is functionalized. On the other hand, in convergent method, surface groups are attached onto the branching units firstly and these small dendron pieces are combined via a multivalent core. Synthesized dendrons are combined either with the help of covalent bond between their focal points or via non-covalent interactions at the end (Figure 1.11) [1].

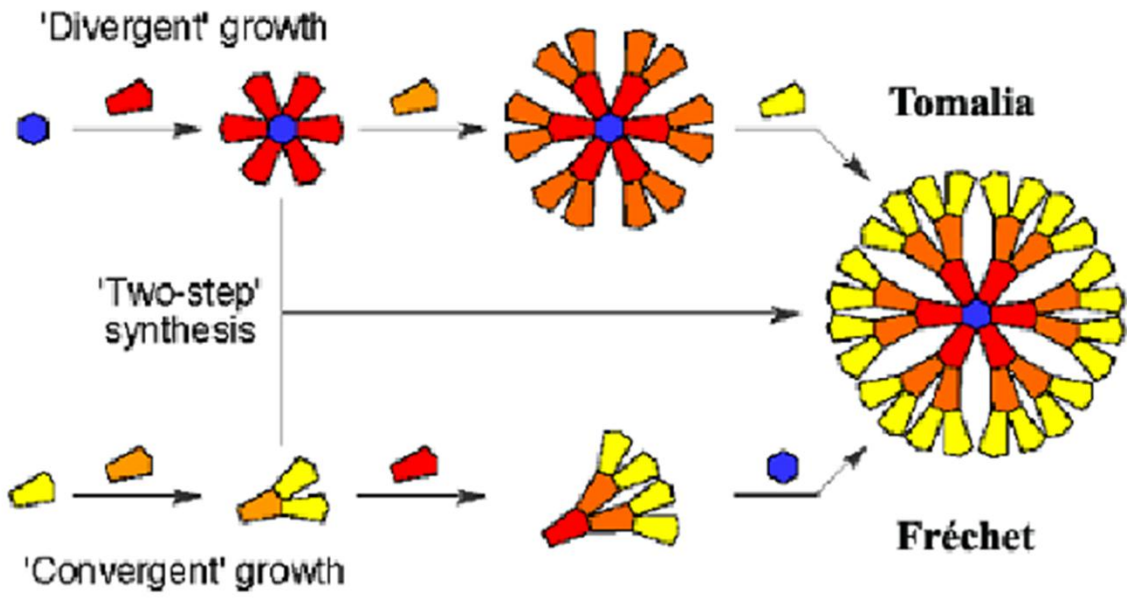

Figure 1.11. Synthesis of dendrimers via divergent and convergent method [1].

Attractive features of dendrimers like nanoscopic size, narrow polydispersity index, excellent control over molecular structure, availability of multiple functional groups at the periphery and cavities in the interior distinguish them among the available polymers. For these reasons, applications of dendrimers in a large variety of fields have been explored. In 1982, Maciejewski proposed, for the first time, the utilization of these highly branched molecules as molecular containers [14].

Clearly, there are many areas of biological chemistry where application of dendrimer systems may be helpful, such as biomedical field [15], controlled and specified drug delivery, which includes nanomedicine [11,16], transdermal drug delivery [17], gene delivery [18], dendrimers as magnetic resonance imaging contrast agents [19] and photodynamic therapy [20].

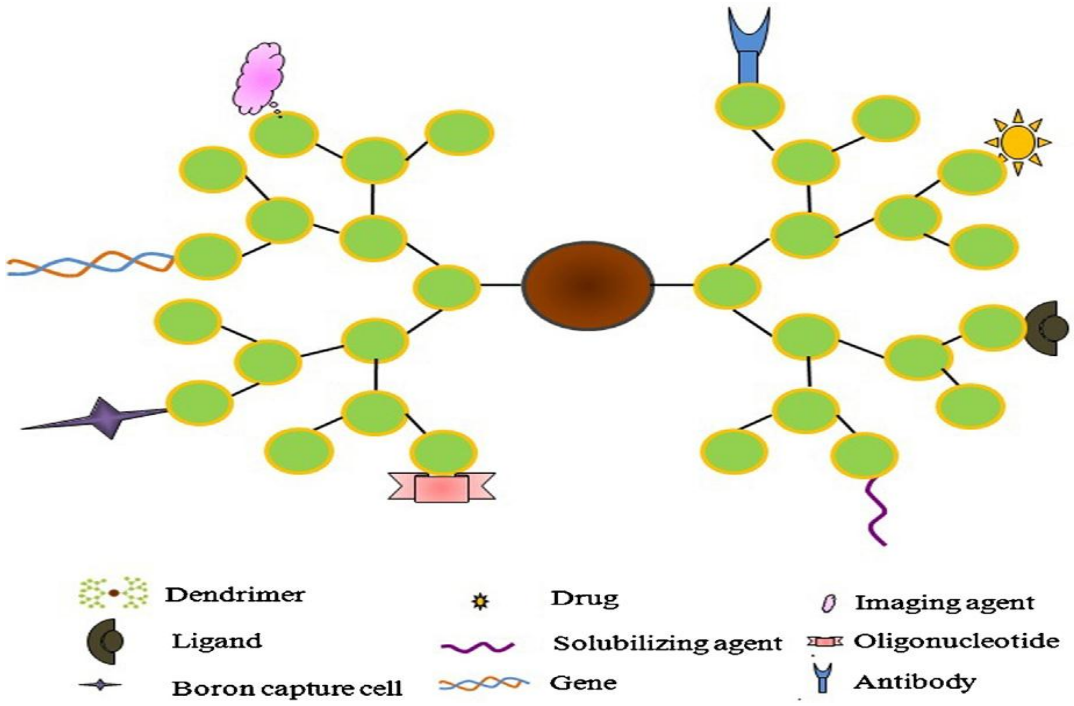

Figure 1.12. Dendrimer as platform for multiple ligands as a tool for various applications [12].

Scientists are especially enthusiastic about possible utility and versatility of dendrimers as drug delivery tool. Terminal functionalities give chance to make conjugation of the drug and targeting moieties.

1.4. Structure of Polymeric Micelles

Polymeric micelles provide a platform that can be carefully designed for drug delivery. Micelles are formed by self-assembly of amphiphilic block copolymers (5-50 nm) in aqueous solutions. These block copolymers are composed of hydrophilic and hydrophobic segments. The amphiphilic copolymers self-assembled into micelles in aqueous environments with the hydrophobic polymer forming the core of the micelle and the hydrophilic polymer forming the corona.

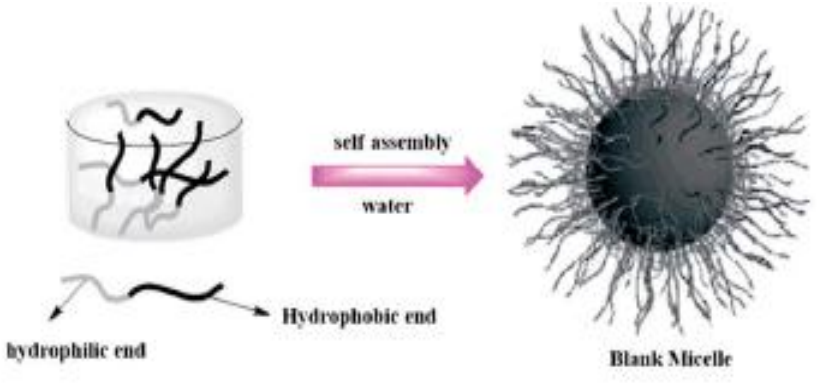

Figure 1.13. Schematic illustration of polymer micelle formation. Amphiphilic copolymers self-assemble to have a hydrophobic core and a hydrophilic corona structure in aqueous environments [21].

The hydrophobic drugs can be physically entered in the core of block copolymer micelles and transported at concentrations that can maintain their water solubility. Moreover, the hydrophilic blocks may form hydrogen bonds with the aqueous environment and form a tight shell around the micellar core. As a result, the inside of the hydrophobic core is effectively protected against hydrolysis and enzymatic degradation. As mentioned before, these amphiphilic block copolymers attractive for drug delivery applications and bring some advantages, such as improving water solubility for drug, prolonged circulation time in the tumor side and passive targeting by means of increased EPR effect. Also, their chemical composition, total molecular weight and segment length ratios can be easily changed, which allows us to control of the size and morphology of the micelles.

1.5. Dendron - Polymer Conjugates

Block copolymers are most commonly studied and already find broad applications in recent years. Besides linear AB diblock or ABA triblock copolymers, branching polymers are emerged as one of the most common field, which gives additional possibilities about structural complexity and unusual structure–property correlations that are clearly separated from those for linear block copolymers. After the first report of a

dendron structure in the 1970s by Vögtle et al. [22], a rapid development in the synthesis of dendrimers and hyperbranched polymers – cascade-branched structures that are often summarized as “dendritic polymers” – has greatly enhanced the spectrum of potential building blocks for segmented macromolecular architectures [23].

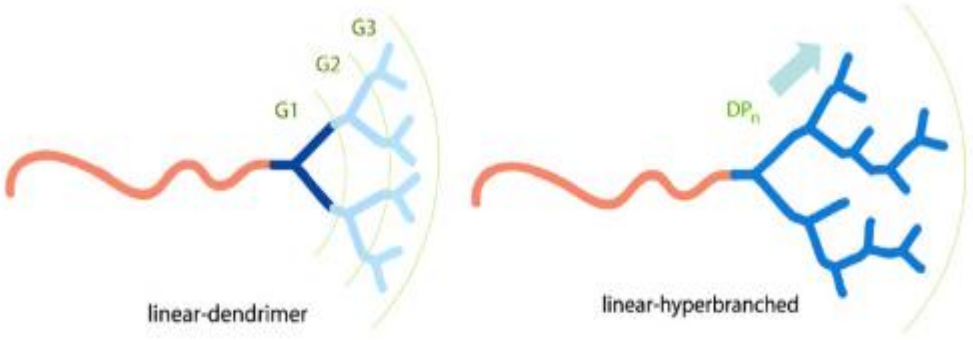

Figure 1.14. Schematic representation of a linear–dendrimer diblock copolymer (left) and a linear–hyperbranched diblock copolymer (right) [23].

In a recent study, the Sanyal group reported Fabrication of “Clickable” Hydrogels via Dendron−Polymer Conjugates. They prepared a family of dendron-polymer conjugates by coupling second- and third-generation alkyne appended polyester dendrons with linear poly(ethylene glycol) diazides, PEG2K and PEG6K via Huisgen type “click” reaction provides a unique precursor for reactive hydrogels [24].

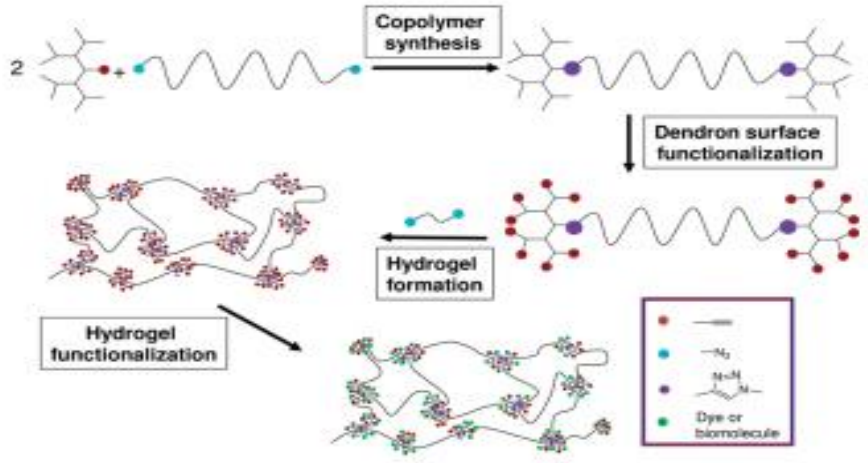

Figure 1.15. General Scheme for the Synthesis of Functionalized Hydrogels [24].

1.6. Dendron – Polymer Conjugates Based Micellar Structures

Self-assembly of dendritic structures under different conditions led to efficient routes to a variety of supramolecular assemblies. For example, dendron-polymer conjugates are one of the most common dendritic structures in the field of drug delivery, especially in pharmaceutical applications of polymeric micelles as well as other drug carriers. In dendron-polymer conjugates, it is possible to obtain micellar structures with the help of differences in solubility of the segments in an aqueous media. Amphiphilic dendritic ABA triblock or AB diblock copolymers which branched dendrimer attached to a linear or branched polymer chain are good candidates to get dendritic micelles. Generally, chemotherapy drugs are hydrophobic in their nature, so in this structure, hydrophobic dendron part forming the core of the micelle provides opportunity to have drug loading.

Frechet and co-workers synthesized a pH-responsive micelle system which linear-dendritic block copolymers include poly(ethylene oxide) and either a polylysine or polyester dendron were prepared and hydrophobic groups were attached to the periphery of dendrimer by highly acid-sensitive cyclic acetals [25].

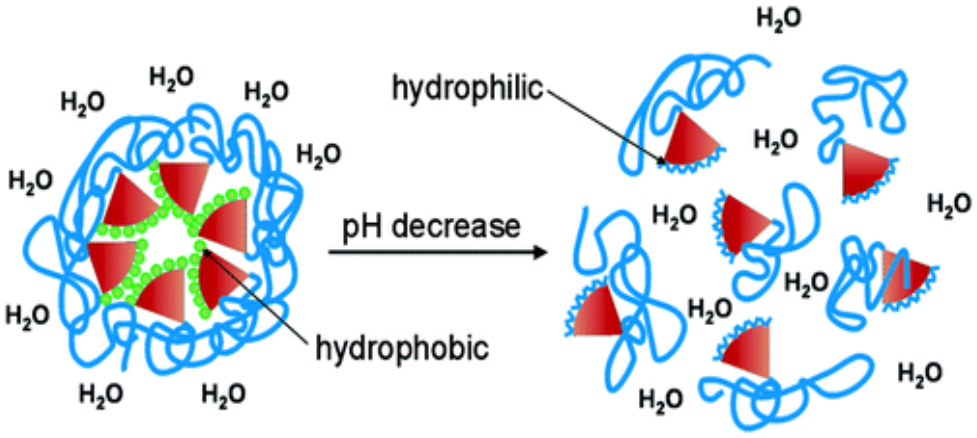

Figure 1.16. Schematic for drug release from a pH-sensitive micelle [25].

These copolymers were designed with the goal of forming stable micelles in aqueous solution at neutral pH but disintegrating into its parts at mildly acidic pH following loss of the hydrophobic groups with acetal hydrolysis. With acetal hydrolysis, the hydrophobic dendrimer periphery becomes hydrophilic, it removes the driving force for self-assembly and destabilizes the micelle. This destabilization enables release of the drugs from the micelle core as illustrated in Figure 1.16 [25].

1.7. Critical Micelle Concentration (CMC)

Amphiphilic polymers self-assemble in aqueous solutions with the hydrophobic chains which aggregate together to form the core of the micelle and the hydrophilic chains extend towards the aqueous environment. The critical micelle concentration (CMC) is the minimum concentration of polymer required to form micelles. Low polymer concentrations are insufficient for self-assemble of polymer chains. When the concentration of polymer increases, more chains are adsorbed at the interface. As a concentration is reached at which both the bulk solution and interface are saturated with polymer chains — this is the CMC. So, to add more polymer chains to the system beyond this CMC point will result in micelle formation in the bulk solution. And at high polymer concentration, the micelles are stable structures unless they are diluted below the CMC point [26].

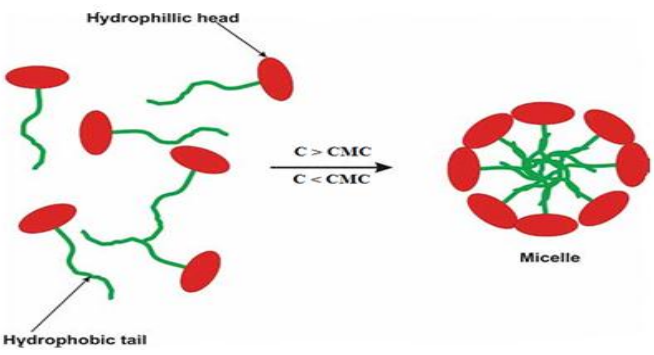

Figure 1.17. General scheme of micelle [27].

Kathryn E. Uhrich and co-workers developed a novel series of amphiphilic macromolecules (AMs) composed of a sugar backbone, aliphatic chains, and branched, hydrophilic poly(oligoethylene glycol) methyl ether methacrylate (POEGMA) for drug delivery applications. They indicate that this design allows them to arrange AM chemical structures and generates a range of physicochemical properties, such as different colloidal stability, aggregation sizes, and thermal properties. They alter the hydrophobic region by increasing the length and number of aliphatic chains attached to the sugar backbone. So, they aim to improve hydrophobic interactions, micelle formation, and micelle stability. Also, they reported that changing the single linear PEG chain with two shorter PEG chains that branched analogues produced AMs that formed micelles of smaller size and higher water solubility. It results in higher micelle stability as compared to analogues containing a single, longer PEG chain. And this micelle stability is favorable for drug delivery systems to achieve sustained release and targeted site accumulation. Also, their AMs possessed low CMC values (10−6 to 10−7 M), and this low CMC was attributed to the strong hydrophobic interactions between the hydrophobic domains, which makes micelle formation easier [28] (Figure 1.18.).

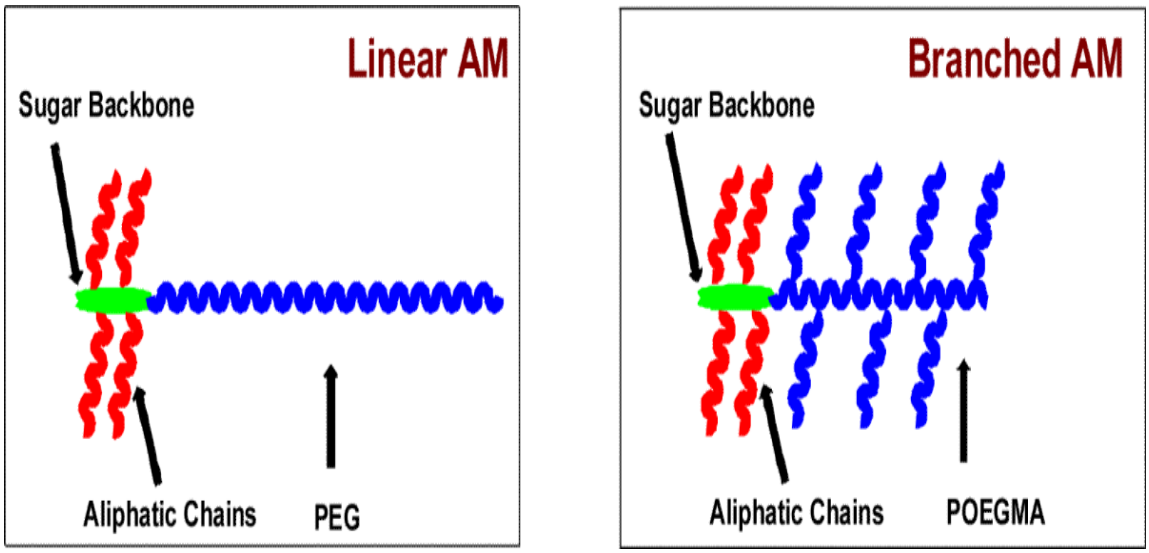

Figure 1.18. Schematic representation of linear and branched AMs [28].

1.8. Atom Transfer Radical Polymerization

Atom transfer radical polymerization (ATRP) is a kind of controlled/living radical polymerization (CRP) technique. It was discovered by Mitsuo Sawamoto [29] and Krzysztof Matyjaszewski in 1995 [30]. Atom Transfer Radical Polymerization is one of the most effective and widely used methods of controlled radical polymerization (CRP). ATRP gives chance to scientists to easily form polymers by putting together component parts which are called monomers, in a controlled manner.

Until the discovery of ATRP, polymer chemists have difficulties in their ability to control the composition and architecture of macromolecules, and to provide materials with highly specific, uniform characteristics. Nowadays, ATRP is widely used to make linear polymers [31], star shaped polymers, core crosslinked star polymers [32], etc.

There are four important variable components of Atom Transfer Radical Polymerizations. They are the monomer, initiator, catalyst and solvent. The atom transfer step is the main reason for the controlled chain growth. The catalyst gives an equilibrium between the active (propagating) and inactive (dormant) form of the polymer. This equilibrium mechanism decreases the concentration of propagating polymer chains and therefore minimizes termination steps (Figure 1.19.) [33].

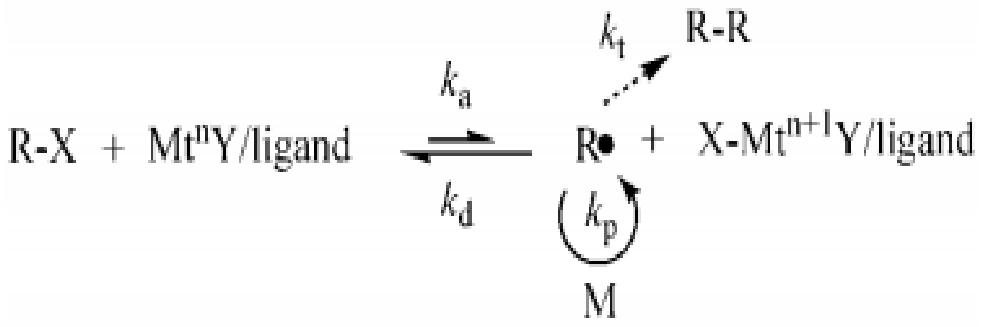

Figure 1.19. Mechanism of ATRP [33].

1.9. Click Chemistry

Click Chemistry [Kolb] describes pairs of functional groups that rapidly and selectively react with each other in mild, aqueous conditions. The concept of Click Chemistry has been transformed into convenient, versatile and reliable two-step coupling procedures of two molecules A and B [34,35], that are widely used in biosciences [36], drug discovery [37] and material science [38].

Mainly there are 4 types of "Click" reactions which are 'nucleophilic opening of highly strained rings' such as epoxides, cyclic sulfates, aziridines, cyclic sulfamidates and aziridinium ions, 'protecting group reactions' such as acetals, ketals and their aza-analogs. And the most famous ones are 'cycloaddition reactions' such as Diels-Alder [4+2] and Copper catalyzed Huisgen [3+2] or Huisgen 1,3 dipolar cycloaddition reactions [39].

1.9.1 Diels-Alder Reaction

Diels-Alder reaction (DA) is a well-known [4+2] cycloaddition reaction between electron rich diene and electron poor dienophile [40]. DA reaction results in a six membered ring formation with the new bonds by inter- or intramolecular interactions. The product obtained is called as an cycloadduct. DA is an electrocyclic reaction that new σ-bonds are formed and these σ-bonds are energetically more stable than the π-bonds. Also, Diels-Alder reaction is a widely used one in synthetic organic chemistry due to its high yields without formation of side products [41].

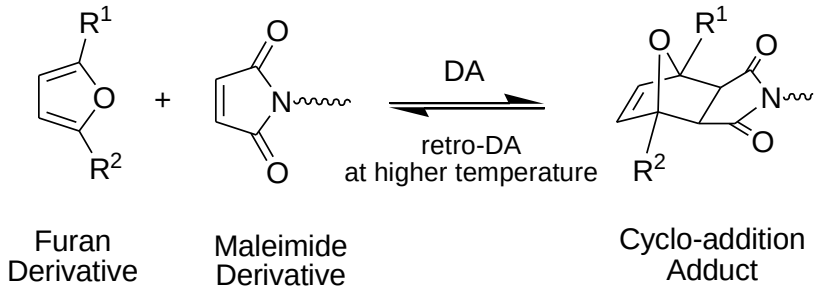

Figure 1.20. Representation of the DA and retro-DA reactions [41].

Diels-Alder reaction can result in two stereoisomers which are named as the endo and exo products. The endo product is the kinetically favored product with a lower activation energy because of the orbital overlap in transition state. It happens at low temperatures. The exo product is one that thermodynamically controlled product due to the formation of a more stable and less sterically hindered final conformation. It happens at high temperatures.

In addition to the advantages of reaction which is stated above, it is possible to shift reaction to the side of reactants by increasing the heat, a process known as “retro Diels-Alder reaction’’ [42]. This property of Diels-Alder reaction can be used for the design of thermo-reversible systems in polymer and material science.

1.9.2 Diels-Alder Reaction in Polymer and Macromolecular Chemistry

The furan-maleimide DA reaction and reversibility of it have been seen in the production of thermally responsive systems which include segment block dendrimers [43], simple linear polymers [41], cross-linking linear polymers [42], alternating copolymers [44], and multiarm star block copolymers [45].

In order to demonstrate the thermo-reversibility property of the dendrimers, Sanyal and co-workers developed segment block dendrimers consisting of polyester and polyaryl ether dendrons using reagent free Diels-Alder cycloaddition reactions. Three generations of maleimide functionalized polyester dendrons were reacted with furan functionalized polyaryl ether dendrons with the same generation to get segment block dendrimers. The thermo-reversible nature of these molecules was investigated by using anthracene as a scavenger diene under elevated temperatures (Figure 1.21.) [43].

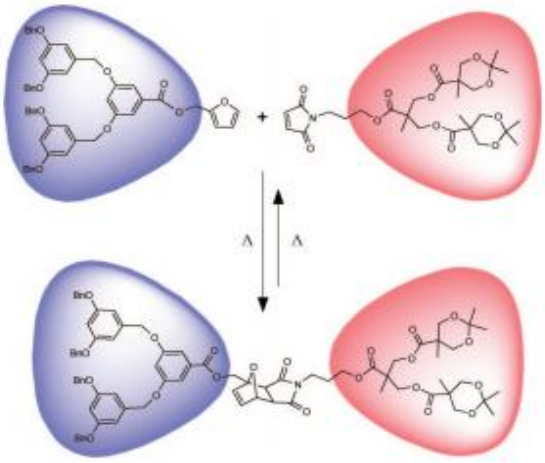

Figure 1.21. Segment block dendrimers consisting of polyester and polyaryl ether dendrons [43].

Another example about the first application of the DA reaction to prepare thermally responsive dendrons and dendrimers which Gandini reported a very original piece of work based on a furan AB2 monomer with aromatic ether moieties at C3 and C4 in conjunction with a maleimide bearing a reactive phenolic moiety. The third generation dendrimer (MW 5469.10) was used [41].

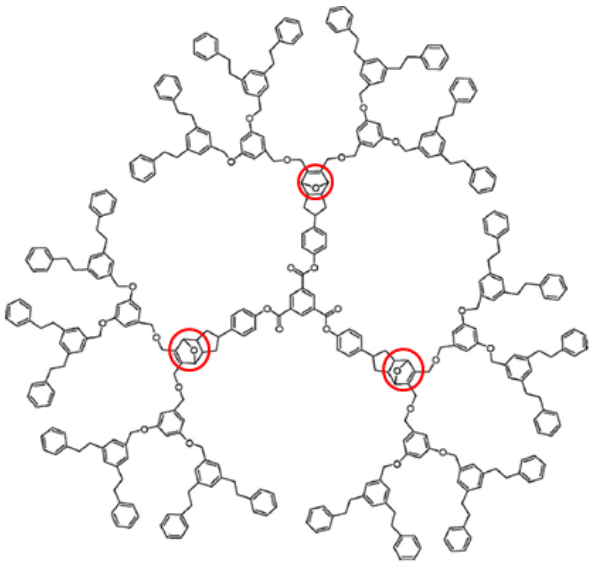

Figure 1.22. A furan AB2 monomer with aromatic ether moieties at C3 and C4 in conjunction with a maleimide bearing a reactive phenolic moiety [41].

These products were heated at 110 °C in DMF in an NMR tube. As a result, the DA-RDA equilibrium was reached within an hour to give 40% dissociation of the adduct sites and when cooling is achieved to 65 °C the dendrimers were fully reconstituted [41].

Besides the furan-maleimide DA reaction, anthracene-maleimide DA reaction is also another example which thermally more stable than the furan-maleimide Diels-Alder cycloadduct and the thermal stability also results in a higher rate of the cycloaddition. For this reason, anthracene-maleimide DA reaction is also more often used in click reactions. It has simple reaction conditions, high yield, and high selectivity that make the reaction valuable in polymer synthesis.

As an example of dendronized polymers via Diels-Alder "Click" reaction, Sanyal and co-workers utilized a styrene- based polymer appended with anthracene groups as reactive side chains. One to three generations of polyester dendrons containing furan-protected maleimide groups at their focal point were synthesized. Then, reagent-free, thermal Diels–Alder cycloaddition reaction between the anthracene-containing polymer and reactive dendrons resulted in functionalization of the polymer chains to obtain dendronized polymers [46].

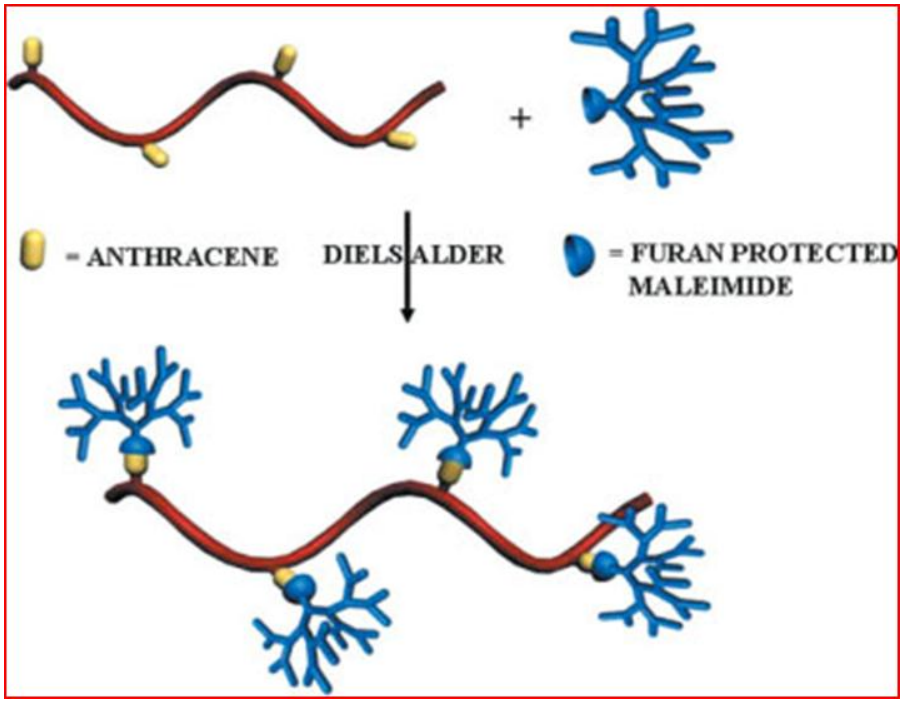

Figure 1.23. Dendronization of polymer via Diels–Alder reaction [46].

They also synthesized diblock and triblock dendron–polymer conjugates containing biodegradable polyester dendron blocks and polyethylene glycol (PEG) polymer using the Diels–Alder "click" cycloaddition reaction. First, they prepared biodegradable polyester dendrons containing an electron-rich anthracene group at their focal point and hydroxyl groups at their periphery. Then, these dendrons were reacted with either mono-functional or telechelic linear PEG polymers containing furan-protected maleimide group at chain ends to get diblock and triblock copolymers, respectively. At the end, reagent-free thermal Diels-Alder cycloaddition reaction gives linear-PEG polymers containing several hydroxyl functional groups at chain ends for further functionalization [47] (Figure 1.24.).

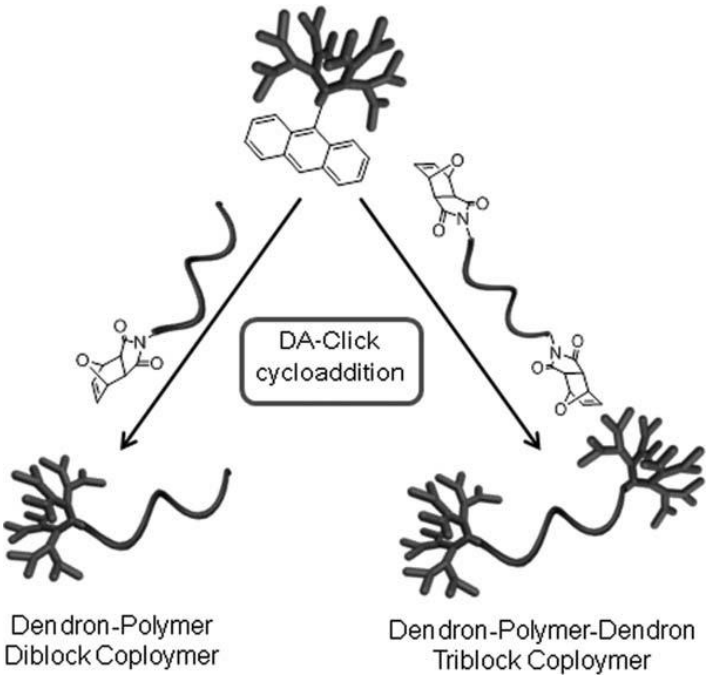

Figure 1.24. Synthesis of dendron–polymer block copolymers via the Diels–Alder "click" reaction [47].

2. AIM OF THE STUDY

The use of micellar structures has been one of the popular methods for the solubilization of hydrophobic drugs in cancer therapy. In this work, micellar structures based on dendron-polymer conjugates which one of the blocks is a hydrophobic dendron and the second block is a hydrophilic multiarm polymer have been prepared to obtain stable drug delivery.

Diblock dendron–polymer conjugates containing biodegradable polyester acetal dendron blocks and biodegradable poly di(ethylene glycol) methyl ether methacrylate p(DEGMEMA) polymer were synthesized using the Diels–Alder “click” cycloaddition reaction. p(DEGMEMA) polymers with furan-protected maleimide functionality were synthesized and reacted with biodegradable polyester acetal dendrons containing an anthracene moiety at their focal point. On this study, we want to examine the effects of macromolecular architecture on the self-assembly of micellar structures, i.e. how does the size and stability of micelles change upon transition from linear to branched structures.

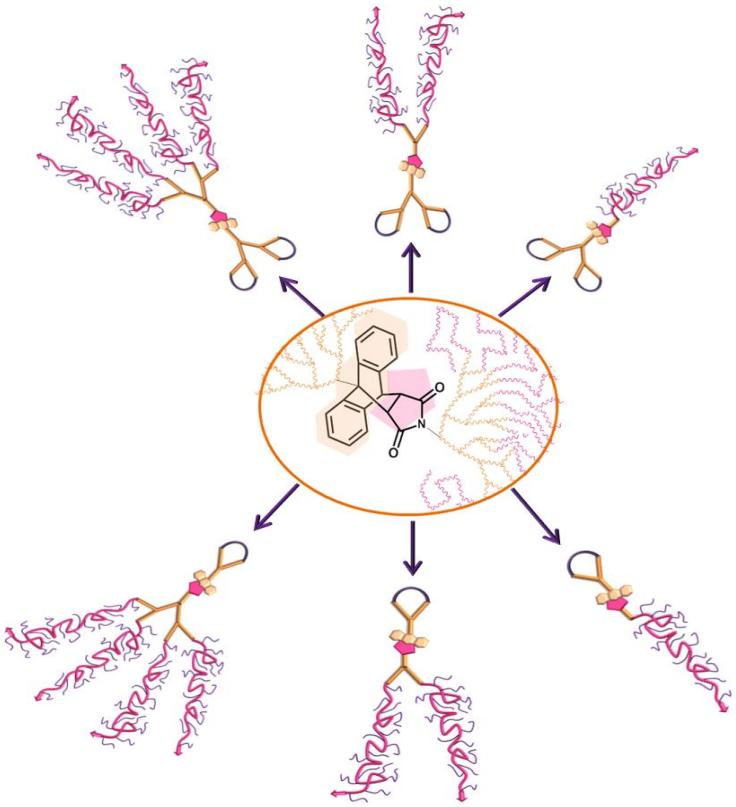

Figure 2.1. General scheme of dendritic macromolecule.

3. RESULTS AND DISCUSSION

3.1. Synthesis of the Building Blocks

In order to synthesize dendron-polymer conjugates, dendron and polymer blocks were synthesized separately. The first block is the hydrophobic biodegradable polyester acetal dendron of G1 and G2 generations containing an anthracene moiety at their focal point. The second block of p(DEGMEMA) polymers containing furan-protected maleimide functionality was synthesized via ATRP. At the end, these two blocks are conjugated with the help of Diels-Alder "click" cycloaddition reaction (Figure 3.1).

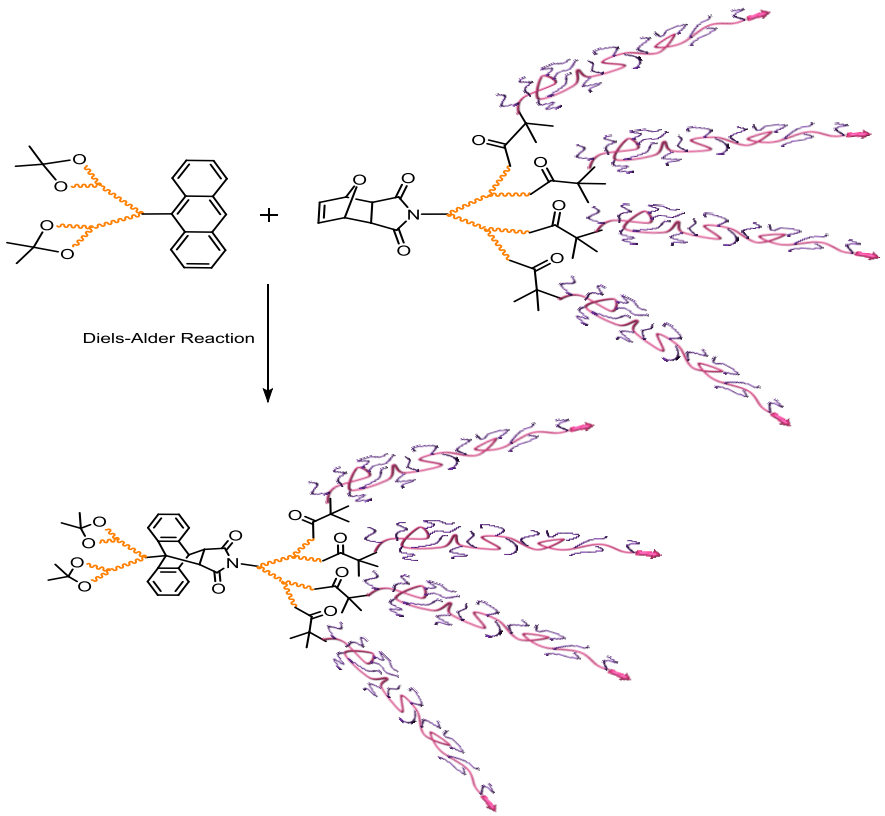

Figure 3.1. General scheme of dendron-polymer synthesis via Diels-Alder "Click" cycloaddition reaction.

3.1.1. Synthesis of Dendrons

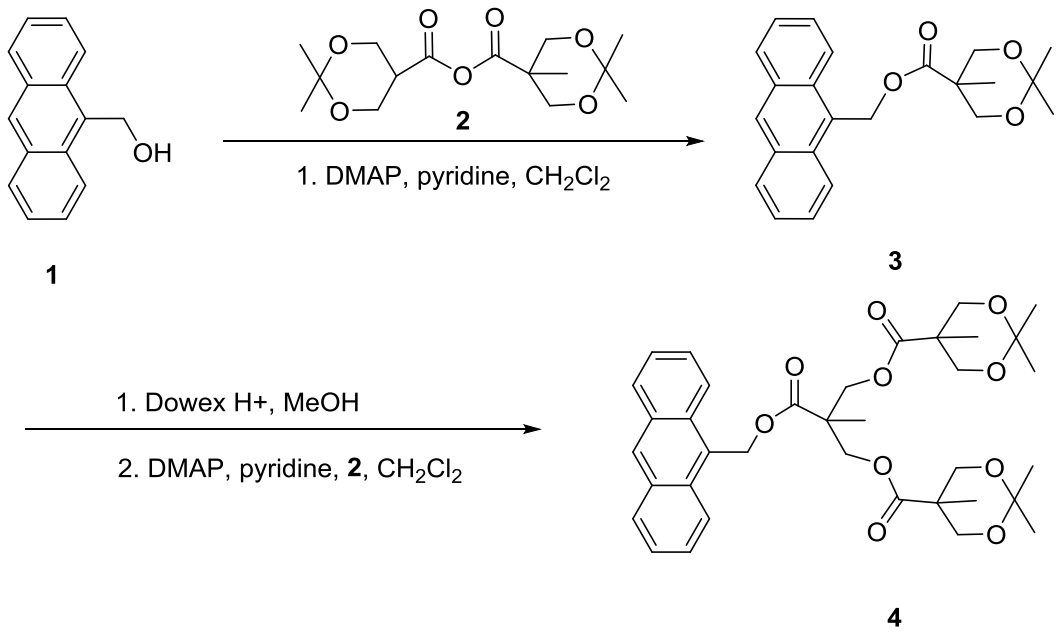

Figure 3.2. General scheme of anthracene functionalized G1-acetal dendron **3** and G2-acetal dendron **4** synthesis.

For the hydrophobic block of the dendron-polymer conjugate, polyester acetal dendrons 3 and 4 which contain anthracene at their focal points were synthesized according to literature [47]. Dendrons are synthesized by the divergent method which means that the growth of the repeating units of the dendron starts from the anthracene core towards the periphery. Reaction of anhydride **2** with 9-anthracene methanol yields formation of G1 acetal dendron bearing anthracene group at its core. The acetonide groups of this G1 acetal dendron is deprotected via treatment with DOWEX, H^+ which yields free alcohol groups to continue the synthesis of 2nd generation acetal dendron in the same manner (Figure 3.2).

The proton spectra of dendrons 3 and 4 can be seen in Figure 3.3. For both dendrons, singlet at 8.51 ppm, doublets at 8.30 ppm and 8.03 ppm, doublet of doublets at 7.57 ppm and 7.49 ppm are specific peaks that belong to aryl protons of anthracene part. Dendron 4 could not be obtained with high purity so further optimization of purification conditions are needed.

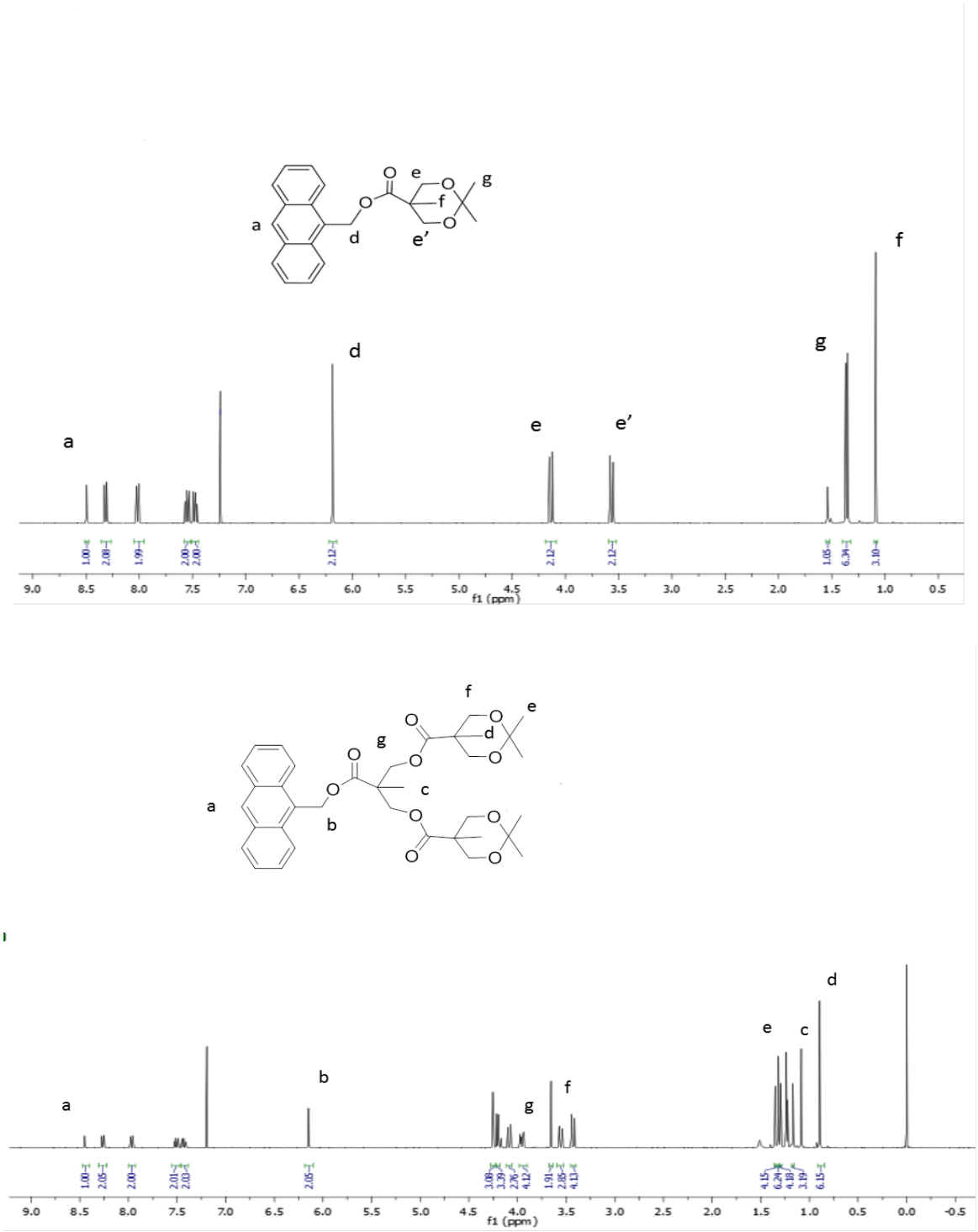

Figure 3.3. ^{1}H NMR of dendron **3** and dendron **4**.

3.1.2. Synthesis of Multiarm Star Polymers

The synthesis of multiarm star polymers bearing reactive maleimide core was synthesized via the Atom Transfer Radical Polymerization (ATRP) method.

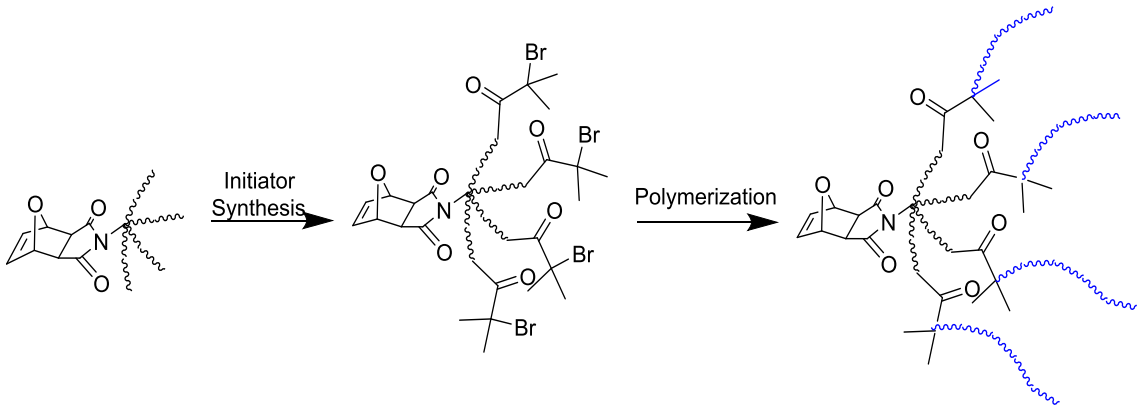

Figure 3.4. General scheme for the synthesis of multiarm star polymers.

For the polymerization, biodegradable polyester dendron with furan protected maleimide functionality at the core was chosen and two different generations of dendrons were synthesized according to the literature procedures [48]. The alcohol groups at the periphery of the dendrons were reacted with a brominated compound, because halogen groups are necessary to initiate the polymerizations.

Double bond of maleimide group can participate into the polymerization reactions, so it is protected by a furan moiety to prevent the reaction from side products. Acetal protected polyester dendrons 7 and 9 were prepared using a divergent growth strategy starting with a furan protected N-hydroxy propyl maleimide. Also, a linear initiator 6 was synthesized from furan protected N-hydroxy propyl maleimide 5. The acetal protecting groups at the periphery of these dendrons were removed via the acidic resin DOWEX 50W-X2. Then, the hydroxyl groups at the periphery of the dendrons were esterified by 2-bromoisobutyryl bromide in the presence of triethylamine to produce the multiarm initiators 8 and 10 (Figure 3.5).

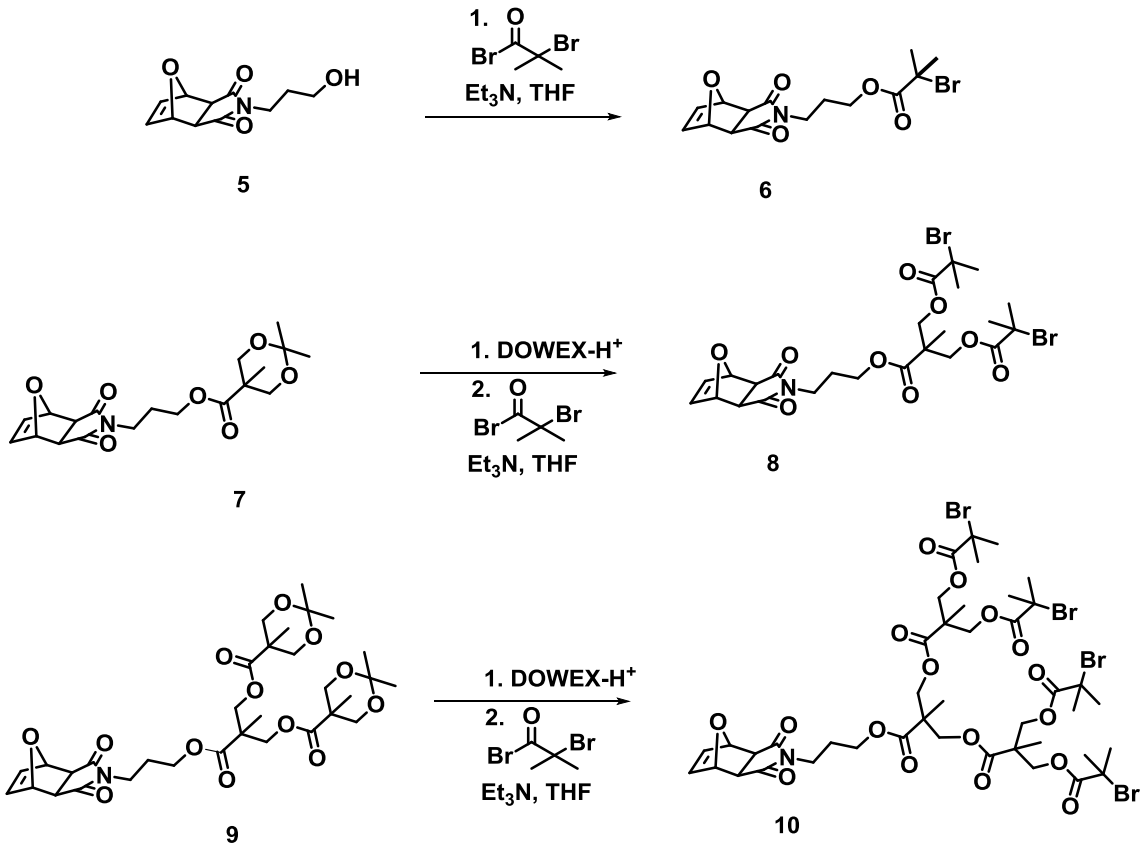

Figure 3.5. General scheme for the synthesis of furan-protected maleimide containing initiators.

After column chromatography, the dendritic multiarm initiators were obtained in pure form. Then, all dendritic initiators were characterized with ^{1}H NMR. For instance, the presence of the bicyclic unit which is furan protected maleimide unit was clear from the proton resonances at 2.83, 5.25 and 6.5 ppm for linear, G1 and G2-maleimide based initiators **6, 8, 10** (Figures 3.5, 6 and 7, respectively).

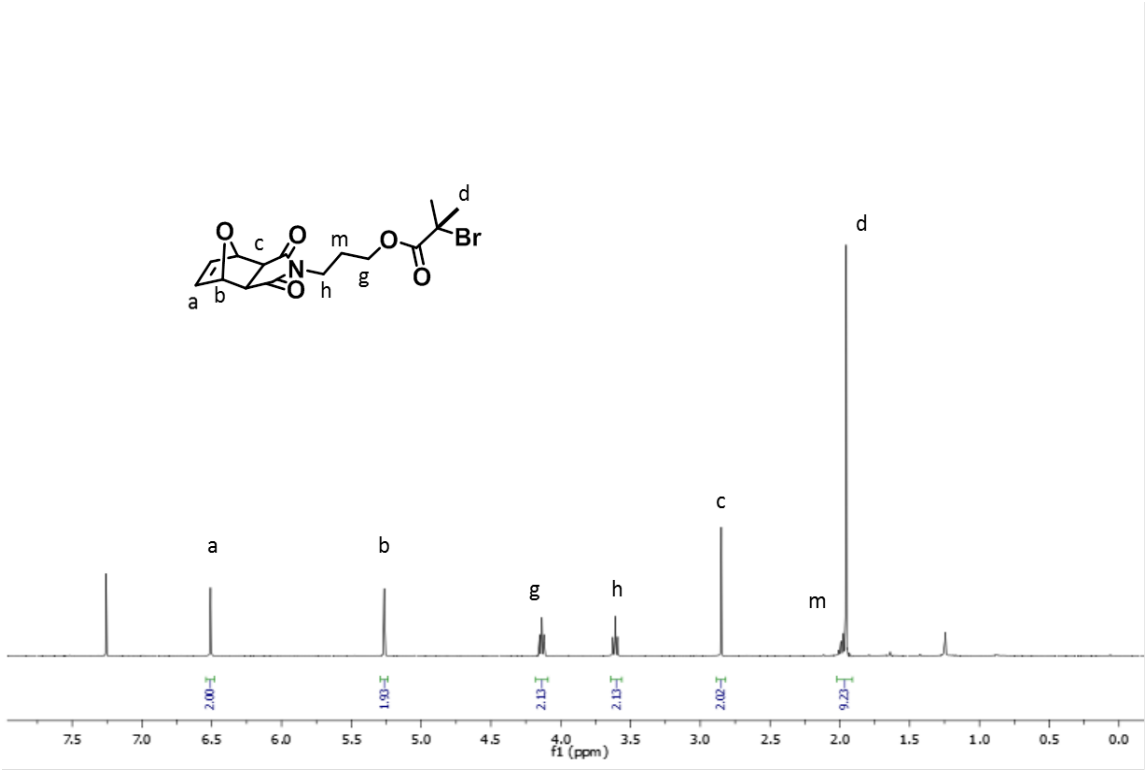

Figure 3.6. ^{1}H NMR spectra of Linear Maleimide Based Initiator (6).

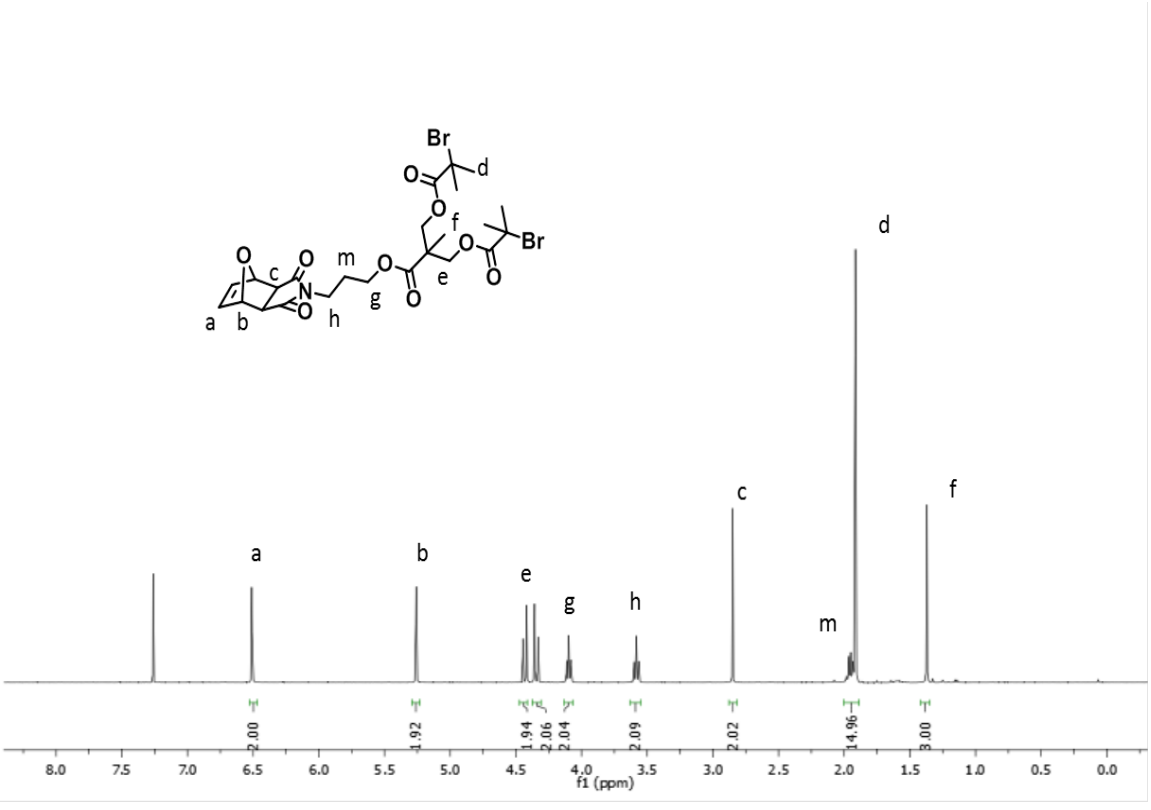

Figure 3.7. ^{1}H NMR spectra of G1-Maleimide Based Initiator (8).

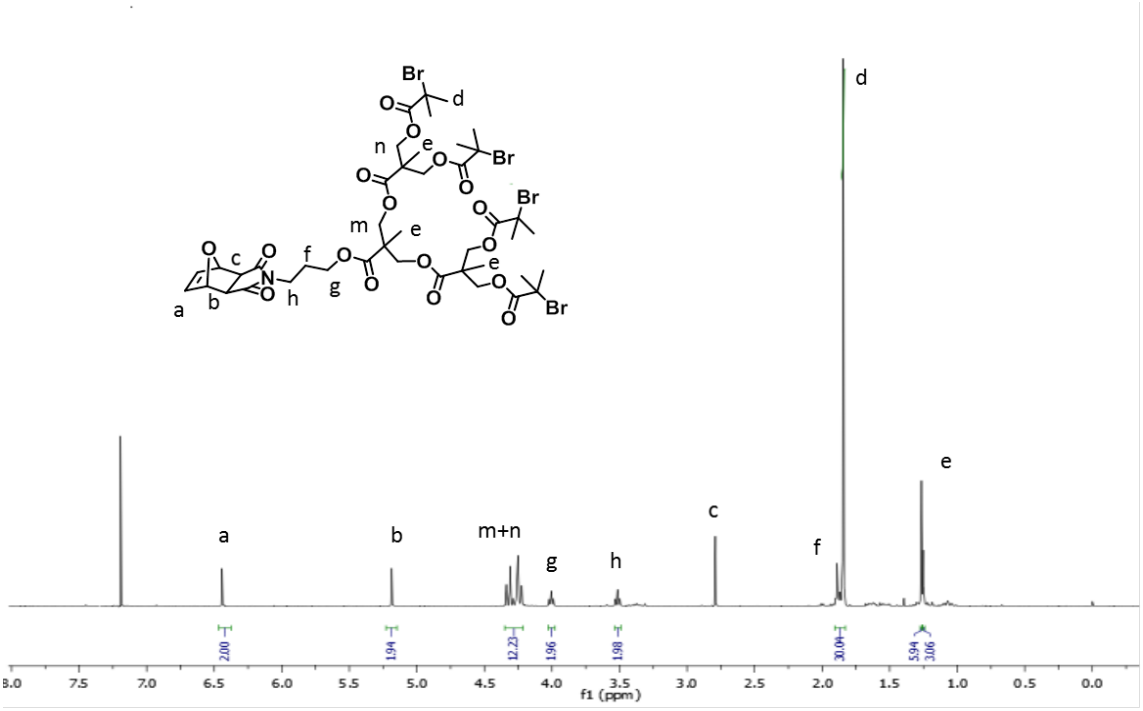

Figure 3.8. ^{1}H NMR spectra of G2-Maleimide Based Initiator **(**10**)**.

It is important to obtain polymers with narrow polydispersities for biological applications. So, in this study, Atom Transfer Radical Polymerization (ATRP) is chosen to obtain desired polymers with good control over their molecular weight distributions. ATRP is initiated by an alkyl halide (R-X) and catalyzed by a transition metal complex. In our case, dendritic initiators were used with CuBr/PMDETA complex which is the catalyst system. Especially, reaction time and solvent ratio were arranged to have polymers with narrow polydispersities.

These polymeric structures are candidates for drug delivery, bioconjugation, etc. and they should have higher water solubility. In this study, water soluble multiarm star polymers with a reactive maleimide core were obtained by using diethylene glycol methylether methacrylate (DEGMEMA) as the monomer. Polymers with low polydispersity and good conversions were obtained at 40°C.

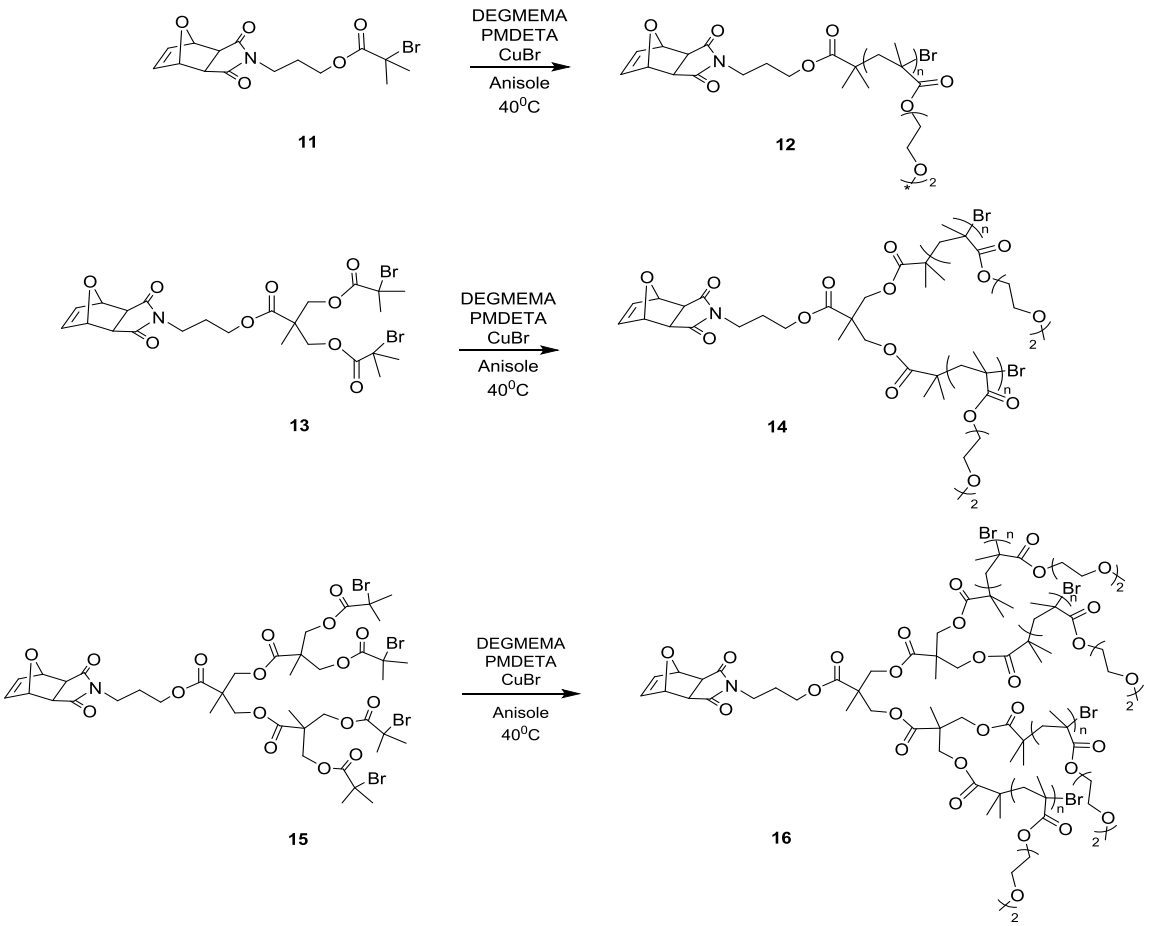

Figure 3.9. Synthesis of furan-protected maleimide-containing linear and multiarm star polymers.

All synthesized polymers were characterized with gel permeation chromatography (GPC). The polymerization conditions are given in Table 3.1.

Table 3.1. Synthesis and Characterization of Linear and Multiarm Star Polymers.

Entry	**Polymer**	**$[M]_0/[I]_0$**	**[I]**	**Time (min)**	**Temp. (^oC)**	**Yield[b] (%)**	**Mn (GPC[a]) (Da)**	**Mw/Mn (GPC)**	**$M_{n,\ theo}$ (Da)**	**$M_{n,\ NMR}$**
12	Linear p(DEGMEMA)	100	**Linear**	120	40	44	14200	1.26	19172	17500
14	G1-p(DEGMEMA)	200	**G1**	120	40	61	16400	1.40	38245	30700
16	G2-p(DEGMEMA)	400	**G2**	120	40	30	14000	1.27	76367	36200

[a] Calibration with linear PS in THF

[b] Determined gravimetrically via dialysis in methanol

After purification of all synthesized polymers, they were characterized with ^{1}H NMR. The presence of the bicyclic unit which is furan protected maleimide unit was clear from the proton resonances at 2.83, 5.25 and 6.5 ppm for linear, G1 and G2-maleimide based polymers 12, 14, 16. Also, singlet at around 3.31 ppm belongs to OCH_3 protons of DEGMEMA units for all synthesized polymers (Figures 3.10, 11 and 12 respectively).

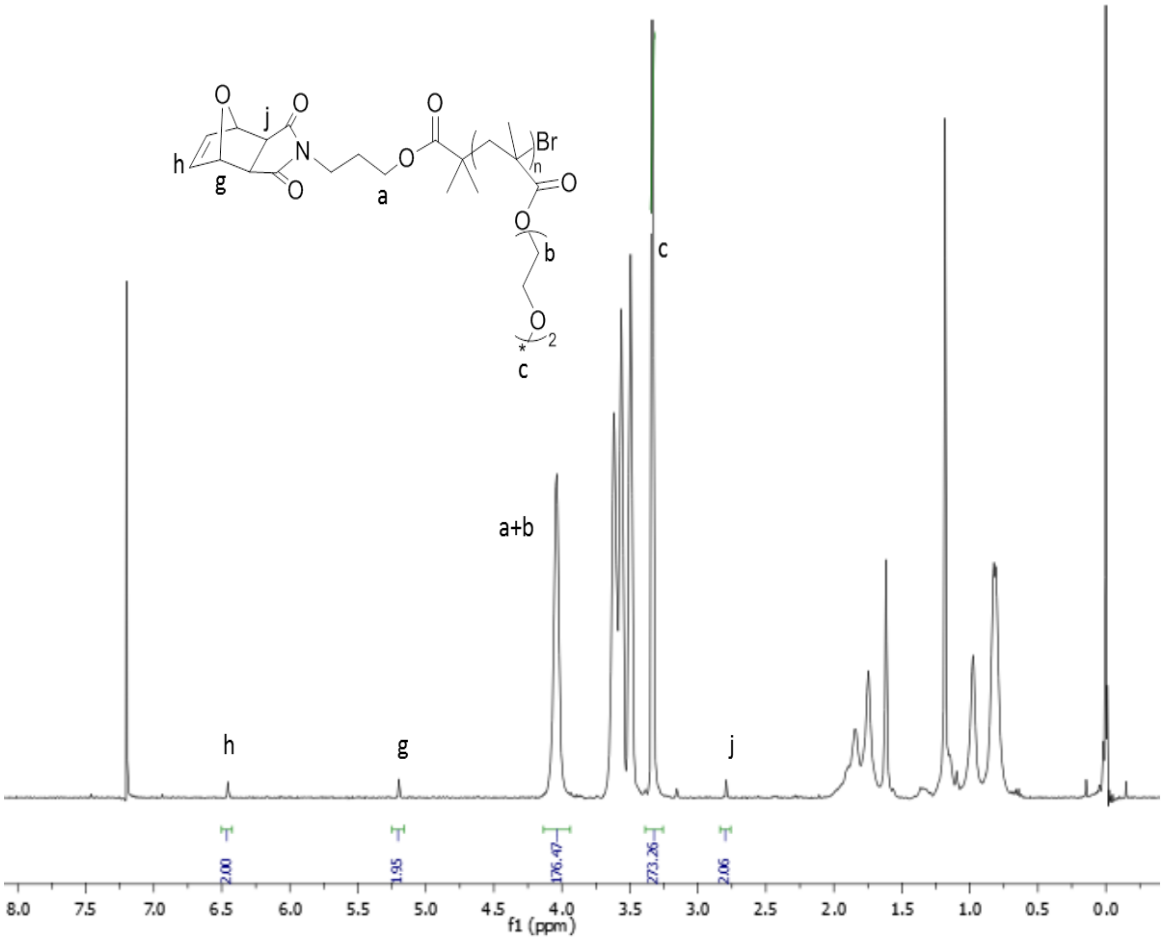

Figure 3.10. ^{1}H NMR spectra of Linear Maleimide Based Polymer (12).

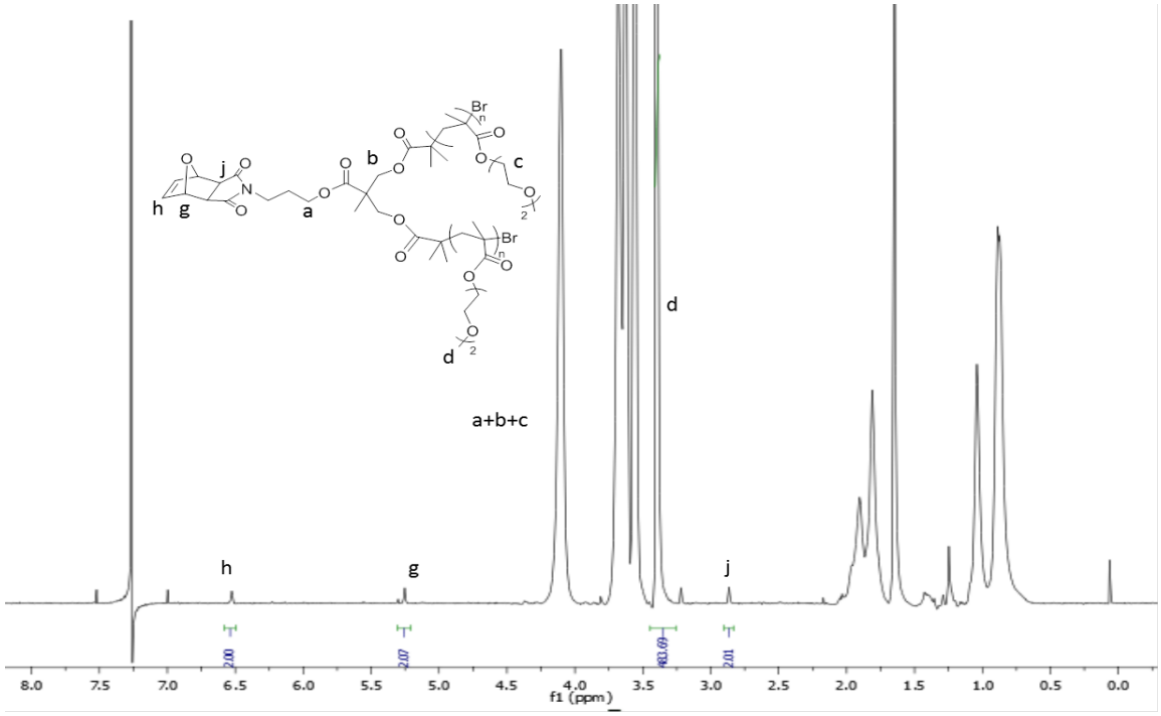

Figure 3.11. ^{1}H NMR spectra of G1-Maleimide Based Polymer (14).

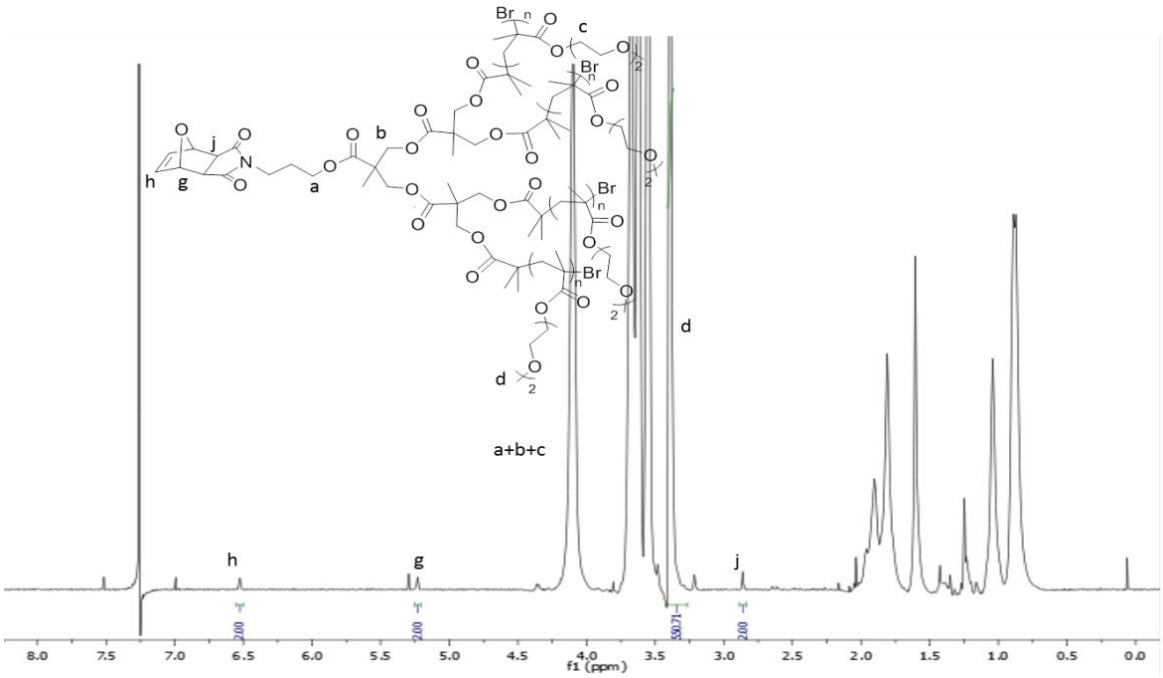

Figure 3.12. ^{1}H NMR spectra of G3-Maleimide Based Polymer (16).

3.2. Synthesis of Dendron-Polymer Conjugates

The obtained polymers with furan-protected maleimide functionality were utilized for further conjugation to first and second generation acetal-protected dendron bearing the anthracene group at its core. For the conjugation of these building blocks, Diels-Alder "Click" cycloaddition reaction was used. Dendron-polymer conjugate was obtained via the reaction between anthracene part of the acetal dendron and reactive maleimide part of the polymer in dimethylformamide (DMF) at 110°C.

Throughout the reaction, at that temperature, unmasking of the maleimide group at the polymer chain end is obtained by the removal of furan via the retro Diels–Alder cycloreversion. Then, the "in situ-generated" maleimide moiety reacts with the anthracene group on the acetal dendron (Figure 3.13).

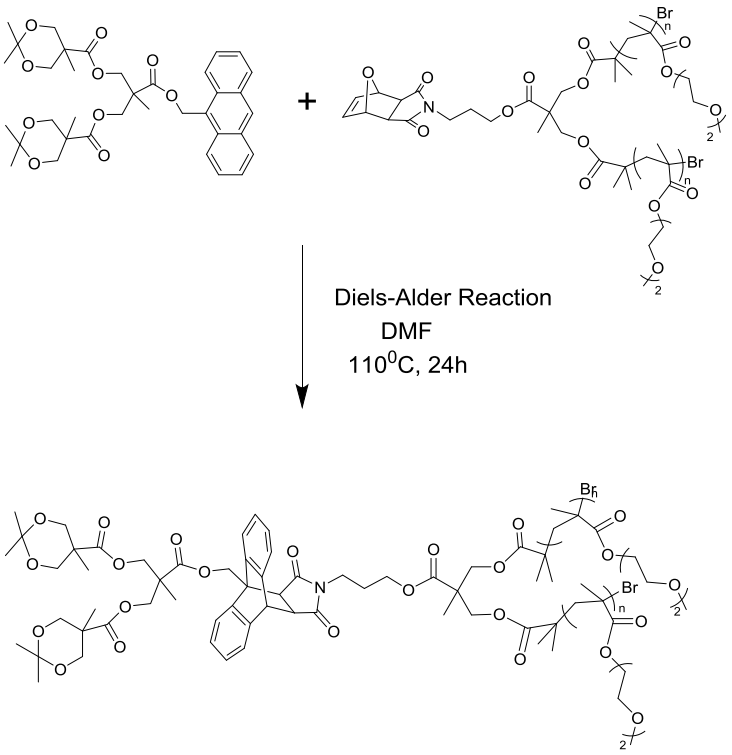

Figure 3.13. Dendron-polymer conjugate via Diels-Alder cycloaddition reaction.

Synthesized dendron-polymer conjugates were purified in methanol by dialysis membrane with 1000 molecular-weight cutoffs (MWCO). This is a separation technique that facilitates the removal or exchange of small molecules from macromolecules in some solvents on the basis of diffusion. After purification, these conjugates were characterized using ^{1}H NMR spectrum.

"Click" reaction produces a cycloadduct where new aromatic protons owing to the anthracene unit can be seen between 7.5 and 7.0 ppm, whereas the bridgehead proton appears at 4.7 ppm (s, 1H, and CH bridgehead proton) and the protons on the methylene unit adjacent to the parent anthracene ring appears around 5.5–5.3 ppm (m, 2H) (Figures 3.14, 15, 16, 17, 18 and 19, peak f). In the Diels–Alder reaction between the p(DEGMEMA) polymers and the acetal dendrons, the disappearance of peaks at 6.48 and 5.23 ppm belonging to bicyclic furan–maleimide cycloadduct at the p(DEGMEMA) polymers is observed (Figures 3.14, 15, 16, 17, 18 and 19).

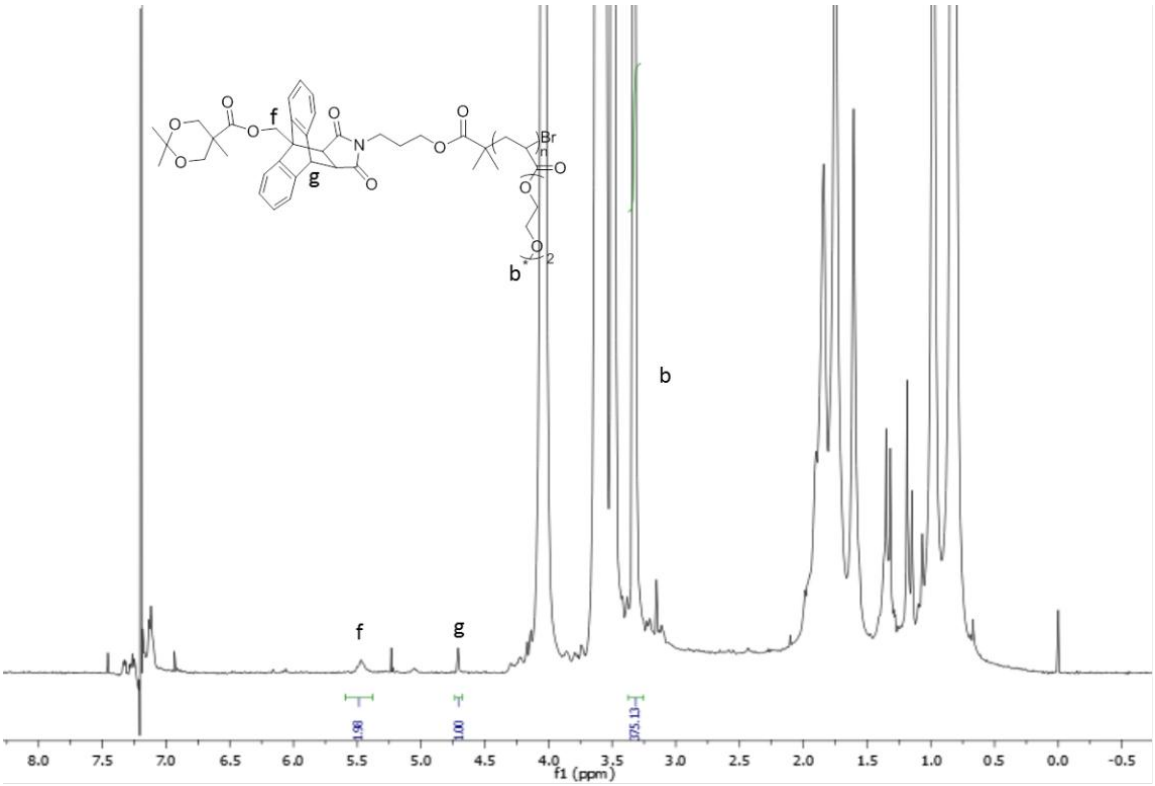

Figure 3.14. ^{1}H NMR spectrum of polymer-dendron conjugate (C1).

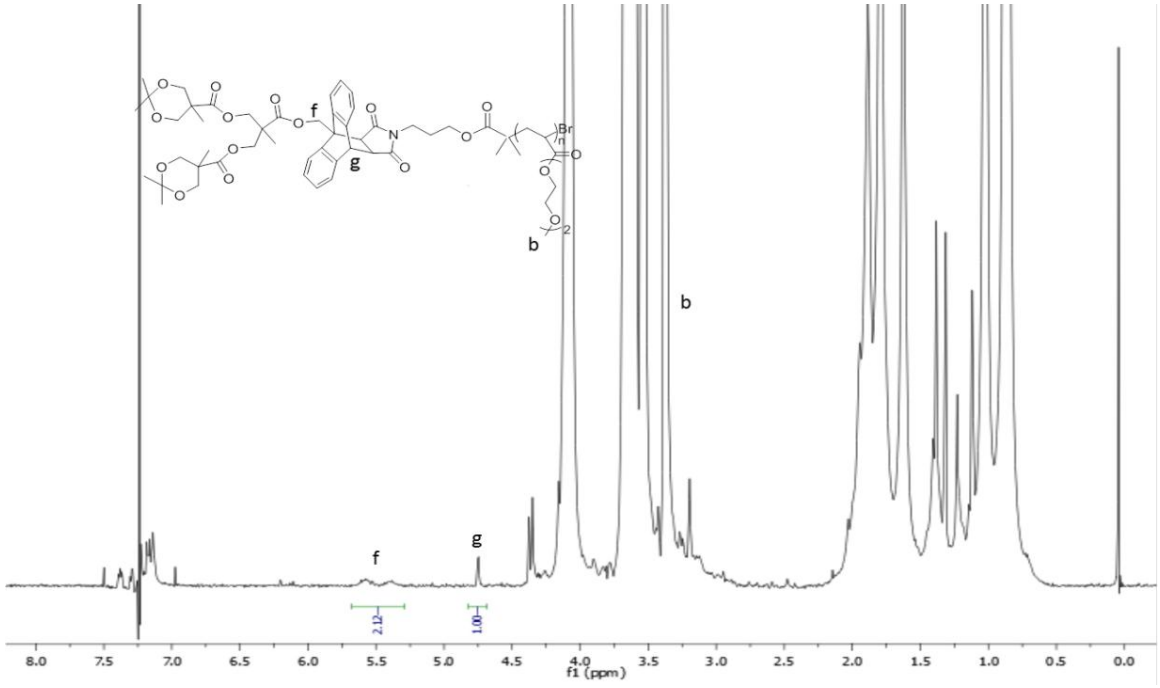

Figure 3.15. ^{1}H NMR spectrum of polymer-dendron conjugate (C2).

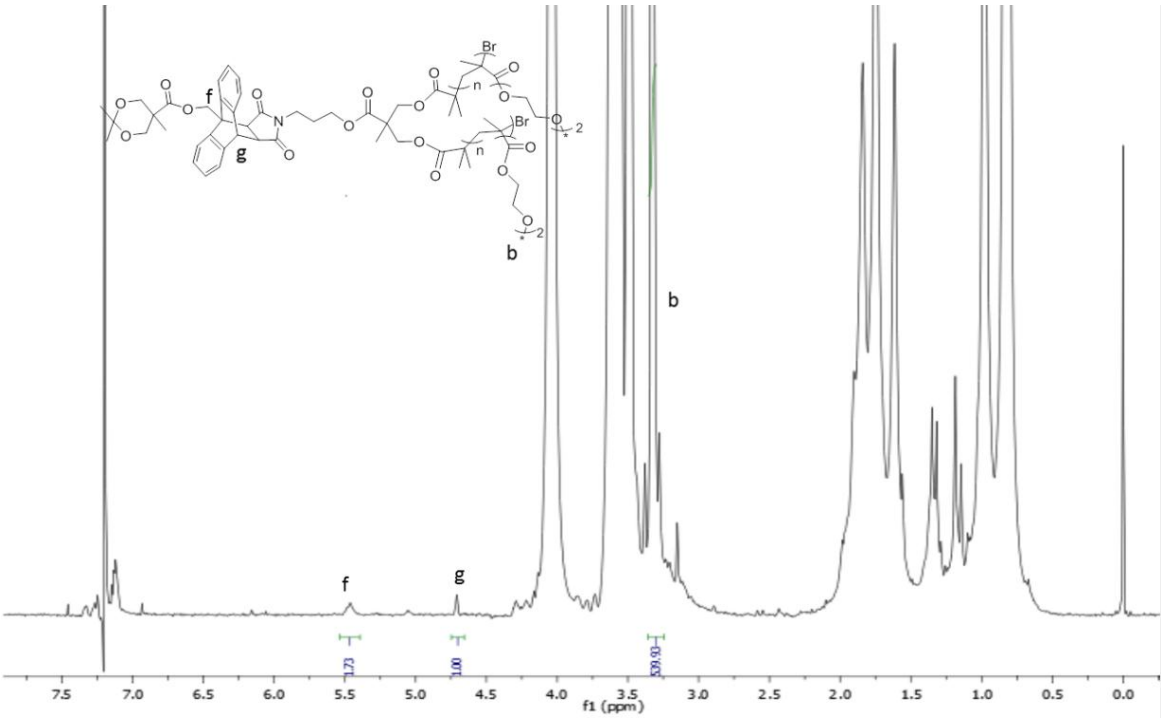

Figure 3.16. ^{1}H NMR spectrum of polymer-dendron conjugate (C3).

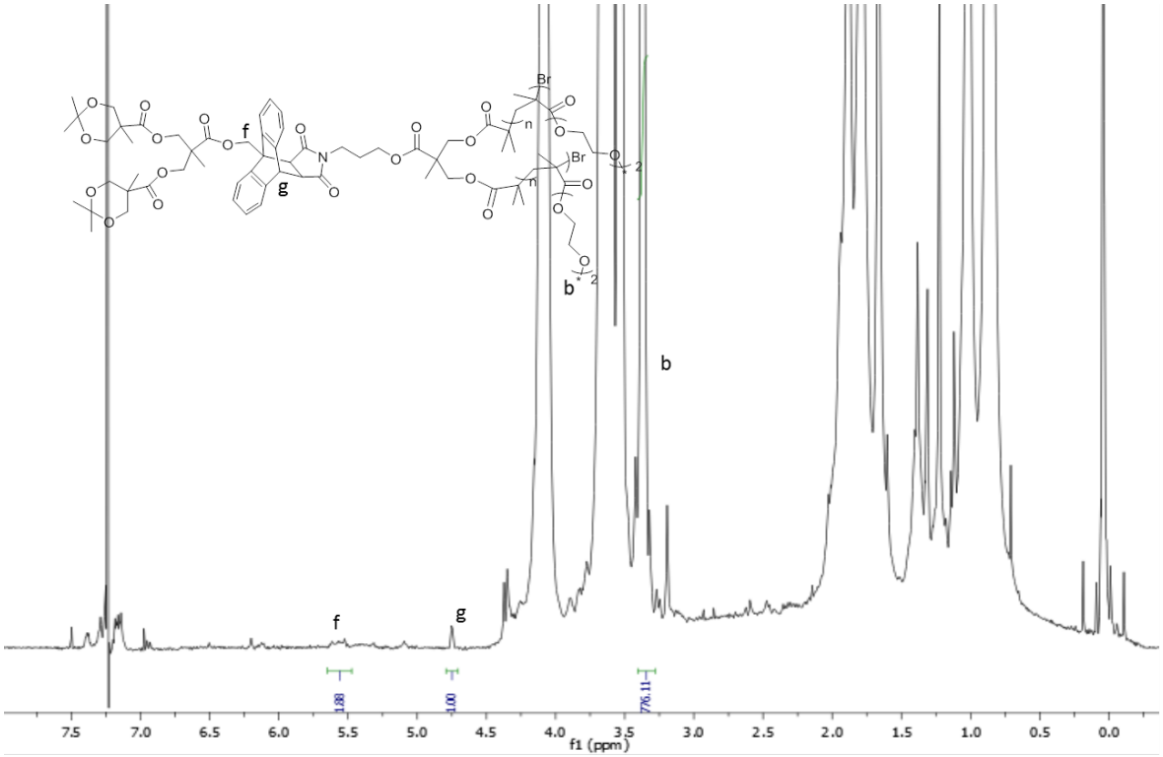

Figure 3.17. ^{1}H NMR spectrum of polymer-dendron conjugate (C4).

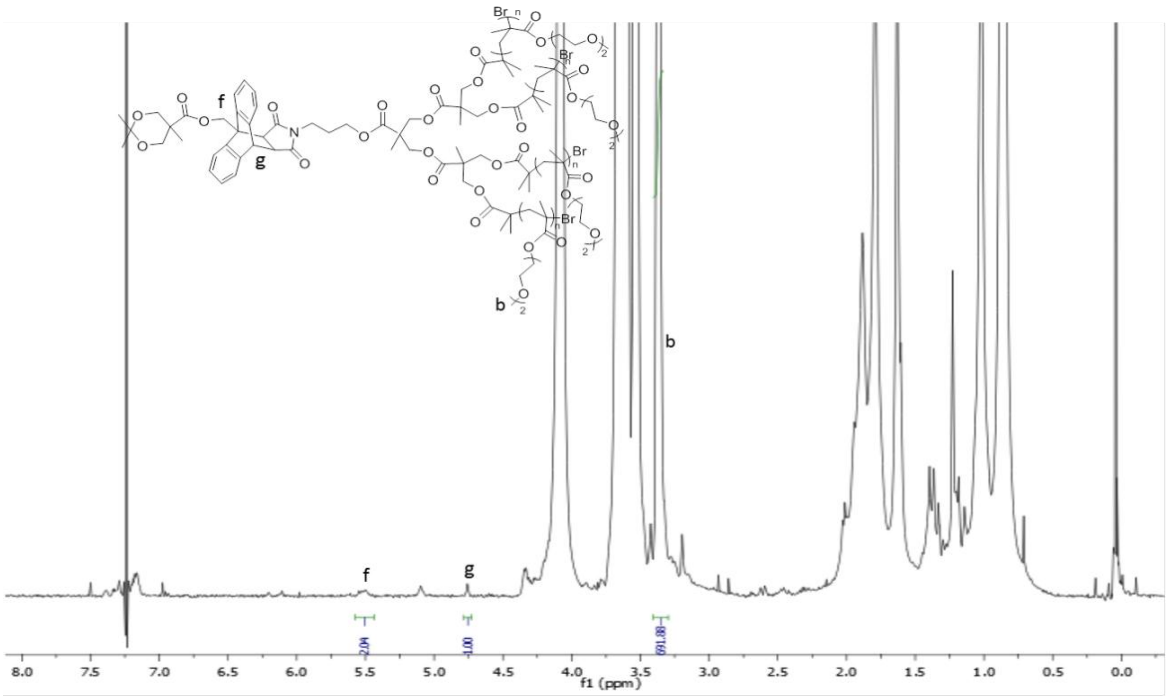

Figure 3.18. ^{1}H NMR spectrum of polymer-dendron conjugate (C5).

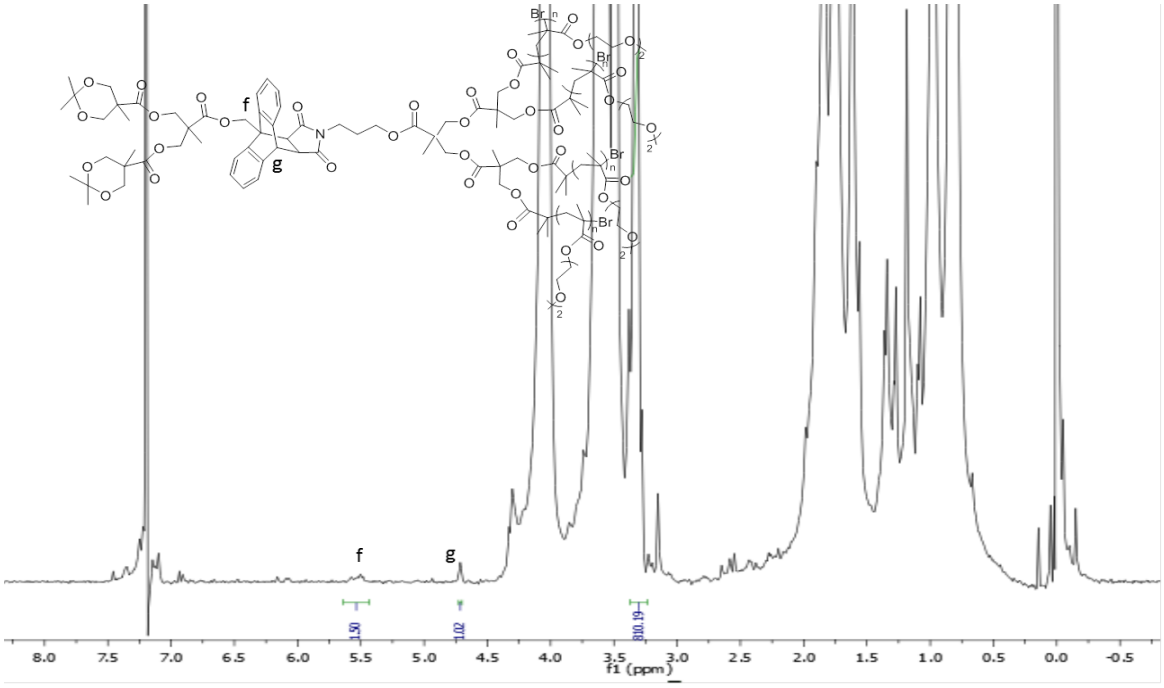

Figure 3.19. ^{1}H NMR spectrum of polymer-dendron conjugate (C6).

Also, Diels Alder reaction is monitored by Gel Permeation Chromatography (GPC) traces of dendron-polymer conjugates and their starting materials (Figure 3.20, 21, 22, 23, 24 and 25).

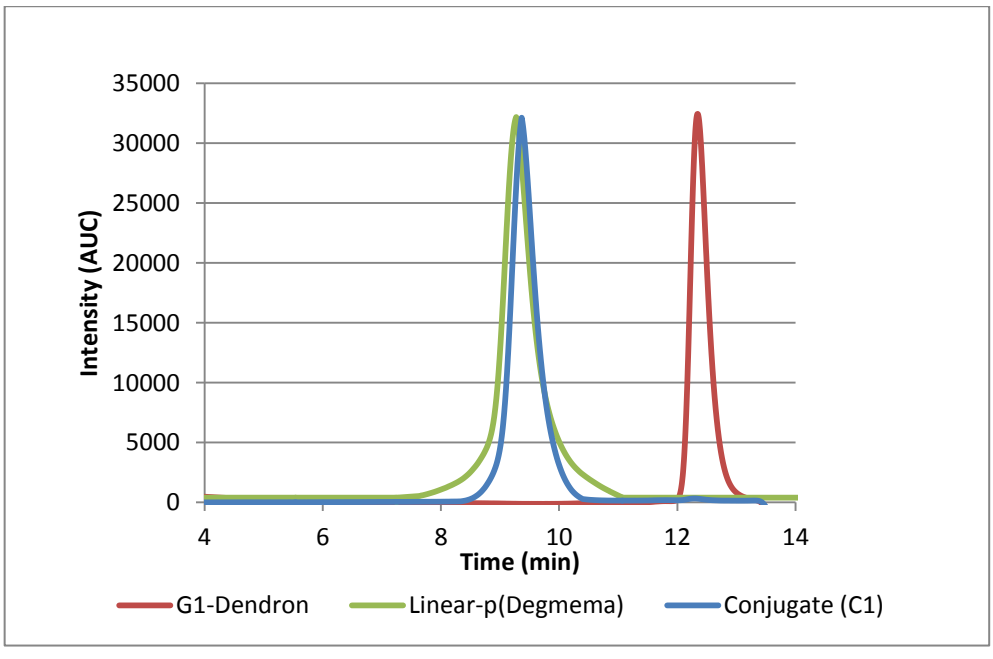

Figure 3.20. GPC traces of polymer 12, dendron 3 and dendron-polymer conjugate C1.

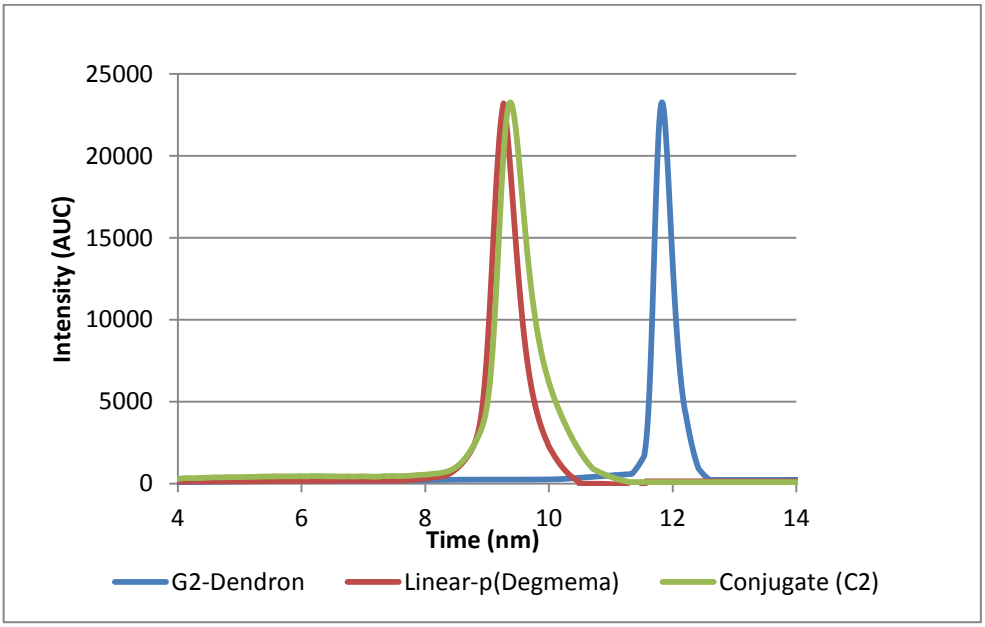

Figure 3.21. GPC traces of polymer 12, dendron 4 and dendron-polymer conjugate C2.

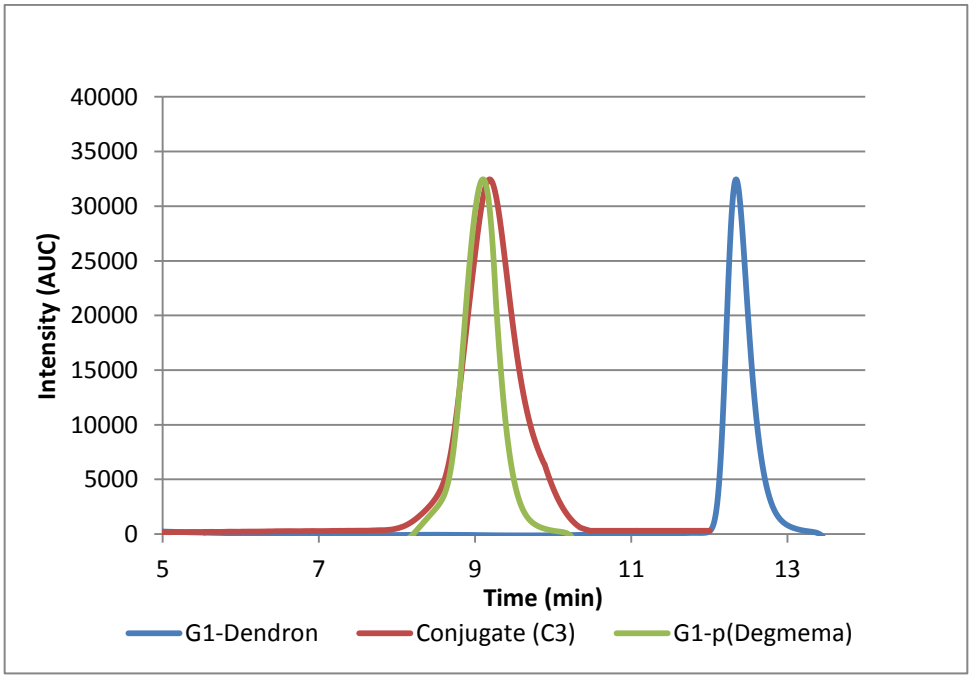

Figure 3.22. GPC traces of polymer 14, dendron 3 and dendron-polymer conjugate C3.

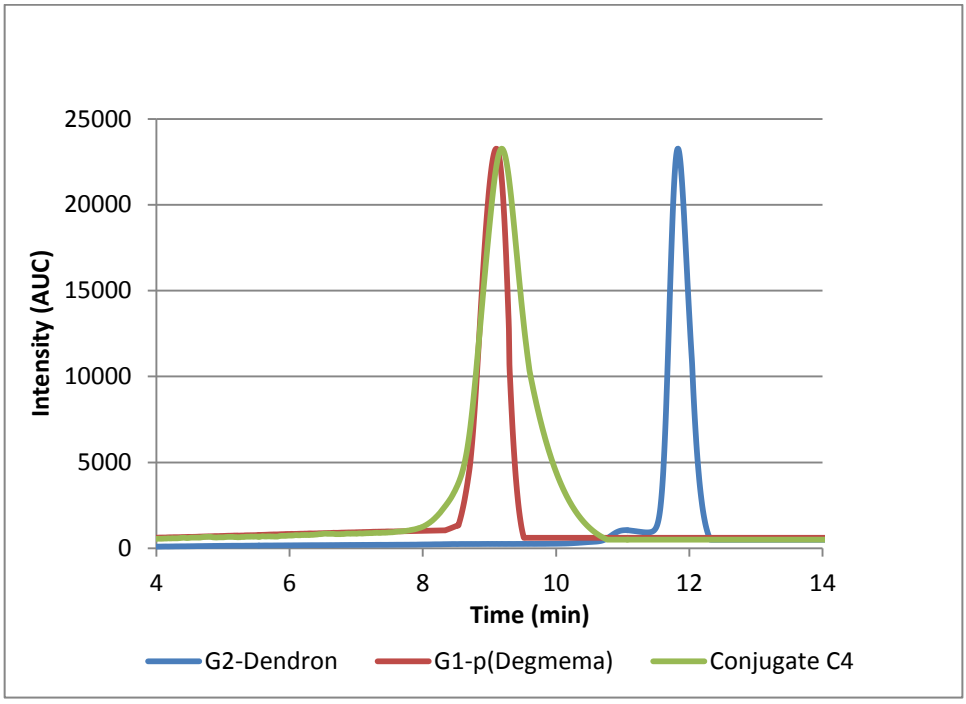

Figure 3.23. GPC traces of polymer 14, dendron 4 and dendron-polymer conjugate C4.

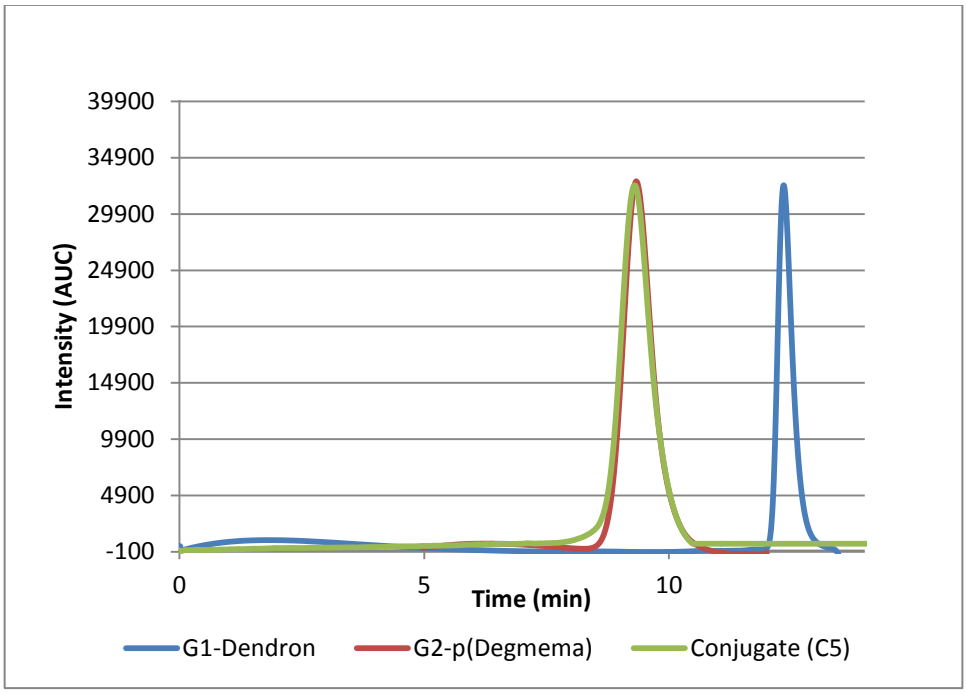

Figure 3.24. GPC traces of polymer 16, dendron 3and dendron-polymer conjugate C5.

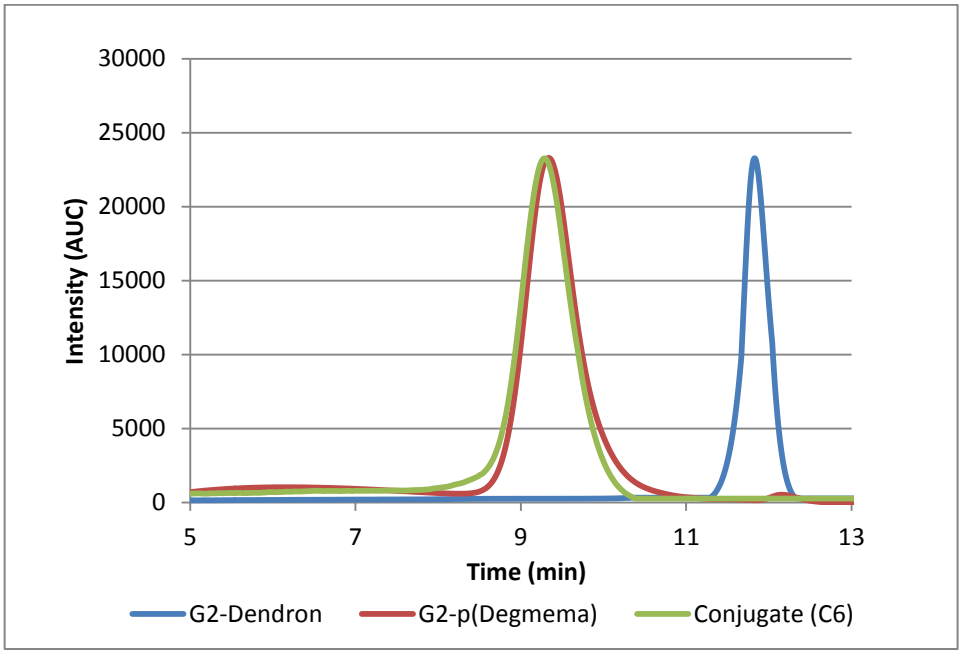

Figure 3.25. GPC traces of polymer 16, dendron 4 and dendron-polymer conjugate C6.

3.3. Micelle Formation from Polymer-Dendron Conjugate

In this study, polymer-dendron conjugates have amphiphilic character having both hydrophilic and hydrophobic groups in their structure. So, in aqueous media, dendron-polymer conjugates form micellar structures with the hydrophilic "tail" region which is p(DEGMEMA) polymers in contact with surrounding solvent, sequestering the hydrophobic "head" region which is acetal dendron part in the micelle core.

3.3.1. Critical Micelle Concentration (CMC)

Critical Micelle Concentration (CMC) is defined as the minimum concentration above which micelles form. At low surfactant concentration, the surfactant molecules become on the surface. As more surfactant is added, the surface tension of the solution starts to decrease, and after a while, more surfactant molecules will be on the surface.

When the surface becomes saturated, the addition of the surfactants will cause formation of micelles. This concentration point is called critical micelle concentration (Figure 3.26).

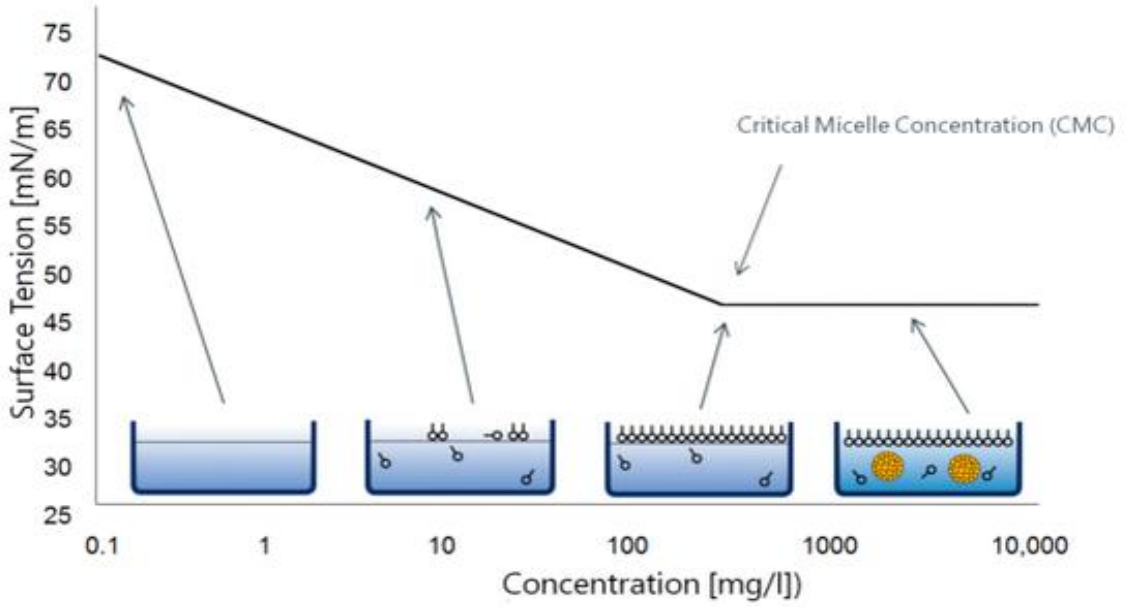

Figure 3.26. Formation of micelles at critical micelle concentration [49].

Before forming micelles, CMC of dendron-polymer conjugate solution should be calculated to determine the effective concentration to get micellar structures. Basically, the CMC value is an effective estimation of the stability of micelles in a thermodynamic manner. For determining the CMC value of the micelles, fluorescence spectrometry measurements were done via using pyrene, a hydrophobic dye. The fluorescence spectrum of pyrene shows characteristic range around 300–360 nm. Additionally, the maximum intensity of pyrene peak shifts to 338 nm from 334 nm which is in aqueous media after micelle formation occurs. Pyrene is located into the core of the micelle and it gives intensity about 338 nm in organic media, showing that pyrene absorption can be a convenient method for probing critical micellar concentration (Figure 3.27).

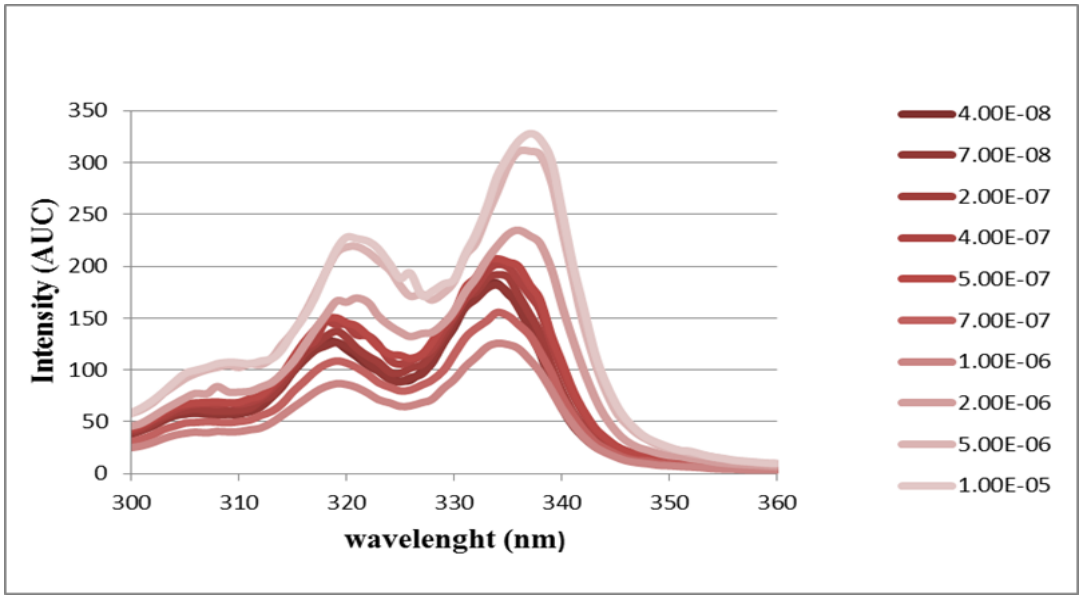

Figure 3.27. Excitation graph of pyrene loaded micelles formed from conjugate C1.

3.3.1.1. Critical Micelle Concentration (CMC) Measurements. After the synthesis of amphiphilic copolymers, preparation of micelles in aqueous media was achieved by self-assembly of the amphiphilic blocks at 25°C. CMC values of polymers and conjugates **12, 14, 16, C1, C2, C3, C4, C5** and **C6** were measured with fluorescence spectroscopy by utilizing the excitation characteristics of pyrene molecule. CMC values of dendron-polymer conjugates were close to each other although their hydrophobic and hydrophilic segments have multiarm character with different generations. Interestingly, polymers without dendron part are able to self-assemble at 25°C in aqueous media, and there is no significant change between the CMC values of polymers and conjugates (Table 3.2).

Table 3.2. CMC values of conjugates and polymers at 25°C.

Conjugates and Polymers	Value of CMC (M)
C1	$9.72x10^{-7}$
C2	$3.26x10^{-7}$
C3	$2.38x10^{-7}$
C4	$1.79x10^{-7}$
C5	$2.29x10^{-7}$
C6	$3.81x10^{-7}$
12	$2.18x10^{-7}$
14	$1.55x10^{-7}$
16	$2.60x10^{-7}$

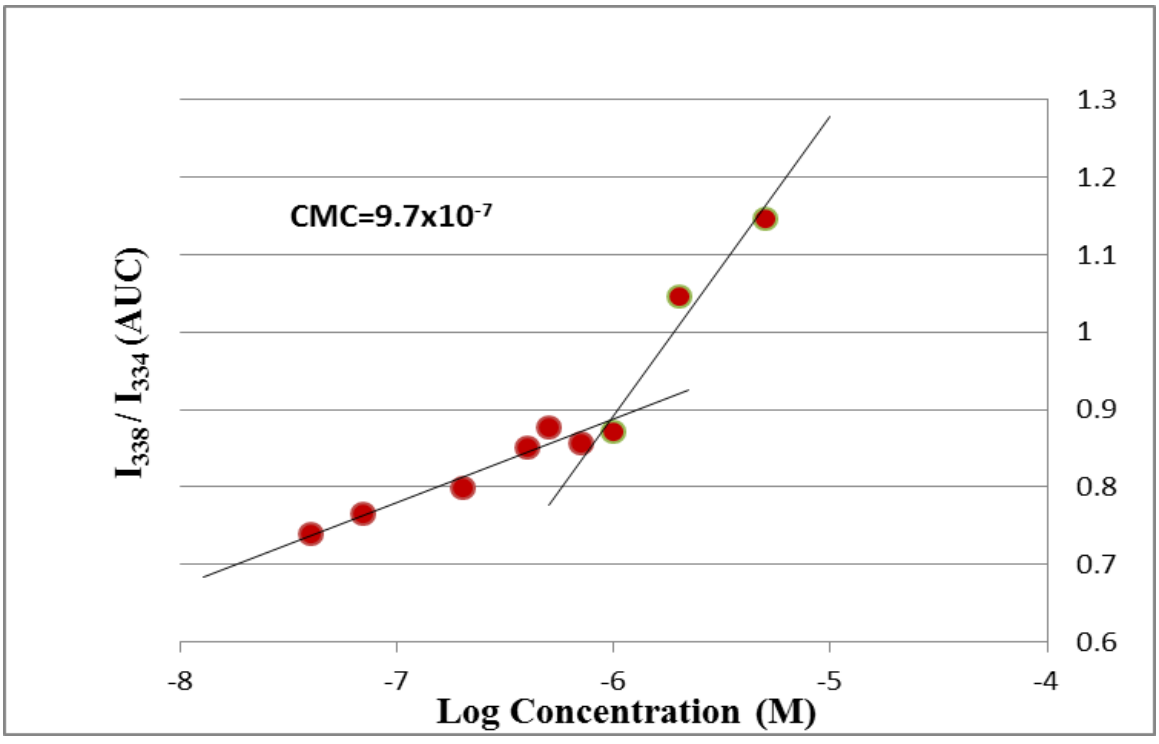

Figure 3.28. CMC graph of micelles formed from conjugate C1.

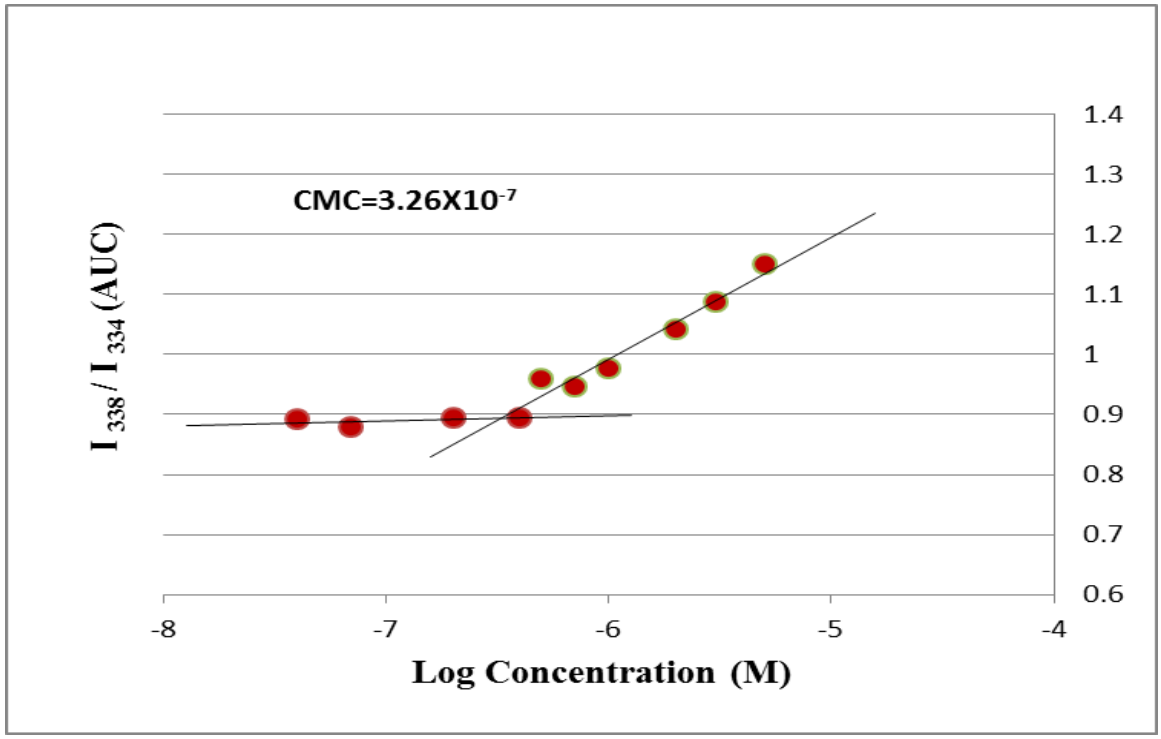

Figure 3.29. CMC graph of micelles formed from conjugate C2.

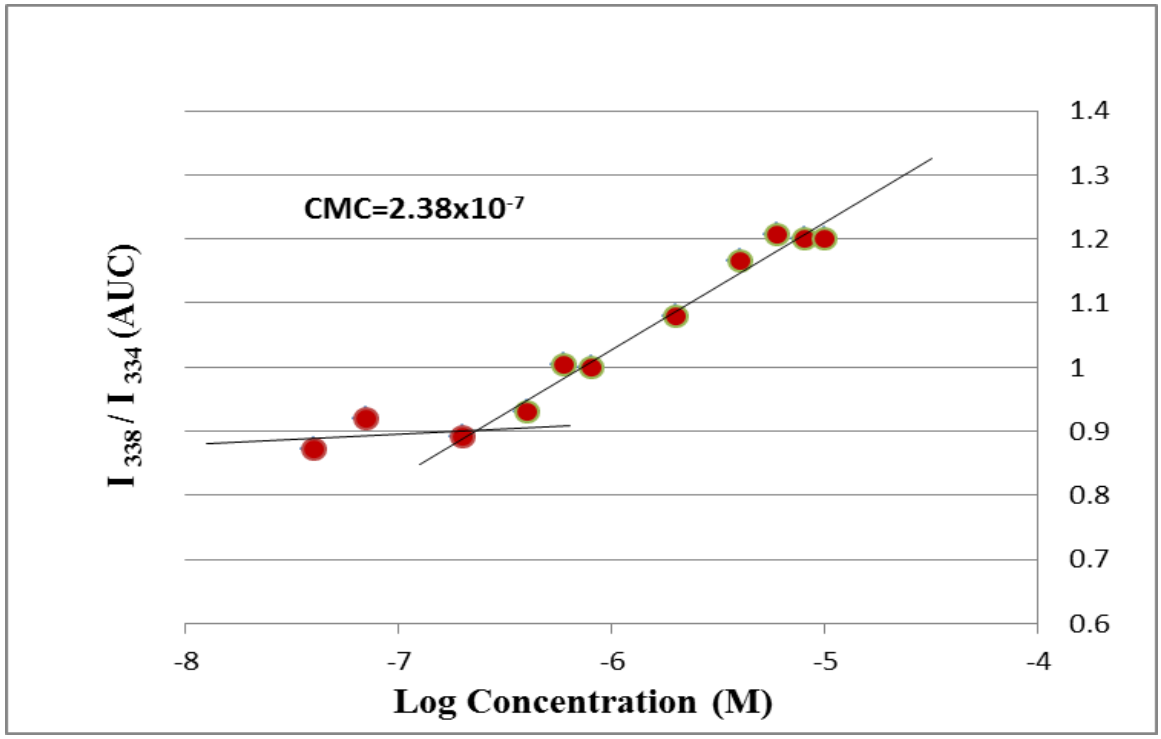

Figure 3.30. CMC graph of micelles formed from conjugate C3.

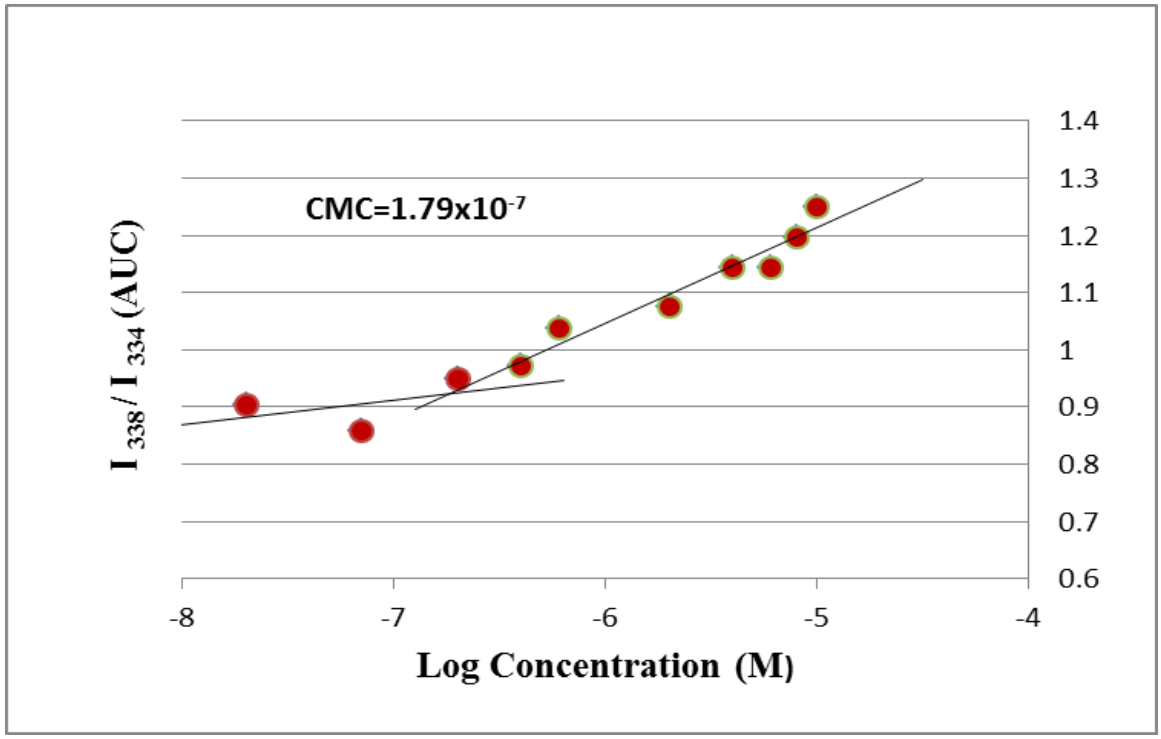

Figure 3.31. CMC graph of micelles formed from conjugate C4.

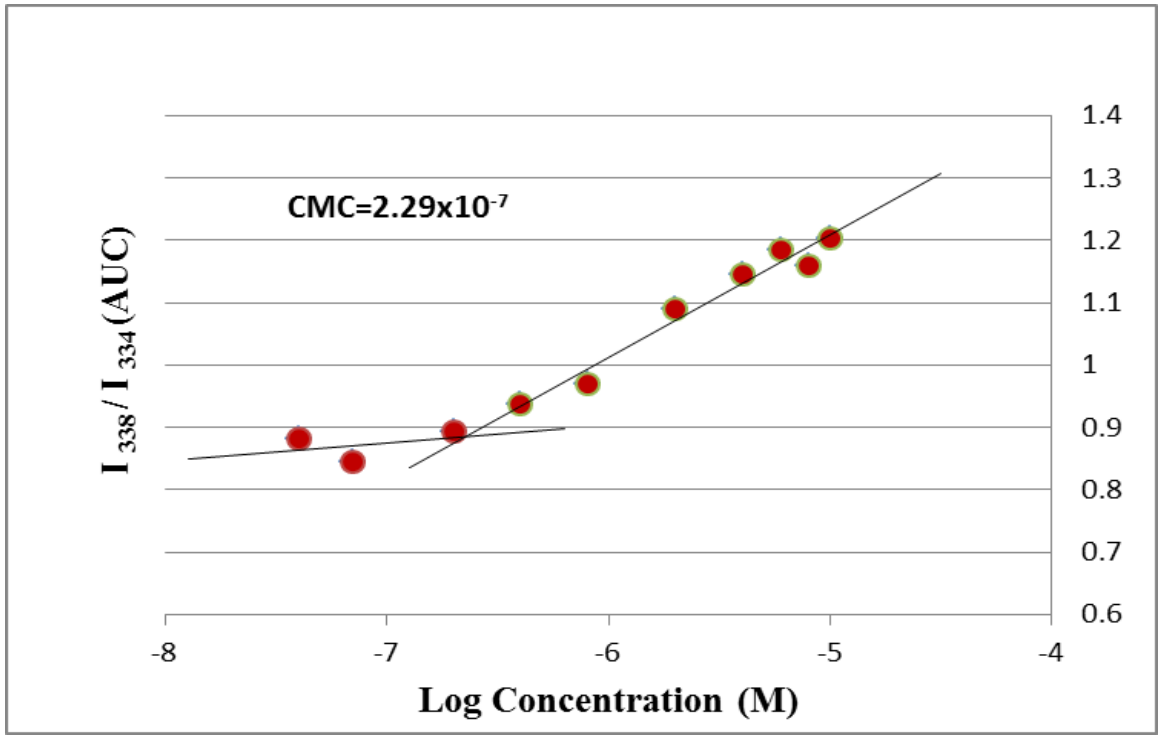

Figure 3.32. CMC graph of micelles formed from conjugate C5.

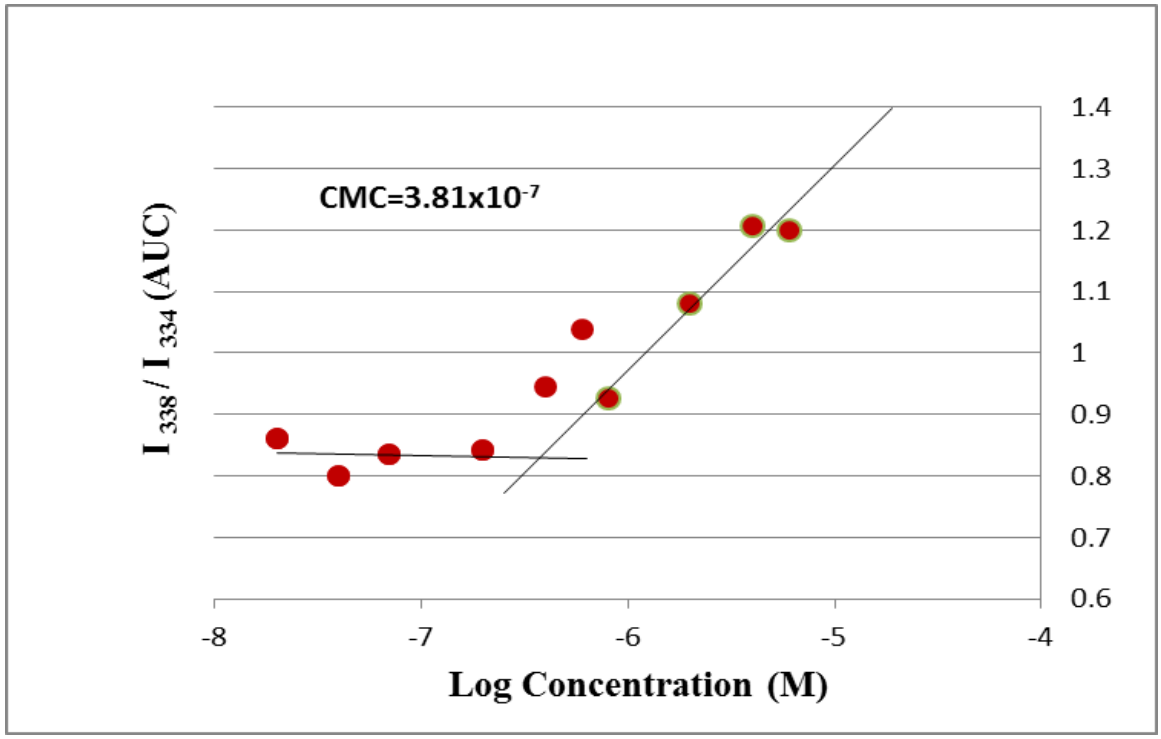

Figure 3.33. CMC graph of micelles formed from conjugate C6.

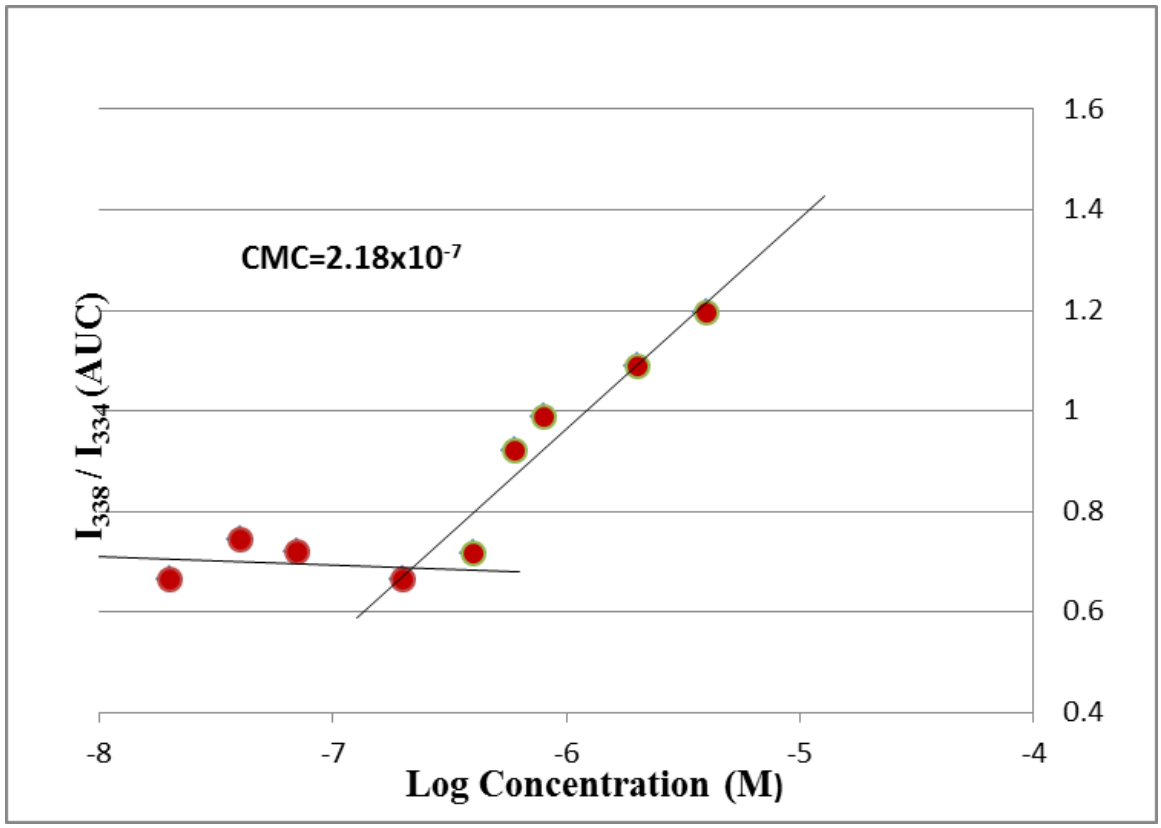

Figure 3.34. CMC graph of micelles formed from polymer 12.

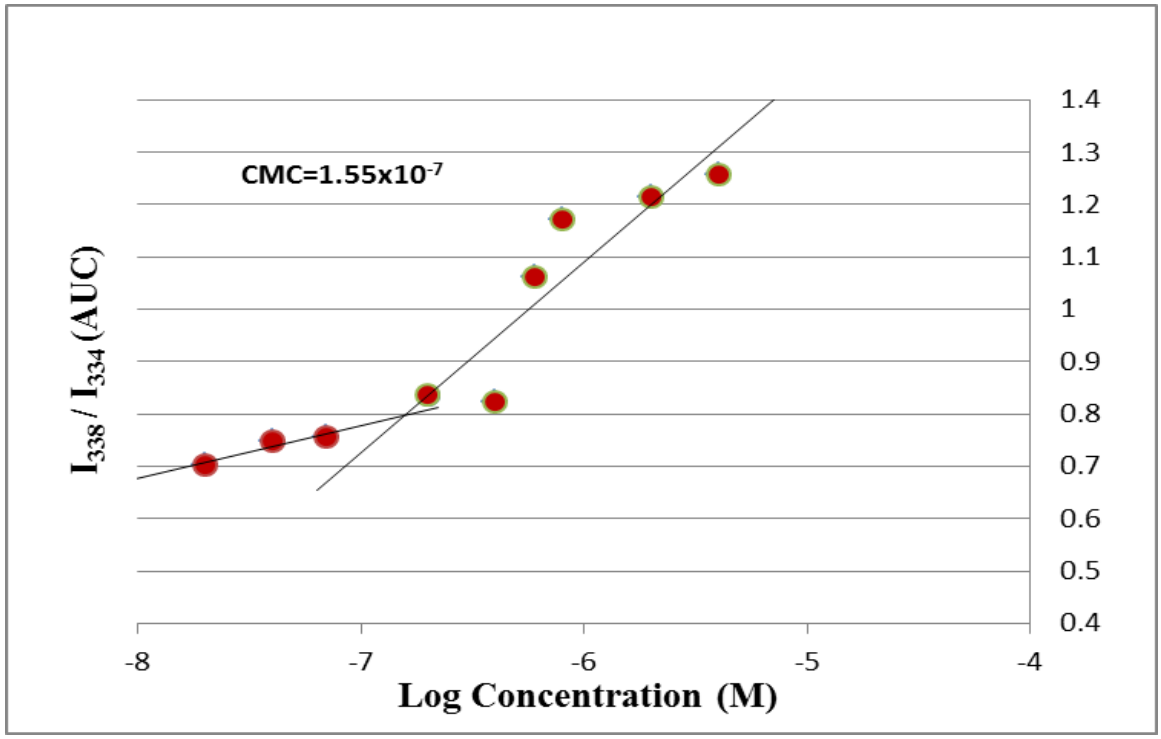

Figure 3.35. CMC graph of micelles formed from polymer 14.

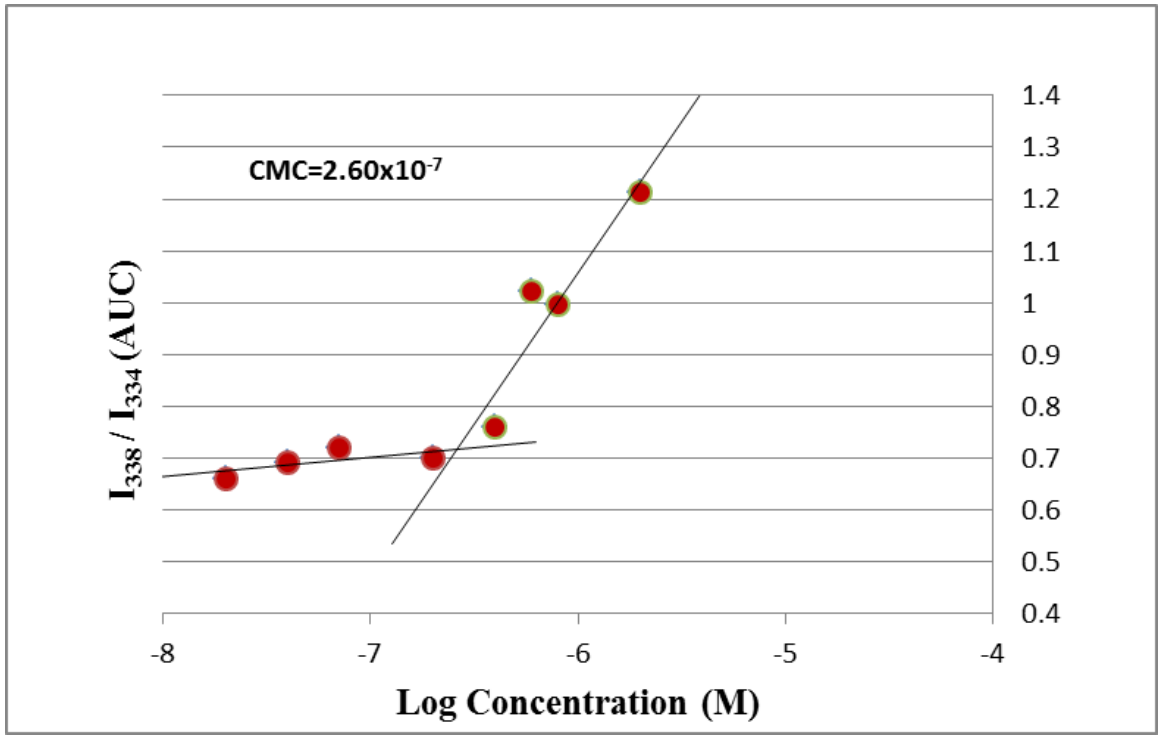

Figure 3.36. CMC graph of micelles formed from polymer 16.

To be an effective drug carrier molecule, micelles should have around 100 nm and narrow PDI value. After finding CMC values via fluorescence probe technique, light scattering measurements were done to determine sizes of micelles formed from conjugates and polymers at 25°C in water.

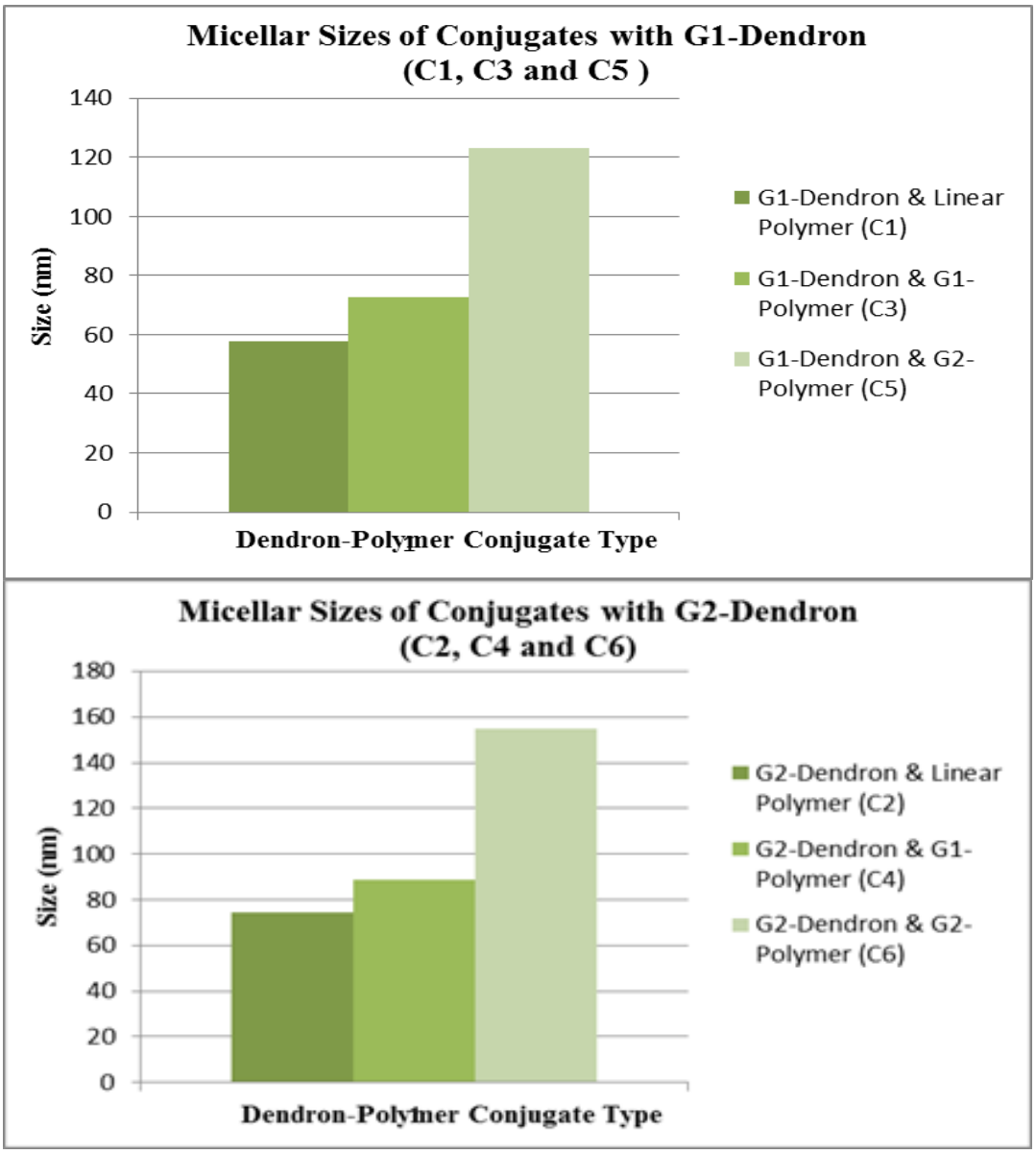

Figure 3.37. Sizes of Conjugates with Changing Polymer Segment.

As in the Figure 3.37, when we change the generation of hydrophilic polymer side by holding the hydrophobic dendron part the same, the micelle construct is growing in size.

In the same way, as we alter the hydrophobic dendron part which is the core of micelle by keeping arms fixed, sizes of micelles are again increasing (Figure 3.38).

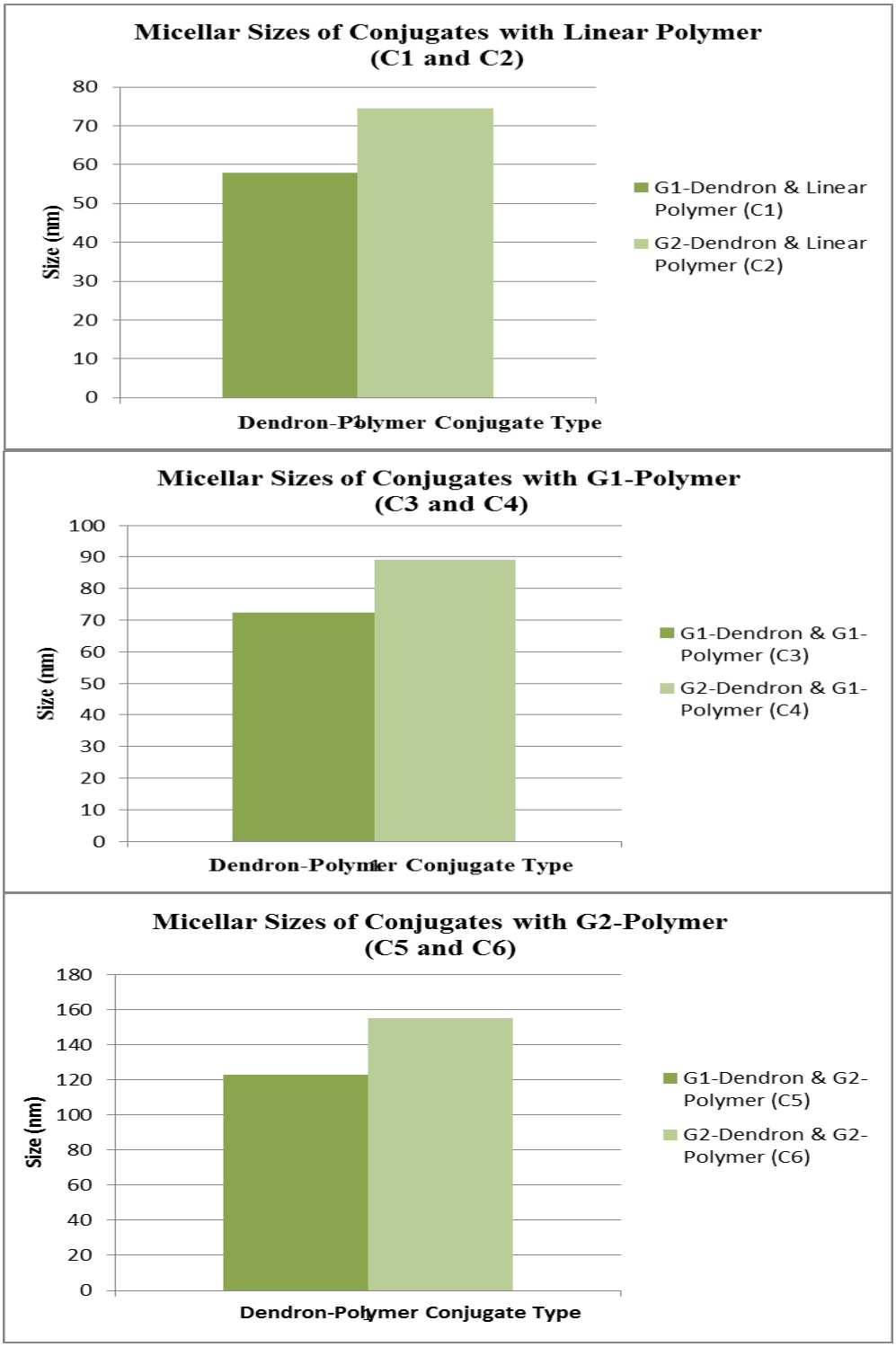

Figure 3.38. Sizes of Conjugates with Changing Dendron Segments.

As mentioned, polymers without dendron part are able to self-assemble at 25°C in aqueous media (Figure 3.39) and their CMC values are nearly the same as the ones of conjugates. But we can observe differences in sizes of micelles between polymers and their conjugates because of the hydrophobic acetal dendron segment. With the addition of acetal dendron, the hydrophobic segments may stick together easily via non-covalent interactions, thus resulting in decrease in the sizes of conjugates. Sizes of these micelles formed from conjugates have been found to be less than 200 nm, a size which is suitable for various drug delivery uses. The micelles formed from polymers have more than 200 nm as figure 3.40, 41 and 42.

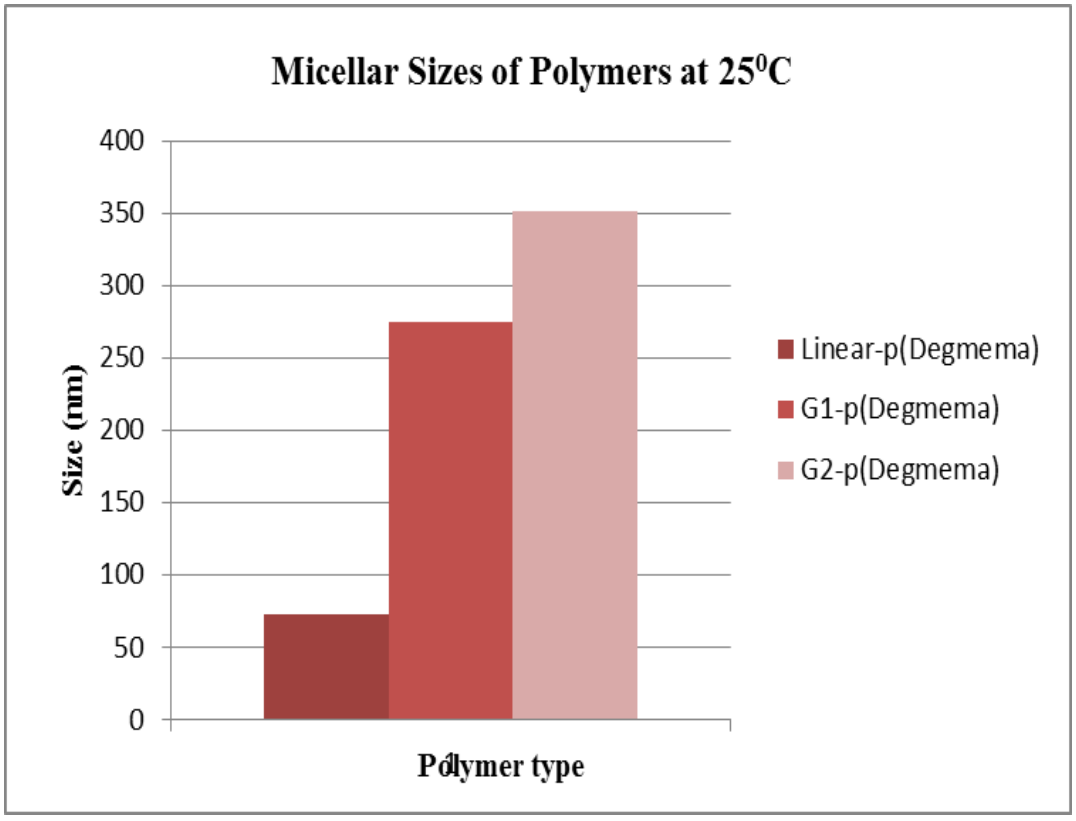

Figure 3.39. Size of Polymers at 25°C.

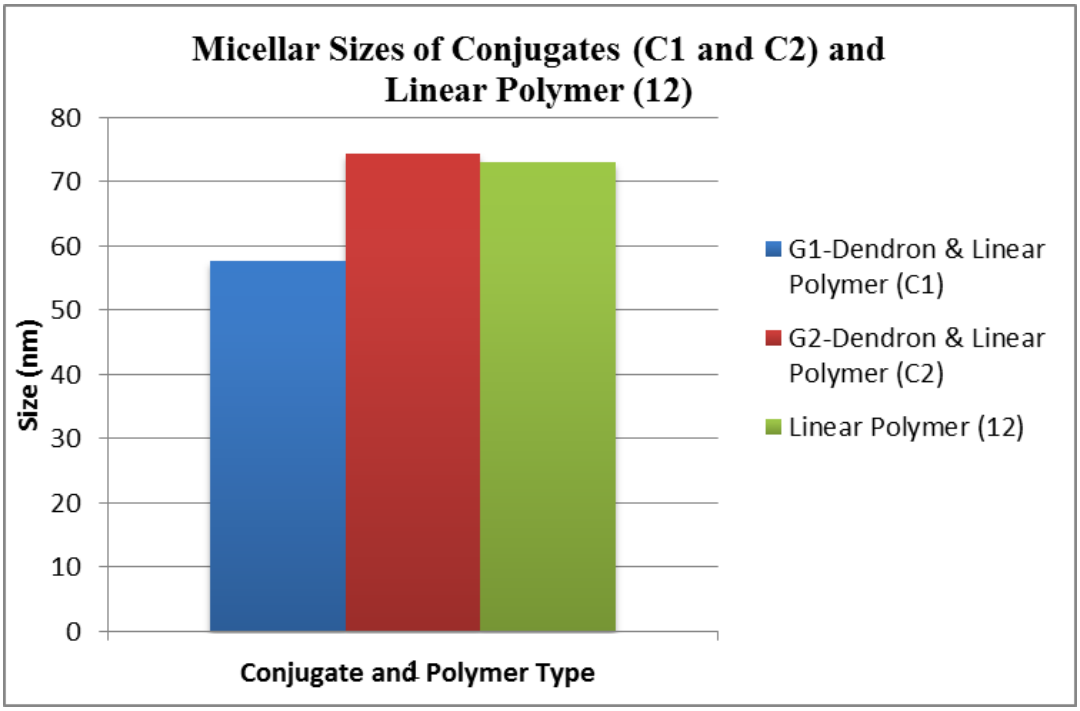

Figure 3.40. Size of Linear Polymer and Its Conjugates.

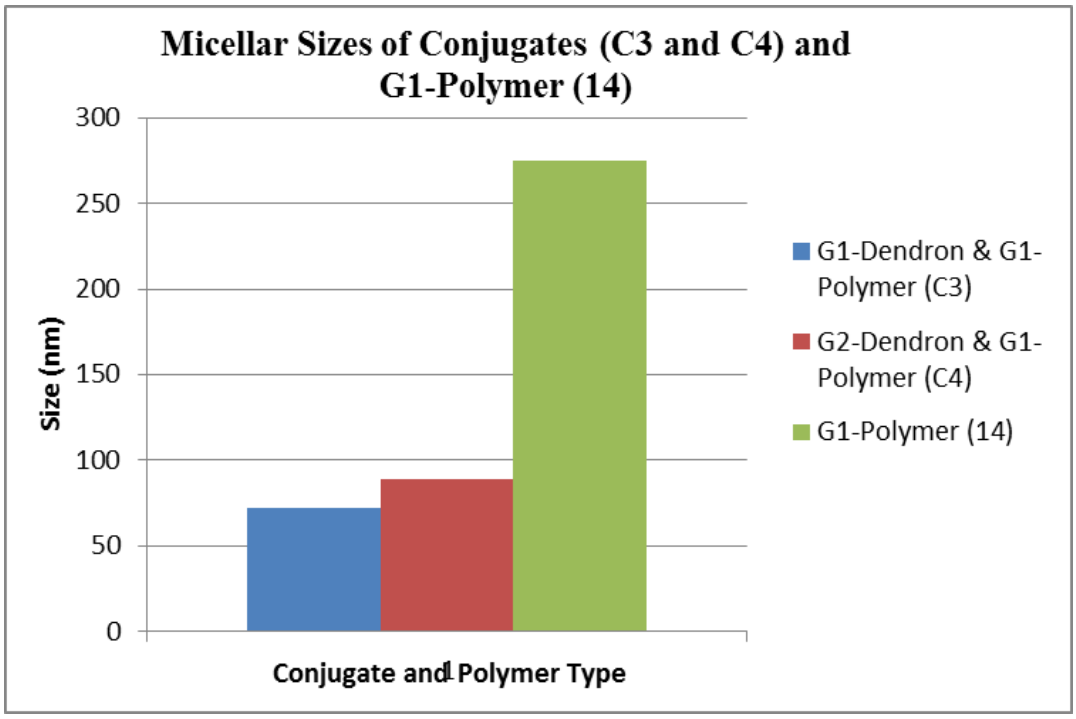

Figure 3.41. Size of G1-Polymer and Its Conjugates.

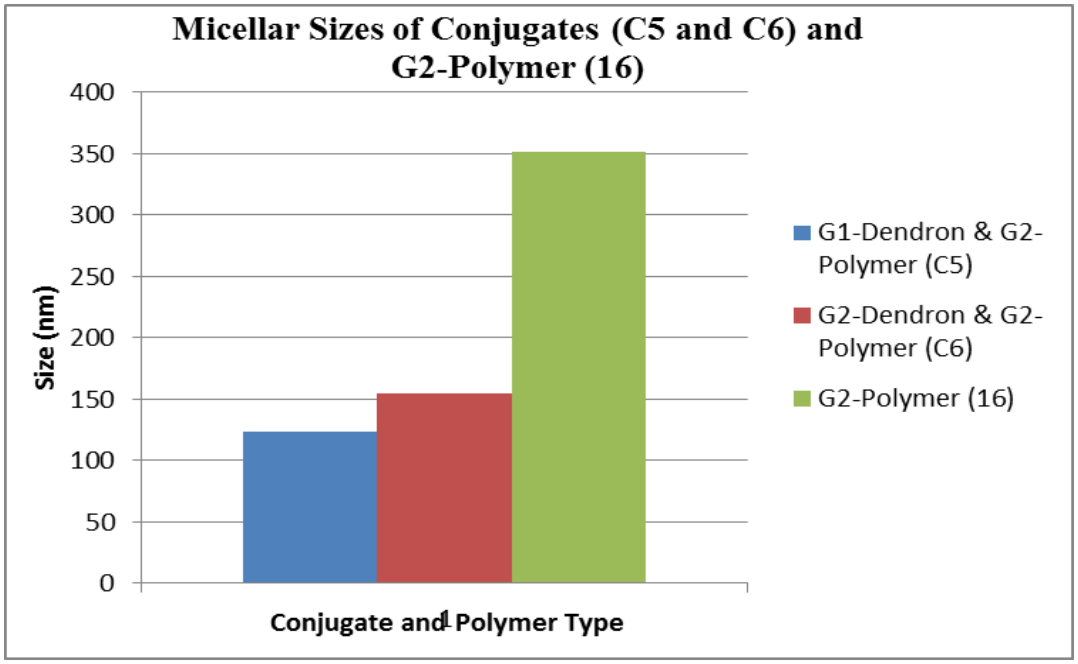

Figure 3.42. Size of G2-Polymer and Its Conjugates.

3.3.1.2. Swelling and Ultra-Dilution Studies of Micelles. Further experiments were undertaken to compare and understand the difference in stability of structures formed by conjugates versus linear polymers alone. THF was added to self-assembled micelles. Since THF is a good solvent for both blocks, its addition results in dissolution of the blocks, thus leading to disassembly of micelle. It can be seen from the figures 3.43 and 3.44 that more THF is needed to disrupt the micelles formed using the dendron-polymer conjugates. Thus, even though same loose structures are formed by the polymers alone, their stability is lower (Figure 3.45). Hence addition of dendron results in better self-assembly to form micelles.

Future studies will be done to understand if the addition of hydrophobic part results in increased drug loading capacity, adding further advantages towards these constructs.

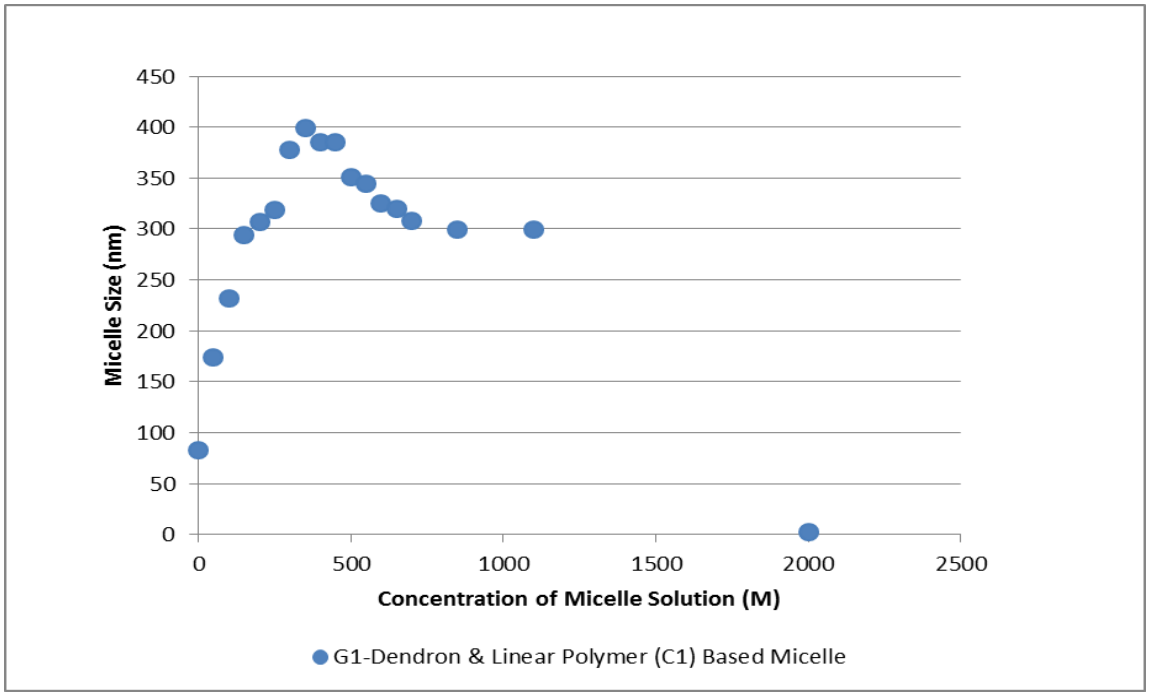

Figure 3.43. Change in the size of micelles of G1-Dendron & Linear Polymer (C1) upon addition of THF.

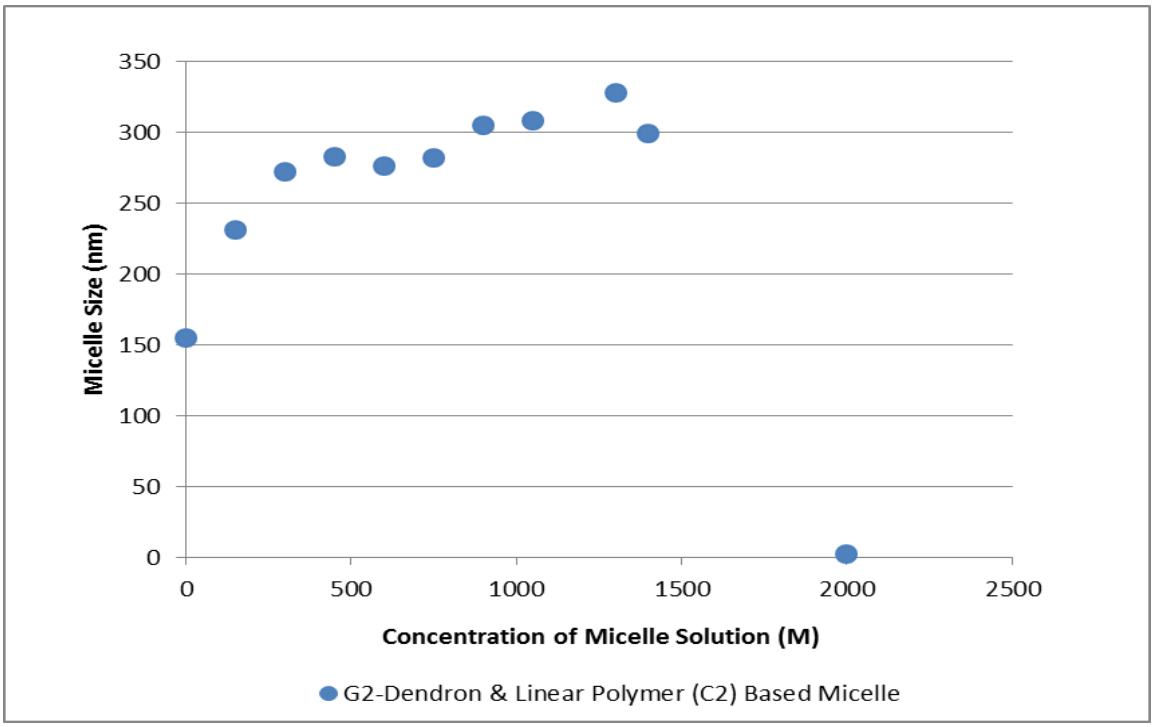

Figure 3.44. Change in the size of micelles G2-Dendron & Linear Polymer (C2) upon addition of THF.

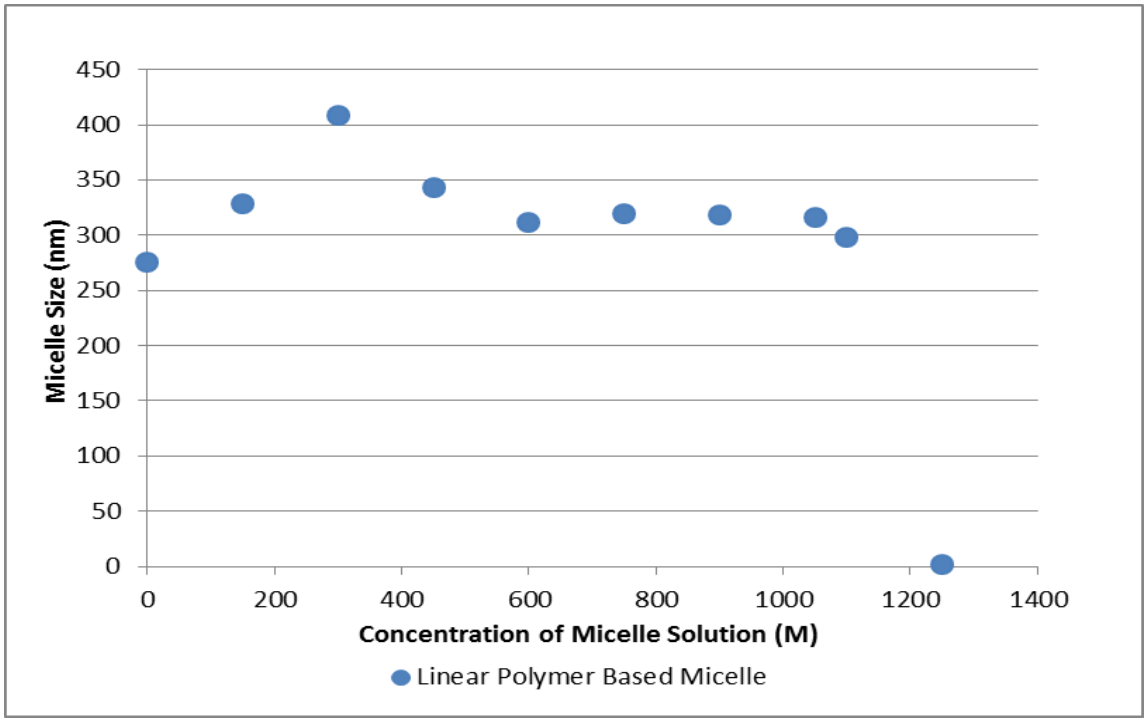

Figure 3.45. Change in the size of micelles of linear polymer upon addition of THF.

4. EXPERIMENTAL

4.1. Materials and General Methods

All chemicals were obtained from commercial sources (Merck, Aldrich and Alfa Aesar) and were used as received unless otherwise stated. Dry solvents (CH_2Cl_2, THF) were obtained from ScimatCo Purification System, other dry solvents were dried over molecular sieves. Di(ethylene glycol) methyl ether methacrylate (Mw = 188) (DEGMA, 99%, Aldrich) was passed through basic alumina column to remove inhibitor and then distilled over CaH_2 in vacuum prior to use. N, N, N', N'', N''-pentamethyldiethylenetriamine (PMDETA, Aldrich) was distilled over NaOH prior to use. 4-Dimethylaminopyridine (DMAP, 99%, Aldrich), CuBr (99.9%, Aldrich) and 2-bromo-2-methylpropionyl bromide (98%, Aldrich) were used as received.

The initiator, dendron and polymer characterizations involved ^1H solution NMR spectroscopy (Varian 400 MHz and Bruker 260 MHz). The molecular weights were estimated by gel permeation chromatography (GPC) analysis using a Shimadzu PSS-SDV (length/ID 8 x 300 mm, 10 nm particle size) mixed-C column calibrated with polystyrene standards (1-150 kDa) using a refractive index detector. THF was used as eluent at a flow rate of 1 mL/min at 30^oC. Micelle formations were characterized using Fluorescence spectroscopy (Cary Eclipse) and Zetasizer Nano particle analyzer series (Malvern).

4.2. Synthesis

4.2.1. Synthesis of Anthracene Functionalized Poly(ester) Acetal Dendrons

4.2.1.1. Synthesis of 1st Generation Anthracene Functionalized Acetal Dendron.

Compounds G1 acid and 2 were synthesized according to the previously reported literature procedures [50].

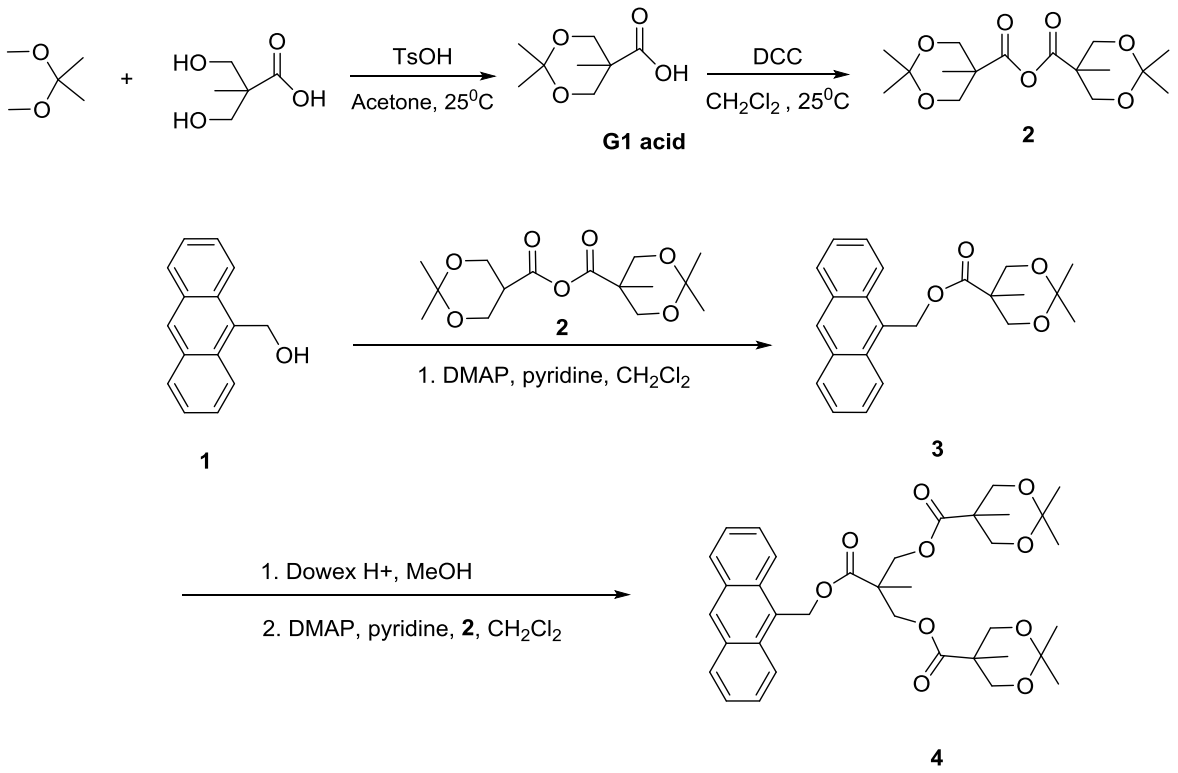

Figure 4.1. Divergent synthesis of anthracene functionalized poly (ester) acetal dendron.

To a solution of 2 (4.25 g, 12.86 mmol) in CH_2Cl_2 (40 mL), 9-anthracene methanol (1.79 g, 8.58 mmol), DMAP (0.42 g, 3.43 mmol) and pyridine (2.50 mL) was added. The mixture was stirred at room temperature for 20 hours followed by quenching of excess anhydride with (1:1) mixture of pyridine and water (8.20 mL) for 5 h. Reaction mixture was extracted with 1 M $NaHSO_4$ (3 x 60 mL), 10 % Na_2CO_3 (3 x 60 mL) and then with brine (1 x 60 mL) combined organic layers were dried over anhydrous Na_2SO_4. The residue was concentrated in vacuo. The product was obtained as a pure yellow solid **3** (5.70 g, 90 %). ^{1}H NMR ($CDCl_3$, δ, ppm) 8.51 (s, 1H, ArH), 8.30 (d, 2H, ArH), 8.03 (d, 2H, ArH), 7.57 (dd, 2H, ArH), 7.49 (dd, 2H, ArH), 6.23 (s, 2H, CH_2-Ar), 4.12 (d, 2H, CH_2 ester protons), 3.60 (d, 2H, CH_2 ester protons), 1.35 (dd, 6H, CH_3), 1.12 (s, 3H, $C(CH_3)$).

4.2.1.2. Synthesis of 2nd Generation Anthracene Functionalized Acetal Dendron. Compound **3** (2.00 g, 5.30 mmol) was dissolved in MeOH (30 mL) and to this solution, Dowex H^+ resin was added with a tip of spatula. The resulting mixture was stirred at room temperature until the consumption of 2 was observed via TLC. The resin was then filtered off and washed with MeOH. The crude product was purified by recrystallization with $CHCl_3$. The product was obtained by filtration to give as a yellow solid. Obtained yellow solid (0.32 g, 0.99 mmol) was added to a solution of DMAP (0.06 g, 0.49 mmol), pyridine (0.72 mL) and compound 2 (1.14 g, 3.45 mmol) in CH_2Cl_2 (10 mL). The mixture was then stirred at room temperature for 20 h followed by quenching of excess anhydride with (1:1) mixture of pyridine and water (2.40 mL) for 5 h. Reaction mixture was diluted with CH_2Cl_2 (30 mL) and extracted with 1 M $NaHSO_4$ (3 x 40 mL), 10 % Na_2CO_3 (3 x 40 mL) and then with brine (1 x 40 mL) combined organic layers were dried over anhydrous Na_2SO_4. The residue was concentrated in vacuo. Crude product was purified by column chromatography to give **4** as a yellow solid (0.48 g, 76 %). ^{1}H NMR ($CDCl_3$, δ, ppm) 8.50 (s, 1H, ArH), 8.26 (d, 2H, ArH), 8.00 (d, 2H, ArH), 7.57 (dd, 2H, ArH), 7.49 (dd, 2H, ArH), 6.23 (s, 2H, CH_2-Ar), 4.34 (d, 2H, CH_2 ester protons), 4.22 (d, 2H CH_2 ester protons), 3.60-3.47 (m, 8H, CH_2 ester protons), 1.25 (s, 3H, $C(CH_3)$), 0.80 (s, 6H, $C(CH_3)$).

4.2.2. Synthesis of Furan-Protected Maleimide-Containing Polymers

4.2.2.1. Synthesis of Furan-Protected Maleimide-Containing Linear Initiator. Furan-protected maleimide containing alcohol **5** (1.00 g, 4.48 mmol) was then added to a solution of triethylamine (1.25 mL, 9.004 mmol) and DMAP (0.094 g, 0.775 mmol) in THF (50 mL) under N_2. The mixture was cooled to 0°C in an ice bath. On the other side, 2-bromo-isobutyryl bromide (0.95 mL, 7.72 mmol) was diluted in THF (15 mL) and added into the former mixture dropwise (30 min).

The obtained white suspension was stirred for 3 h at 0^0C, then warmed to room temperature and stirred for 22 hours. The ammonium salt formed was filtered off and the residue was concentrated in vacuo. The product was obtained as a pure white solid **6** (1.95 g, 70 %). ^{1}H NMR ($CDCl_3$, δ, ppm) 6.50 (s, 2H, CH=CH), 5.25 (s, 2H, CH bridgehead protons), 4.20 (t, 2H, OCH_2), 3.56 (t, 2H, NCH_2), 2.83 (s, 2H, CH-CH bridge protons), 2.00-1.96 (m, 14H, $NCH_2CH_2CH_2O$, $CBr(CH_3)$), 1.35 (s, 3H, $C(CH_3)$).

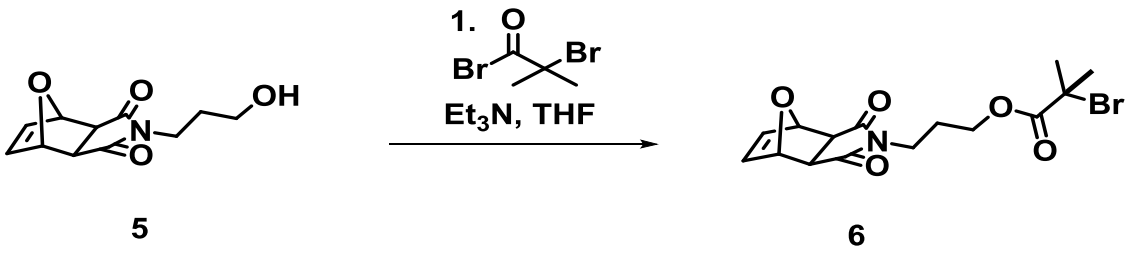

5 **6**

Figure 4.2. Furan-Protected Maleimide-Containing Linear Initiator Synthesis.

4.2.2.2 Synthesis of G1-Maleimide Initiator. Compound **7** (1.0 g, 2.6 mmol) was dissolved in MeOH (15 mL) and to this solution Dowex H^+ resin was added with a tip of spatula. The resulting mixture was stirred at ambient temperature until the consumption of 7 was observed via TLC. The resin was then filtered off and washed with MeOH. The crude product was purified by recrystallization with $CHCl_2$. The product was obtained by filtration to give a white solid (0.89 g, 99% yield). The solid (1.00 g, 3.01 mmol) was then added to a solution of triethylamine (1.5 mL, 10.55 mmol) and DMAP (0.11 g, 0.90 mmol) in THF (15 mL) under N2. The mixture was cooled to 0^oC in an ice bath. On the other side, 2-bromo-isobutyryl bromide (1.12 mL, 9.04 mmol) was diluted in THF (60 mL) and added into the former mixture dropwise (30 min). The obtained white suspension was stirred for 3 h at 0^oC, then warmed to room temperature and stirred for 22 hours. The ammonium salt formed was filtered off and the residue was concentrated in vacuo. The product was purified with column chromatography and white solid **8** is obtained (1.34 g, 70 %). ^{1}H NMR ($CDCl_3$, δ, ppm) 6.50 (s, 2H, CH=CH), 5.25 (s, 2H, CH bridgehead protons), 4.41

(d, 2H, CH_2 ester protons), 4.32 (d, 2H, CH_2 ester protons), 4.10 (t, 2H, OCH_2), 3.56 (t, 2H, NCH_2), 2.83 (s, 2H, CH-CH bridge protons), 2.00-1.96 (m, 14H, $NCH_2CH_2CH_2O$, $CBr(CH_3)$), 1.35 (s, 3H, $C(CH_3)$).

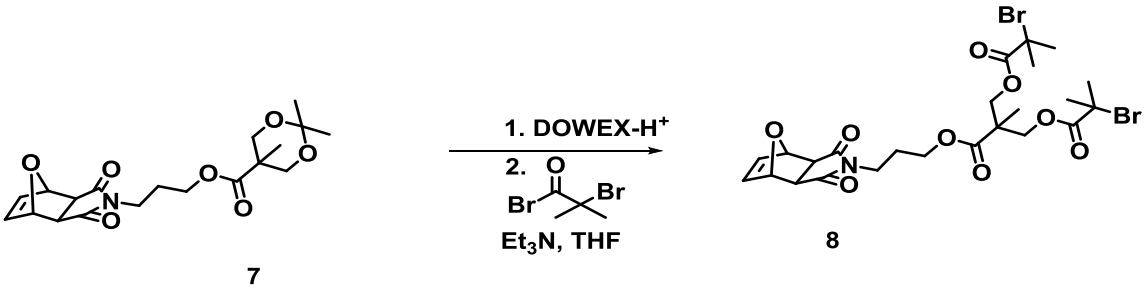

Figure 4.3. G1-Maleimide Initiator Synthesis.

4.2.2.3. Synthesis of G2-Maleimide Initiator. Compound **9** (1.00 g, 1.52 mmol) was dissolved in MeOH (20 mL) and to this solution Dowex H^+ resin was added with a tip of spatula. The resulting mixture was stirred at ambient temperature until the consumption of 9 was observed via TLC. The resin was then filtered off and washed with MeOH. The crude product was purified by recrystallization with $CHCl_2$. The product was obtained by filtration to give a white solid (0.85 g, 98% yield). The solid (1.00 g, 1.75 mmol) was then added to a solution of triethylamine (1.365 mL, 9.78 mmol) and DMAP (0.102 g, 0.84 mmol) in THF (15 mL) under N_2. The mixture was cooled to 0^oC in an ice bath. On the other side, 2-bromo-isobutyryl bromide (1.04 mL, 8.39 mmol) was diluted in THF (60 mL) and added into the former mixture dropwise (30 min). The obtained white suspension was stirred for 3 h at 0^oC, then warmed to room temperature and stirred for 22 hours. The ammonium salt formed was filtered off and the residue was concentrated in vacuo. The product was purified with column chromatography, and white solid is obtained **10** (0.52 g, 50 %). ^1H NMR ($CDCl_3$, δ, ppm) 6.48 (s, 2H, CH=CH), 5.23 (s, 2H, CH bridgehead protons), 4.38-4.27 (m, 12H, CH_2 ester protons), 4.05 (t, 2H, OCH_2), 3.55 (t, 2H, NCH_2), 2.83 (s, 2H, CH-CH bridge protons), 1.94-1.84 (m, 26H, $NCH_2CH_2CH_2O$, $CBr(CH_3)$), 1.31 (s, 9H, $C(CH_3)$).

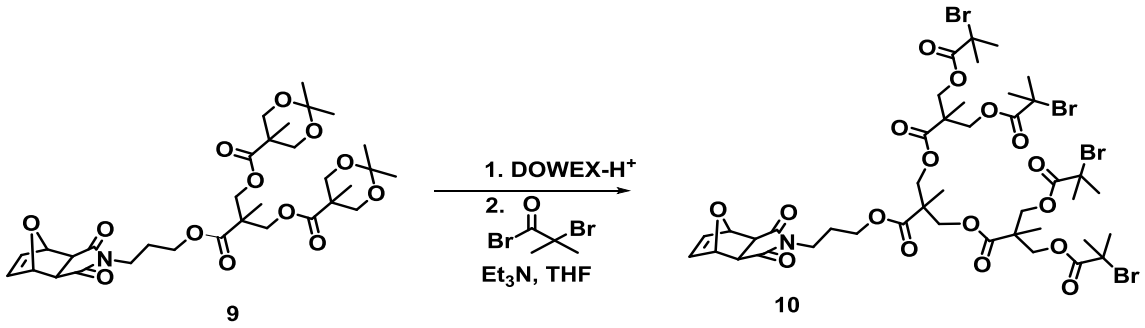

Figure 4.4. G2-Maleimide Initiator Synthesis.

4.2.2.4. Synthesis of furan protected maleimide end-functionalized Linear-p(DEGMEMA) (12). Linear p(DEGMEMA) was prepared by ATRP of DEGMEMA. Furan protected linear-initiator **11** (40 mg, 0.107 mmol) dissolved in minimum amount of degassed anisole was introduced into a flask containing CuBr (30.8 mg, 0.215 mmol), degassed PMDETA (74.5 mg, 0.43 mmol) and degassed DEGMEMA (1.98mL, 10.74 mmol) dissolved in degassed anisole (10 ml) under stirring. The flask was then placed in an oil bath at 40°C for 120 min. After polymerization, dialysis with 3500 cutoff was done for the reaction mixture to remove the catalyst. Linear-p(DEGMEMA) **12** was obtained as a white solid. $[M]_0/[I]_0$= 100; $[I]_0$:[CuBr]:[PMDETA]=1:2:4; conversion = 42 %. $Mn,_{theo}$=19172, $Mn,_{NMR}$= 17500, $Mn,_{GPC}$= 14200, Mw/Mn= 1.26, relative to PS. ^{1}H NMR ($CDCl_3$, δ, ppm) 6.50 (s, 2H, CH=CH), 5.24 (s, 2H, CH bridgehead protons), 4.06 (br s, 4H, OCH_2 and OCH_2 of DEGMEMA), 3.62-3.49 (m, 2H, OCH_2 of DEGMEMA), 3.33 (br s, 5H, OCH_3 of DEGMEMA and NCH_2), 2.79 (s, 2H, CH-CH bridge protons), 1.85–0.82 (m, 13H, $NCH_2C\mathit{H}_2CH_2O$, $O=CC(CH_3)$, CH_2 and CH_3 along polymer backbone).

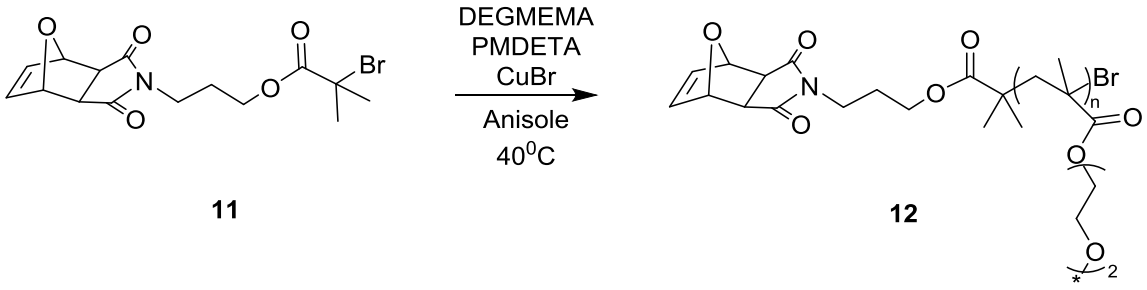

Figure 4.5. Linear Maleimide Based Polymer Synthesis.

4.2.2.5. Synthesis of furan protected maleimide end-functionalized G1-p(DEGMEMA) (14). G1-DEGMEMA was prepared by ATRP of DEGMEMA. Furan protected G1-initiator **13** (20 mg, 0.031 mmol) dissolved in minimum amount of degassed anisole was introduced into a flask containing CuBr (17.8 mg, 0.124 mmol), degassed PMDETA (42.97 mg, 0.248 mmol) and degassed DEGMEMA (1.143 mL, 6.20 mmol) dissolved in degassed anisole (5.70 ml) under stirring. The flask was then placed in an oil bath at 40°C for 120 min. After polymerization dialysis with 3500 cutoff was done for the reaction mixture to remove the catalyst. G1-p(DEGMEMA) **14** was obtained as a white solid. $[M]_0/[I]_0$= 200; [I]:[CuBr]:[PMDETA]=1:4:8; conversion = 60 %. Mn,theo=38245, $Mn,_{NMR}$= 30700, $Mn,_{GPC}$= 16400, Mw/Mn= 1.4, relative to PS. ^{1}H NMR ($CDCl_3$, δ, ppm) 6.51 (s, 2H, CH=CH), 5.25 (s, 2H, CH bridgehead protons), 4.10 (br s, 8H, CH_2 ester protons and OCH_2 of DEGMEMA), 3.68-3.56 (m, 2H, OCH_2 of DEGMEMA), 3.40 (br s, 5H, OCH_3 and NCH_2), 2.87 (s, 2H, CH-CH bridge protons), 1.92–0.89 (m, 22H, $NCH_2CH_2CH_2O$, $C(CH_3)$, $O=CC(CH_3)$, CH_2 and CH_3 along polymer backbone).

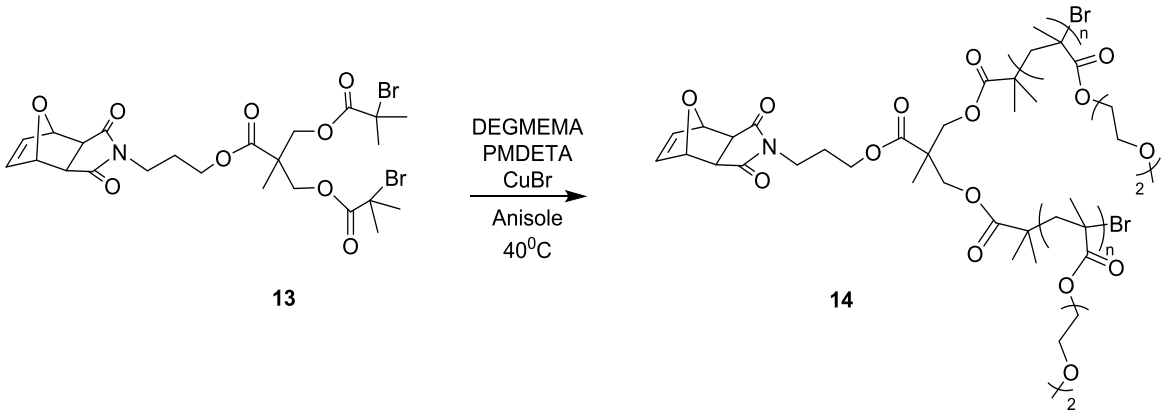

Figure 4.6. G1-Maleimide Based Polymer Synthesis.

4.2.2.6. Synthesis of furan protected maleimide end-functionalized G2-p(DEGMEMA) (16). G2-DEGMEMA was prepared by ATRP of DEGMEMA. Furan protected G2-initiator **15** (20 mg, 0.0171 mmol) dissolved in minimum amount of degassed anisole was introduced into a flask containing CuBr (9.83 mg, 0.0685 mmol), degassed PMDETA (23.7 mg, 0.1371 mmol) and degassed DEGMEMA (1.262 mL, 6.8521 mmol) dissolved in degassed anisole (6.30 ml) under stirring. The flask was then placed in an oil bath at 40°C for 120 min. After polymerization dialysis with 3500 cutoff was done for the reaction mixture to remove the catalyst. G2-p(DEGMEMA) **16** was obtained as a white solid. $[M]_0/[I]_0$= 400; [I]:[CuBr]:[PMDETA]=1:4:8; conversion = 23 %. Mn,theo=76367, $Mn,_{NMR}$= 36200, $Mn,_{GPC}$= 14000, Mw/Mn= 1.27, relative to PS. ^{1}H NMR ($CDCl_3$, δ, ppm) 6.51 (s, 2H, CH=CH), 5.24 (s, 2H, CH bridgehead protons), 4.10 (br s, 8H, CH_2 ester protons and OCH_2 of DEGMEMA), 3.68-3.55 (m, 2H, OCH_2 of DEGMEMA), 3.40 (br s, 5H, OCH_3 and NCH_2), 2.86 (s, 2H, CH-CH bridge protons), 1.96–0.89 (m, 40H, $NCH_2C\mathit{H}_2CH_2O$, $C(CH_3)$, $O{=}CC(CH_3)$, CH_2 and CH_3 along polymer backbone.

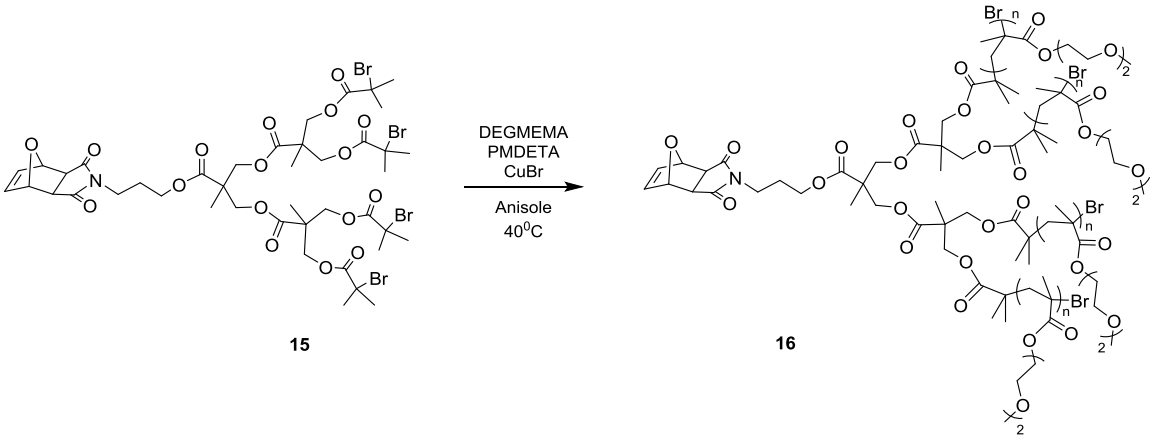

Figure 4.7. G2-Maleimide Based Polymer Synthesis.

4.2.3. Synthesis of Dendron-Polymer Conjugates

4.2.3.1. Synthesis of Dendron-Polymer Conjugate (C1). Furan protected maleimide end-functionalized linear p(DEGMEMA) **12** (20 mg, 0.0014 mmol) and G1-anthracene acetal dendron **3** (1.041 mg, 0.0285 mmol) were dissolved in dimethylformamide (DMF) (0.5 mL) and the mixture was heated under nitrogen at 110°C for 24 hours. Then all volatiles were removed by vacuo and after dialysis with 1000 cutoff membrane with methanol to get rid of excess anthracene dendron, the product was obtained and dried under vacuum to give as a white solid (13.4 mg, 64 %). ^{1}H NMR data for dendron-polymer conjugate **C1** ($CDCl_3$, δ, ppm) 7.45-7.12(m, 8H, ArH), 5.53-5.41 (m, 2H, $CH_2OC{=}O$), 4.71 (s, 1H, CH bridgehead proton), 4.04 (br s, 4H, OCH_2 ester protons), 3.62-3.49 (m, 6H, OCH_2 of DEGMEMA and OCH_2 of acetal unit), 3.33 (br s, 5H, OCH_3 of DEGMEMA and NCH_2), 1.90–0.83 (m, 22H, $NCH_2C\mathit{H}_2CH_2O$, $C(CH_3)$, $O{=}CC(CH_3)$, $C(CH_3)_2$ of acetal unit, CH_2 and CH_3 along polymer backbone).

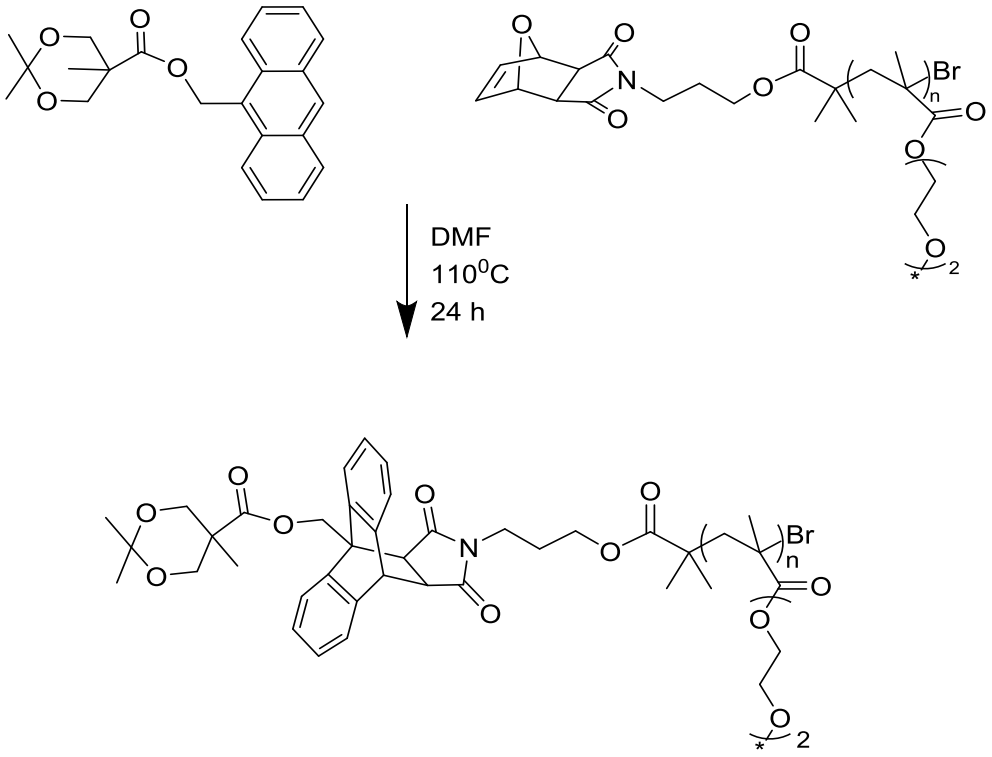

Figure 4.8. Synthesis of dendron-polymer conjugate (C1).

4.2.3.2. Synthesis of Dendron-Polymer Conjugate (C2). Furan protected maleimide end-functionalized linear p(DEGMEMA) **12** (30 mg, 0.00214 mmol) and G2-anthracene acetal dendron **4** (2.73 mg, 0.0043 mmol) were dissolved in dimethylformamide (DMF) (0.5 mL) and the mixture was heated under nitrogen at 110°C for 24 hours. Then all volatiles were removed by vacuo and after dialysis with 1000 cutoff membrane with methanol to get rid of excess anthracene dendron, the product was obtained and dried under vacuum to give as a white solid (23 mg, 70 %). ^{1}H NMR data for dendron-polymer conjugate **C2** ($CDCl_3$, δ, ppm) 7.49-7.10(m, 8H, ArH), 5.60-5.27 (m, 2H, $CH_2OC=O$), 4.71 (s, 1H, CH bridgehead proton), 4.04 (br s, 8H, OCH_2 ester protons), 3.62-3.49 (m, 10H, OCH_2 of DEGMEMA and OCH_2 of acetal unit), 3.33 (br s, 5H, OCH_3 of DEGMEMA and NCH_2), 1.90–0.83 (m, 34H, $NCH_2CH_2CH_2O$, $C(CH_3)$, $O=CC(CH_3)$, $C(CH_3)_2$ of acetal unit, CH_2 and CH_3 along polymer backbone).

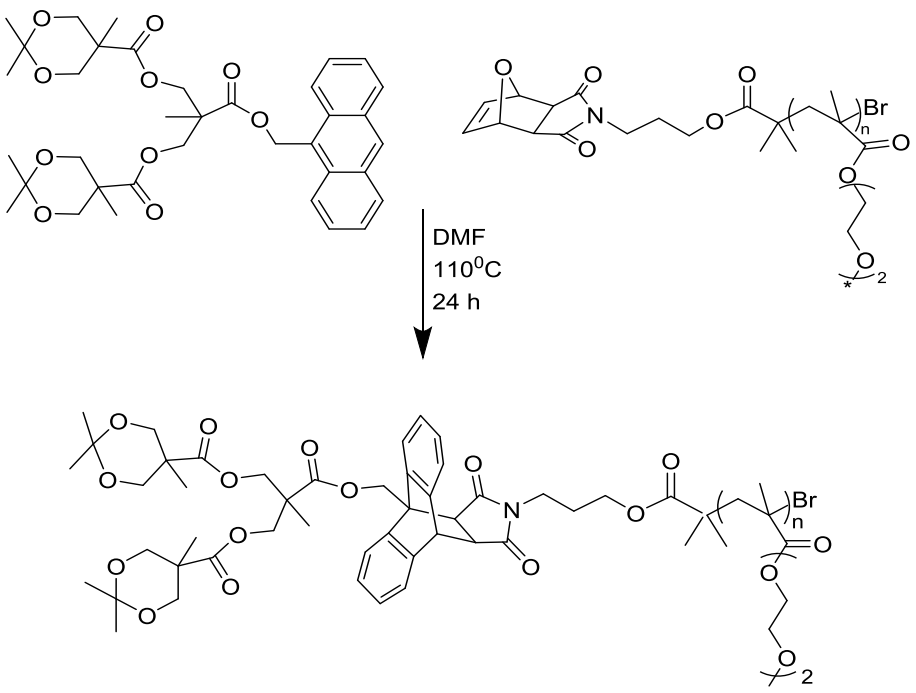

Figure 4.9. Synthesis of dendron-polymer conjugate (C2).

4.2.3.3. Synthesis of Dendron-Polymer Conjugate (C3). Furan protected maleimide end-functionalized G1-p(DEGMEMA) **14** (30 mg, 0,00097 mmol) and G1-anthracene acetal dendron **3** (0.71 mg, 0.0019 mmol) were dissolved in dimethylformamide (DMF) (0.5 mL) and the mixture was heated under nitrogen at 110°C for 24 hours. Then all volatiles were removed by vacuo and after dialysis with 1000 cutoff membrane with methanol to get rid of excess anthracene dendron, the product was obtained and dried under vacuum to give as a white solid (14 mg, 45 %). ^{1}H NMR data for dendron-polymer conjugate **C3** ($CDCl_3$, δ, ppm) 7.46-7.10(m, 8H, ArH), 5.53-5.38 (m, 2H, $CH_2OC=O$), 4.71 (s, 1H, CH bridgehead proton), 4.04 (br s, 8H, OCH_2 ester protons), 3.62-3.49 (m, 6H, OCH_2 of DEGMEMA and OCH_2 of acetal unit), 3.33 (br s, 5H, OCH_3 of DEGMEMA and NCH_2), 1.90–0.81 (m, 31H, $NCH_2C\mathit{H}_2CH_2O$, $C(CH_3)$, $O=CC(CH_3)$, $C(CH_3)_2$ of acetal unit, CH_2 and CH_3 along polymer backbone).

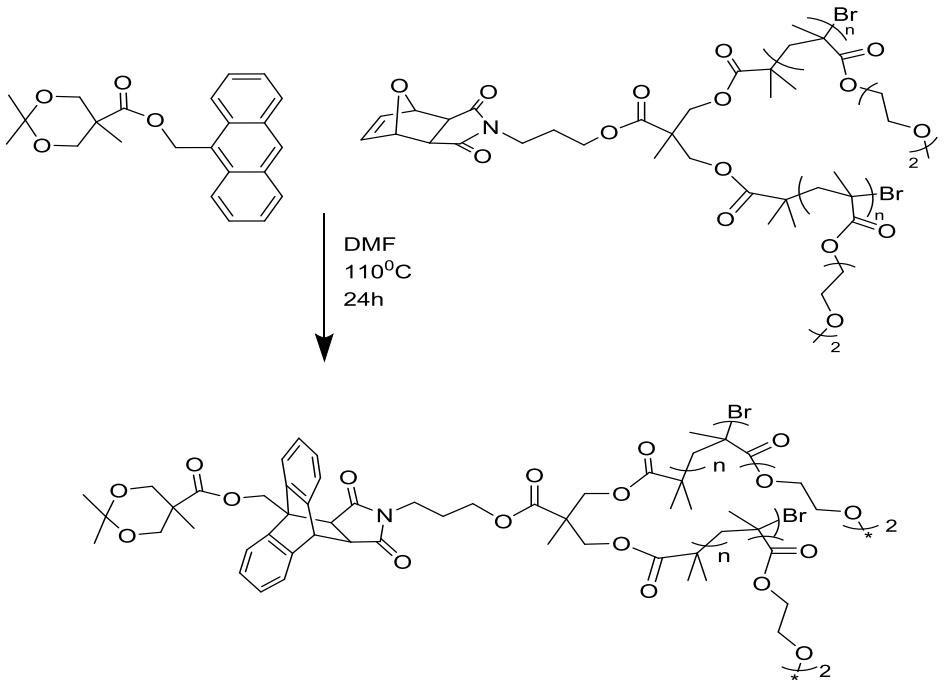

Figure 4.10. Synthesis of dendron-polymer conjugate (C3).

4.2.3.4. Synthesis of Dendron-Polymer Conjugate (C4). Furan protected maleimide end-functionalized G1-p(DEGMEMA) **14** (30 mg, 0,00097 mmol) and G2-anthracene acetal dendron **4** (1.25 mg, 0.0019 mmol) were dissolved in dimethylformamide (DMF) (0.5 mL) and the mixture was heated under nitrogen at 110°C for 24 hours. Then all volatiles were removed by vacuo and after dialysis with 1000 cutoff membrane with methanol to get rid of excess anthracene dendron, the product was obtained and dried under vacuum to give as a white solid (27.8 mg, 88 %). 1H NMR data for dendron-polymer conjugate **C4** ($CDCl_3$, δ, ppm) 7.49-7.10(m, 8H, ArH), 5.66-5.49 (m, 2H, CH_2OC=O), 4.75 (s, 1H, CH bridgehead proton), 4.08 (br s, 8H, CH_2 ester protons), 3.62-3.49 (m, 10H, OCH_2 of DEGMEMA and OCH_2 of acetal unit), 3.33 (br s, 5H, OCH_3 of DEGMEMA and NCH_2), 1.90–0.81 (m, 34H, $NCH_2CH_2CH_2O$, $C(CH_3)$, $O=CC(CH_3)$, $C(CH_3)_2$ of acetal unit, CH_2 and CH_3 along polymer backbone).

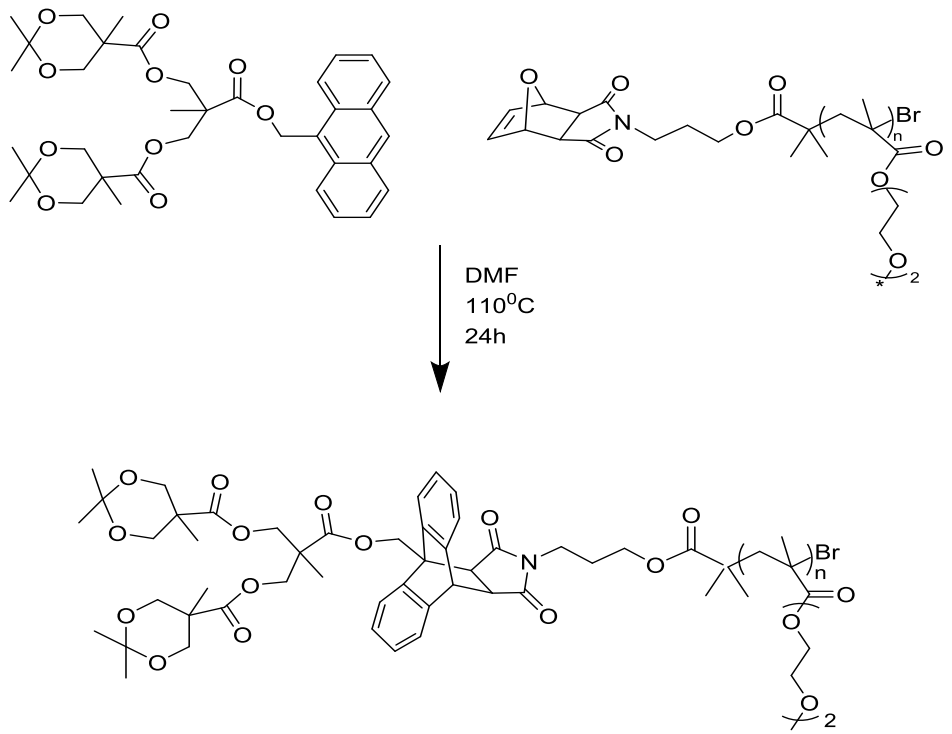

Figure 4.11. Synthesis of dendron-polymer conjugate (C4).

4.2.3.5. Synthesis of Dendron-Polymer Conjugate (C5). Furan protected maleimide end-functionalized G2-p(DEGMEMA) **16** (30 mg, 0,00084 mmol) and G1-anthracene acetal dendron **3** (0.62 mg, 0.0017 mmol) were dissolved in dimethylformamide (DMF) (0.5 mL) and the mixture was heated under nitrogen at 110°C for 24 hours. Then all volatiles were removed by vacuo and after dialysis with 1000 cutoff membrane with methanol to get rid of excess anthracene dendron, the product was obtained and dried under vacuum to give as a white solid (28mg, 94 %). 1H NMR data for dendron-polymer conjugate **C5** ($CDCl_3$, δ, ppm) 7.49-7.10(m, 8H, ArH), 5.58-5.42 (m, 2H, CH_2OC=O), 4.76 (s, 1H, CH bridgehead proton), 4.08 (br s, 16H, OCH_2 ester protons), 3.66-3.53 (m, 6H, OCH_2 of DEGMEMA and OCH_2 of acetal unit), 3.37 (br s, 5H, OCH_3 of DEGMEMA and NCH_2), 1.90–0.87 (m, 49H, $NCH_2CH_2CH_2O$, $C(CH_3)$, $O=CC(CH_3)$, $C(CH_3)_2$ of acetal unit, CH_2 and CH_3 along polymer backbone).

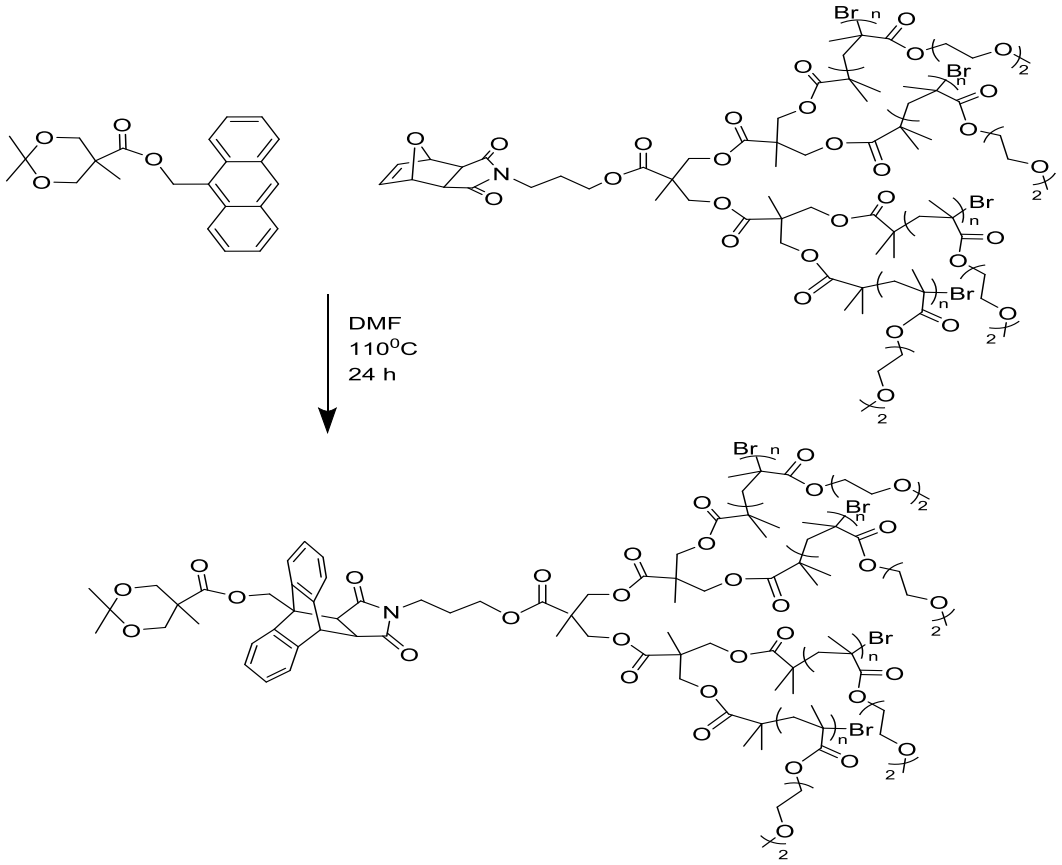

Figure 4.12. Synthesis of dendron-polymer conjugate (C5).

4.2.3.6. Synthesis of Dendron-Polymer Conjugate (C6). Furan protected maleimide end-functionalized G2-p(DEGMEMA) **16** (30 mg, 0,00084 mmol) and G2-anthracene acetal dendron **4** (1.07 mg, 0.0017 mmol) were dissolved in dimethylformamide (DMF) (0.5 mL) and the mixture was heated under nitrogen at 110°C for 24 hours. Then all volatiles were removed by vacuo and after dialysis with 1000 cutoff membrane with methanol to get rid of excess anthracene dendron, the product was obtained and dried under vacuum to give as a white solid (23.4 mg, 75 %). 1H NMR data for dendron-polymer conjugate C5 ($CDCl_3$, δ, ppm) 7.46-7.10(m, 8H, ArH), 5.65-5.32 (m, 2H, C*H*$_2$OC=O), 4.71 (s, 1H, CH bridgehead proton), 4.04 (br s, 20H, OCH_2 ester protons), 3.62-3.49 (m, 10H, OCH_2 of DEGMEMA and OCH_2 of acetal unit), 3.33 (br s, 5H, OCH_3 of DEGMEMA and NCH_2), 1.84–0.83 (m, 61H, $NCH_2CH_2CH_2O$, $C(CH_3)$, $O=CC(CH_3)$, $C(CH_3)$ of acetal unit, CH_2 and CH_3 along polymer backbone).

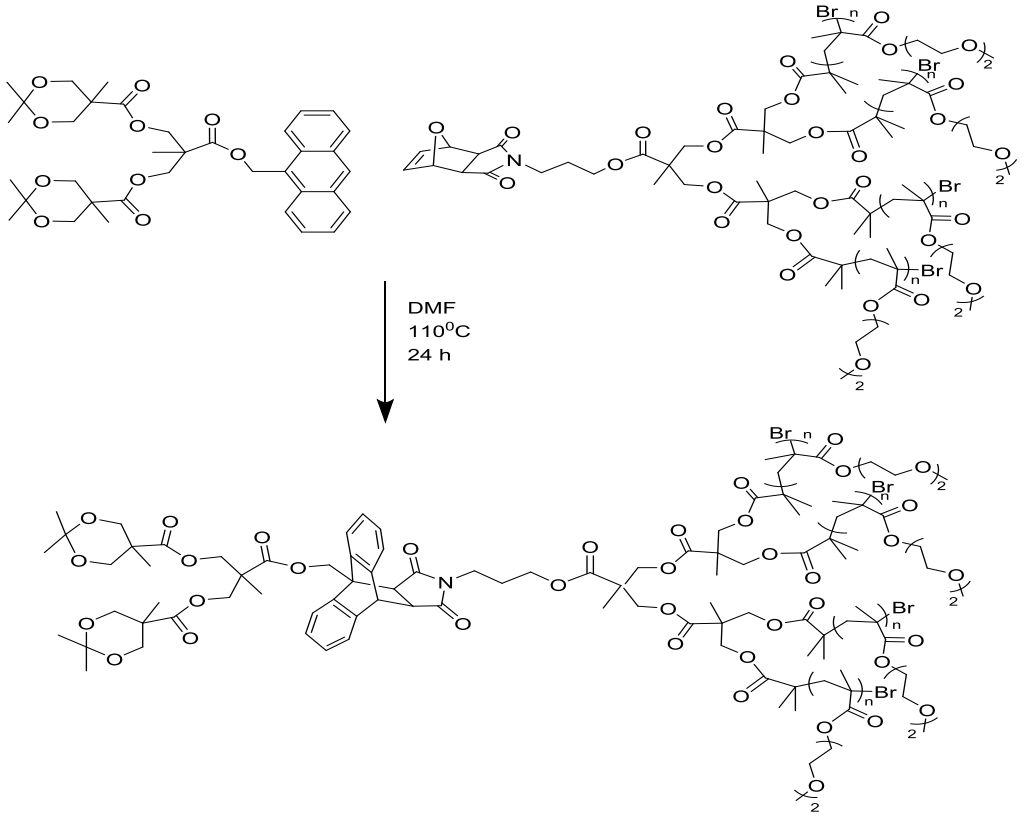

Figure 4.13. Synthesis of dendron-polymer conjugate (C6).

4.3. Micelle Formation from Dendron-polymer Conjugates and Measurements

For six different dendron-polymer conjugates and three polymers, florescence spectroscopy was used to determine CMC values. Pyrene has hydrophobic character in its nature, and it was also used in these experiments to determine CMC of each conjugates and their sizes in aqueous media. The fluorescence spectrum of pyrene shows characteristic range around 300–360 nm, and the maximum intensity of pyrene peak is 338 nm which pyrene is located into the core of the micelle showing that pyrene absorption can be a convenient method for determining critical micellar concentration.

4.3.1. Micelle Preparation Method

Various concentrations of the conjugates ranging from 10^{-5} M to 10^{-8} M were dissolved in 200 µL THF. Then Milli-Q water (1 mL) was added to all samples. Then, pyrene solution was added to all samples and the last concentration of pyrene was 6.10-7 M and 20 µL for each sample in 1 mL water. For the self-assembly, these mixtures were opened to the air to evaporate organic phase. At the end, fluorescence spectroscopy which is in excitation mode and at 390 nm emission wavelength, and DLS measurements were done for all samples.

5. CONCLUSION

In this study, several micellar structures were synthesized for targeted drug delivery by using novel polymer-dendron conjugates. Diblock dendron–polymer conjugates containing biodegradable polyester dendron blocks and p(DEGMEMA) polymer were synthesized using the Diels–Alder "click" cycloaddition reaction which is as a powerful metal-free conjugation reaction to obtain a wide variety of discrete macromolecular constructs efficiently. First, generations of biodegradable polyester dendrons containing an anthracene unit at their focal point were synthesized using a divergent strategy. Then, p(DEGMEMA) polymers with furan-protected maleimide functionality were synthesized via atom transfer radical polymerization (ATRP) and reacted with biodegradable polyester dendrons containing an anthracene moiety at their focal point to obtain biodegradable dendritic macromolecules at the end.

In addition, several kinds of micelles were obtained from various polymer-dendron conjugates where p(DEGMEMA) polymers with furan-protected maleimide functionality were behaved as the hydrophilic component of micelles and biodegradable polyester dendrons containing an anthracene moiety acted as the hydrophobic core of micelles. Their stabilities were measured using fluorescence spectroscopy and DLS. And we could see that dendron-polymer conjugates are good candidates to obtain micellar structures less than 200 nm. Furthermore, addition of THF, a good solvent for both blocks, proved that dendron-polymer conjugates provide more stable micelles than polymer alone. Further studies, as drug loading will be pursued to assess their possible use in drug delivery.

REFERENCES

1. Matthews, O. a., A.N. Shipway, and J.F. Stoddart, “Dendrimers—Branching Out From Curiosities Into New Technologies.”, *Progress in Polymer Science*, Vol. 23, pp. 1–56, 1998.

2. Sikes, S.S., and R.D. Schwartz-Bloom, “Direction Discovery: A Science Enrichment Program For High School Students.”, *Biochemistry and molecular biology education : a bimonthly publication of the International Union of Biochemistry and Molecular Biology*, Vol. 37, pp. 77–83, 2009.

3. Ringsdorf, H., “Structure And Properties Of Pharmacologically Active Polymers.”, *Journal of Polymer Science: Polymer Symposia*, Vol. 51, pp. 135–153, 1975.

4. Duncan, R., M.J. Vicent, F. Greco, and R.I. Nicholson, “Polymer-drug Conjugates: Towards A Novel Approach For The Treatment Of Endrocine-related Cancer.”, *Endocrine-Related Cancer*, Vol. 12, pp. 189–200, 2005.

5. Park, J.H., S. Lee, J.H. Kim, K. Park, K. Kim, and I.C. Kwon, “Polymeric Nanomedicine For Cancer Therapy.”, *Progress in Polymer Science (Oxford)*, Vol. 33, pp. 113–137, 2008.

6. Maeda, H., J. Wu, T. Sawa, Y. Matsumura, and K. Hori, “Tumor Vascular Permeability And The EPR Effect In Macromolecular Therapeutics: A Review.”, *Journal of Controlled Release*, Vol. 65, pp. 271–284, 2000.

7. Haag, R., and F. Kratz, “Polymer Therapeutics: Concepts And Applications.”, *Angewandte Chemie - International Edition*, Vol. 45, pp. 1198–1215, 2006.

8. Kaparissides, C., and S. Alexandridou, “Recent Advances In Novel Drug Delivery Systems.”, *Journal of Nanotechnology*, Vol. 2, pp. 1–10, 2006.

9. Lee, C.C., J. a MacKay, J.M.J. Fréchet, and F.C. Szoka, “Designing Dendrimers For Biological Applications.”, *Nature biotechnology*, Vol. 23, pp. 1517–1526, 2005.

10. Gillies, E.R., E. Dy, J.M.J. Fréchet, and F.C. Szoka, “Biological Evaluation Of Polyester Dendrimer: Poly(ethylene Oxide) ‘Bow-tie’ Hybrids With Tunable Molecular Weight And Architecture.”, *Molecular Pharmaceutics*, Vol. 2, pp. 129–138, 2005.

11. Abbasi, E., S.F. Aval, A. Akbarzadeh, M. Milani, and H.T. Nasrabadi, “Dendrimers : Synthesis , Applications , And Properties.”, *Nanoscale Research Letters*, Vol. 9, pp. 1–10, 2014.

12. Kesharwani, P., K. Jain, and N.K. Jain, “Dendrimer As Nanocarrier For Drug Delivery.”, *Progress in Polymer Science*, Vol. 39, pp. 268–307, 2014.

13. Valle, J.W., A. Armstrong, C. Newman, V. Alakhov, G. Pietrzynski, J. Brewer, S. Campbell, P. Corrie, E.K. Rowinsky, and M. Ranson, “A Phase 2 Study Of SP1049C, Doxorubicin In P-glycoprotein-targeting Pluronics, In Patients With Advanced Adenocarcinoma Of The Esophagus And Gastroesophageal Junction.”, *Investigational New Drugs*, Vol. 29, pp. 1029–1037, 2011.

14. Sobczak, R.L., M.E. Osborn, and L.A. Paquette, “Derivatives . Chemical Transformations Along The Fluted Perimeter Of A Topologically Spherical Molecule.”, Vol. 44, pp. 4886–4890, 1979.

15. Duncan, R., and L. Izzo, “Dendrimer Biocompatibility And Toxicity.”, *Advanced Drug Delivery Reviews*, Vol. 57, pp. 2215–2237, 2005.

16. Gillies, E.R., and J.M.J. Fréchet, “Dendrimers And Dendritic Polymers In Drug Delivery.”, *Drug Discovery Today*, Vol. 10, pp. 35–43, 2005.

17. Taylor, M.J., S. Tanna, and T. Sahota, “In Vivo Study Of A Polymeric Glucose-sensitive Insulin Delivery System Using A Rat Model.”, *Journal of pharmaceutical sciences*, Vol. 99, pp. 4215–4227, 2010.

18. Konishi, M., K. Kawamoto, M. Izumikawa, H. Kuriyama, and T. Yamashita, “Gene Transfer Into Guinea Pig Cochlea Using Adeno-associated Virus Vectors.”, *The journal of gene medicine*, Vol. 10, pp. 610–618, 2008.

19. Patel, H.N., and P.M. Patel, “Dendrimer Applications - A Review.”, *International Journal of Pharma and Bio Sciences*, Vol. 4, pp. 454–463, 2013.

20. Triesscheijn, M., P. Baas, J.H.M. Schellens, and F. a Stewart, “Photodynamic Therapy In Oncology.”, *The oncologist*, Vol. 11, pp. 1034–1044, 2006.

21. Ahmad, Z., A. Shah, M. Siddiq, and H.-B. Kraatz, “Polymeric Micelles As Drug Delivery Vehicles.”, *RSC Advances*, Vol. 4, pp. 17028–17038, 2014.

22. Buhleier, E., W. Wehner, and F. Vögtle, “‘Cascade’- And ‘Nonskid-Chain-like’ Syntheses Of Molecular Cavity Topologies.”, *Synthesis*, Vol. 1978, pp. 155–158, 1978.

23. Wurm, F., and H. Frey, “Linear-dendritic Block Copolymers: The State Of The Art And Exciting Perspectives.”, *Progress in Polymer Science (Oxford)*, Vol. 36, pp. 1–52, 2011.

24. Altin, H., I. Kosif, and R. Sanyal, “Fabrication Of ‘Clickable’ Hydrogels Via Dendron-polymer Conjugates.”, *Macromolecules*, Vol. 43, pp. 3801–3808, 2010.

25. Gillies, E.R., T.B. Jonsson, and J.M.J. Fréchet, “Stimuli-responsive Supramolecular Assemblies Of Linear-dendritic Copolymers.”, *Journal of the American Chemical Society*, Vol. 126, pp. 11936–11943, 2004.

26. Owen, S.C., D.P.Y. Chan, and M.S. Shoichet, “Polymeric Micelle Stability.”, *Nano Today*, Vol. 7, pp. 53–65, 2012.

27. Held, P., “Rapid Critical Micelle Concentration (CMC) Determination Using Fluorescence Polarization Analysis Of The Physical-Chemical Properties Of Detergents.” , *Application Note*, Vol. 7, pp. 39-44, 2014.

28. Manuscript, A., “NIH Public Access.”, *Changes*, Vol. 29, pp. 997–1003, 2012.

29. Kato, M., M. Kamigaito, M. Sawamoto, and T. Higashimuras, “Polymerization Of Methyl Methacrylate With The Carbon.”, *Macromolecules*, Vol. 28, pp. 1721–1723, 1995.

30. Wang, J., and K. Matyjaszewski, “Control1ed‘Living’ Radical Polymerization. Atom Transfer Radical Polymerization In The Presence Of Transition-Metal Complexes.”, *Journal of American Chemical Society*, Vol. 117, pp. 5614–5615, 1995.

31. Baek, K.Y., M. Kamigaito, and M. Sawamoto, “Star-shaped Polymers By Metal-catalyzed Living Radical Polymerization. 1. Design Of Ru(II)-based Systems And Divinyl Linking Agents.”, *Macromolecules*, Vol. 34, pp. 215–221, 2001.

32. Zhang, X., J. Xia, and K. Matyjaszewski, “End-Functional Poly(Tert -butyl Acrylate) Star Polymers By Controlled Radical Polymerization.”, *Macromolecules*, Vol. 33, pp. 2340–2345, 2000.

33. Matyjaszewski, K., and J. Xia, “Atom Transfer Radical Polymerization.”, *Chemical reviews*, Vol. 101, pp. 2921–2990, 2001.

34. Kolb, H.C., and K.B. Sharpless, “The Growing Impact Of Click Chemistry On Drug Discovery.”, *Drug Discovery Today*, Vol. 8, pp. 1128–1137, 2003.

35. Lallana, E., R. Riguera, and E. Fernandez-Megia, “Reliable And Efficient Procedures For The Conjugation Of Biomolecules Through Huisgen Azide-alkyne Cycloadditions.”, *Angewandte Chemie - International Edition*, Vol. 50, pp. 8794–8804, 2011.

36. Grammel, M., and H.C. Hang, “Chemical Reporters For Biological Discovery.”, *Nature Chemical Biology*, Vol. 9, pp. 475–484, 2013.

37. Manuscript, A., “Development Of Radiopharmaceuticals.”, Vol. 54, pp. 829–832, 2014.

38. Evans, R.A., “The Rise Of Azide–Alkyne 1,3-Dipolar ‘Click’ Cycloaddition And Its Application To Polymer Science And Surface Modification.”, *Australian Journal of Chemistry*, Vol. 60 , pp. 384–395, 2007.

39. Das, R., Majumdar, N., and Lahiri, A., “A Review On 1,3-dipolar Cycloaddition Reactions In Bioconjugation And It’s Importance In Pharmaceutical Chemistry.”, Vol. 4, pp. 467–472, 2014.

40. Fringuelli, F., A. Taticchi, and E. Wenkert, “Diels-Alder Reactions Of Cycloalkenones In Organic Synthesis.”, *Organic Preparations and Procedures International*, Vol. 22, pp. 131–165, 1990.

41. Gandini, A., “The Application Of The Diels-Alder Reaction To Polymer Syntheses Based On Furan/maleimide Reversible Couplings.”, *Polímeros*, Vol. 15, pp. 95–101, 2005.

42. Gheneim, R., C. Perez-Berumen, and A. Gandini, “Diels-Alder Reactions With Novel Polymeric Dienes And Dienophiles: Synthesis Of Reversibly Cross-linked Elastomers.”, *Macromolecules*, Vol. 35, pp. 7246–7253, 2002.

43. Kose, M.M., G. Yesilbag, and A. Sanyal, “Segment Block Dendrimers Via Diels-alder Cycloaddition.”, *Organic Letters*, Vol. 10, pp. 2353–2356, 2008.

44. Kamahori, K., S. Tada, K. Ito, and S. Itsuno, “Optically Active Polymer Synthesis By Diels-Alder Polymerization With Chirally Modified Lewis Acid Catalyst.”, *Macromolecules*, Vol. 32, pp. 541–547, 1999.

45. Dag, A., H. Durmaz, U. Tunca, and G. Hizal, “Multiarm Star Block Copolymers Via Diels-Alder Click Reaction.”, *Journal of Polymer Science Part A: Polymer Chemistry*, Vol. 47, pp. 178–187, 2009.

46. Tonga, M., N. Cengiz, M. Merve Kose, T. Dede, and A. Sanyal, “Dendronized Polymers Via Diels-alder ‘Click’ Reaction.”, *Journal of Polymer Science, Part A: Polymer Chemistry*, Vol. 48, pp. 410–416, 2010.

47. Gok, O., S. Yigit, M. Merve Kose, R. Sanyal, and A. Sanyal, “Dendron-polymer Conjugates Via The Diels-alder ‘Click’ Reaction Of Novel Anthracene-based Dendrons.”, *Journal of Polymer Science, Part A: Polymer Chemistry*, Vol. 51, pp. 3191–3201, 2013.

48. Gok, O., H. Durmaz, E.S. Ozdes, G. Hizal, U. Tunca, and A. Sanyal, “Maleimide-based Thiol Reactive Multiarm Star Polymers Via Diels-Alder/retro Diels-Alder Strategy.”, *Journal of Polymer Science Part A: Polymer Chemistry*, Vol. 48, pp. 2546–2556, 2010.

49. Khan, A., “Surface Tension, Density And Viscosity Studies On The Associative Behaviour Of Oxyethylene-Oxybutylene Diblock Copolymers In Water At Different Temperatures.”, *International Journal of Organic Chemistry*, Vol. 2, pp. 82–92, 2012.

50. Ihre, H., A. Hult, J.M.J. Fréchet, and I. Gitsov, “Double-Stage Convergent Approach For The Synthesis Of Functionalized Dendritic Aliphatic Polyesters Based On 2,2-Bis(hydroxymethyl)propionic Acid.”, *Macromolecules*, Vol. 31, pp. 4061–4068, 1998.